

Buckybowl Synthesis | Hot Paper|**2,7,11,16-Tetra-*tert*-Butyl Tetraindenopyrene Revisited by an “Inverse” Synthetic Approach**

Sven M. Elbert,^[a] Anika Haidisch,^[a] Tobias Kirschbaum,^[a] Frank Rominger,^[a] Ute Zschieschang,^[b] Hagen Klauk,^[b] and Michael Mastalerz*^[a]

Abstract: A new synthetic route to tetraindenopyrene (TIP)—a bowl-shaped cut-out structure of C_{70} —is reported. The key step in this approach is a fourfold palladium-catalyzed C–H activation that increases the yield more than 50 times in comparison to the approach originally described by Scott and co-workers. Besides examination of its optoelec-

tronic properties and study of its aggregation in solution, TIP was also re-investigated by dispersion-corrected DFT methods, which showed that dispersion interactions significantly increase the bowl-to-bowl inversion barrier. Furthermore, TIP was used as a semiconductor in p-channel thin-film transistors (TFTs).

The discovery of fullerene C_{60} in 1985^[1] stimulated chemists to synthesize this molecule,^[2] other fullerenes or cut-outs thereof—the so called buckybowl.^[3] Buckybowls have interesting properties themselves, but have also been used for the bottom-up synthesis of fullerenes, for example, by flash vacuum pyrolysis.^[4] Besides corannulene,^[5] sumanene^[6] is the simplest substructure of C_{60} and therefore it is not surprising that these two compounds are the most frequently studied.^[3a] In contrast to C_{60} -related buckybowl, similar approaches to compounds representing substructures of C_{70} (Figure 1) are much rarer.^[7] In this respect, Kuo’s $C_{38}H_{14}$ and $C_{40}H_{14}$ bowls are among the largest realized so far, with bowl depths of up to 2.33 Å.^[8] Other substructures of C_{70} ^[9] such as rubicenes^[10] or dibenzorubicenes show smaller bowl depths of 1.68 Å^[10b] or twisted^[10a,11] conformations in the solid state. Some of these molecules have been employed as the semiconductor in p-channel thin-film field-effect transistors, with a maximum reported charge-carrier mobility of $1\text{ cm}^2\text{ V}^{-1}\text{ s}^{-1}$.^[11]

Another substructure of C_{70} is tetraindenopyrene (TIP, 2, Figure 1), which had been the subject of theoretical investiga-

tions by Havenith et al.^[12] and was later synthesized by Scott and co-workers.^[13] The key step of Scott’s TIP synthesis was a quadruple Pd-catalyzed direct arylation of pyrene 1, which provides a yield of only about 0.5% of TIP 2. In the same publication, a one-pot procedure from 1,3,6,8-tetrabromopyrene and 2-bromophenyl boronic acid was described, but yields were again in the range of 0.5%.^[13] Despite the very low yield of the cyclization step, the photophysics of TIP 2 were thoroughly investigated at that time. Based on these properties, the authors suggested that TIP may be a potential candidate for organic electronics or materials chemistry, such as long wavelength dyes for special high-temperature applications. Very recently,

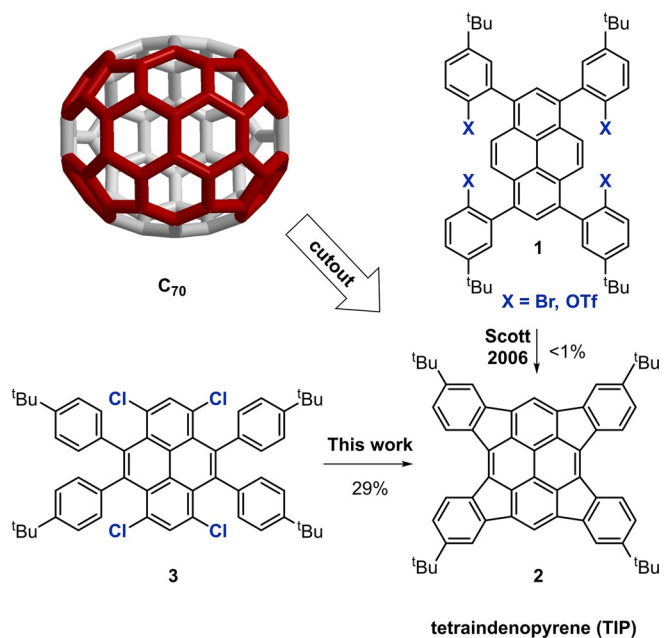


Figure 1. Top left: structure of C_{70} with tetraindenopyrene (TIP) 2 highlighted in red. Right: synthetic approach by Scott,^[13] bottom: this work.

[a] Dr. S. M. Elbert, A. Haidisch, T. Kirschbaum, Dr. F. Rominger,

Prof. Dr. M. Mastalerz

Organisch-Chemisches Institut

Ruprecht-Karls Universität Heidelberg

Im Neuenheimer Feld 270, 69120 Heidelberg (Germany)

E-mail: michael.mastalerz@oci.uni-heidelberg.de

[b] Dr. U. Zschieschang, Dr. H. Klauk

Max Planck Institute for Solid State Research

Heisenbergstr. 1, 70569 Stuttgart (Germany)

Supporting information and the ORCID identification numbers for the authors of this article can be found under:

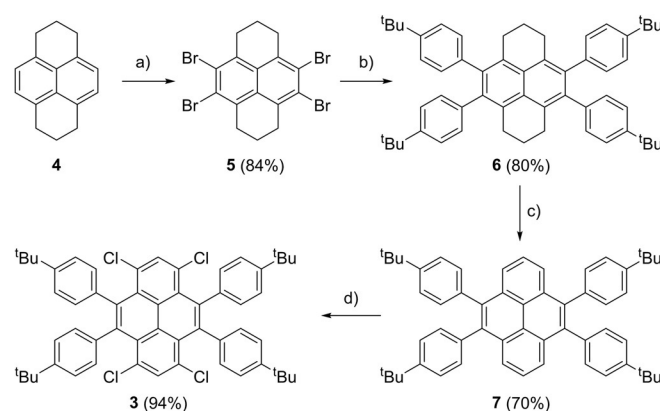
<https://doi.org/10.1002/chem.202001555>.

© 2020 The Authors. Published by Wiley-VCH Verlag GmbH & Co. KGaA. This is an open access article under the terms of Creative Commons Attribution NonCommercial-NoDerivs License, which permits use and distribution in any medium, provided the original work is properly cited, the use is non-commercial and no modifications or adaptations are made.

the synthesis of a structurally related tetra-*n*-octyl TIP by an alumina-mediated HF elimination was reported.^[14] Unfortunately, neither full characterization nor detailed discussion on photophysical or electrochemical properties were included. It is known that the K region of pyrene has a substantial olefin character, and thus the C–H activation may occur by a Heck coupling mechanism, rather than by a C–H activation in which the hydrogen is abstracted from a benzene ring.^[15] Therefore, we developed an alternative approach towards TIP **2** based on C–H activation of tetrachloropyrene **3** (Figure 1).^[16]

The synthesis of pyrene derivative **3** was described previously, starting from pyrene in six consecutive steps.^[16,17] We developed a different synthetic route for **3**, starting from the commercially available hexahydropyrene **4** (Scheme 1) which was selectively fourfold-brominated to **5** and isolated in 84% yield by simple filtration.^[18] Subsequent Suzuki–Miyaura cross-coupling under Fu conditions (Pd_2dba_3 , $HptBu_3BF_4$) and oxidation of the unsaturated propylene tethers by DDQ gave pyrene **7** in 56% yield over two steps (for details, see the Supporting Information).

The next step was the tetrachlorination of pyrene **7**, which was achieved with a slight excess (4.5 equiv) of *N*-chlorosuccinimide (NCS) in chloroform to obtain **3** in 94% yield (Scheme 1). It is worth mentioning that the chlorination was described previously using a large excess (>50 equiv) of sulfurylchloride.^[16] With the modified synthetic route described here, pyrene derivative **3** can be synthesized in just four steps from commercially available hexahydropyrene **4** in an overall yield of 44%. Furthermore, no purification by column chromatography is required, allowing the synthesis of **2** on gram scale. In comparison, the previously described synthetic route started from pyrene with an overall yield of 4% in six steps and required two steps of purification by column chromatography.^[16–17,19]



Scheme 1. Synthesis of tetrachloro tetraaryl pyrene **3**. a) Br_2 , Fe , CH_2Cl_2 , $80^\circ C$, 30 min; b) $4-tBuPh_2(OH)_2$, 8 mol % Pd_2dba_3 , 30 mol % $HptBu_3BF_4$, THF , K_2CO_3 aq (1 M), $80^\circ C$, 16 h; c) 3 equiv DDQ, toluene, $130^\circ C$, 4 h; d) NCS , $CHCl_3$, $80^\circ C$, 42 h.

All compounds were fully characterized (see the Supporting Information). By vapor diffusion of *n*-pentane into saturated solutions of **5** and **6** in dichloromethane, crystals of sufficient quality for single-crystal X-ray diffraction analyses were obtained (Figure 2). Tetrabromide **5** crystallized in the orthorhombic space group *Pnna* with $Z=4$. The crystal packing is driven by halogen bonding between two bromides with $d_{C-Br\cdots Br}=3.63\text{ \AA}$ and dispersion interactions of the bromides with the aliphatic hydrogen ($d_{C-H\cdots Br}=3.08\text{--}3.36\text{ \AA}$, Figure 2a), forming two-dimensional sheets.^[20] The distance between adjacent sheets is dominated by $Br\cdots\pi$ interactions ($d_{Br\cdots\pi}=3.63\text{ \AA}$),^[21] and these layers are twisted by 16.0° with respect to each other (Figure 2b, c). Tetraaryl hexahydropyrene **6** crystallized in the triclinic space group *P-1* with $Z=2$ (Figure 2d). The molecules interact only by weak dispersion interactions of the pe-

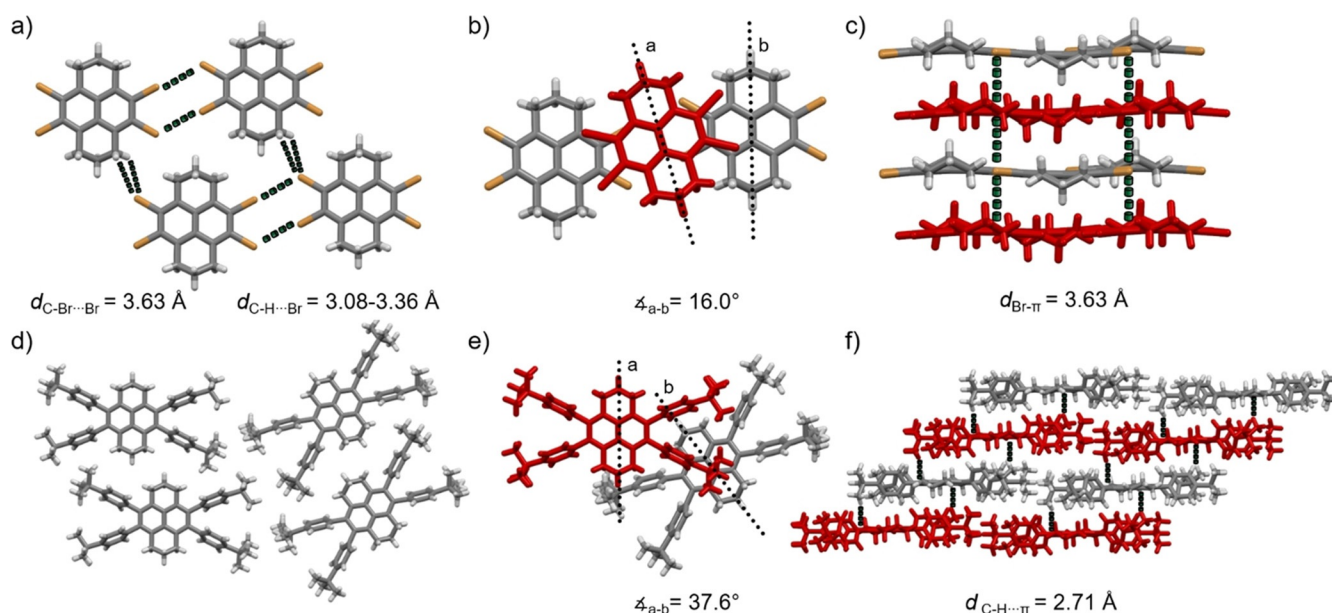
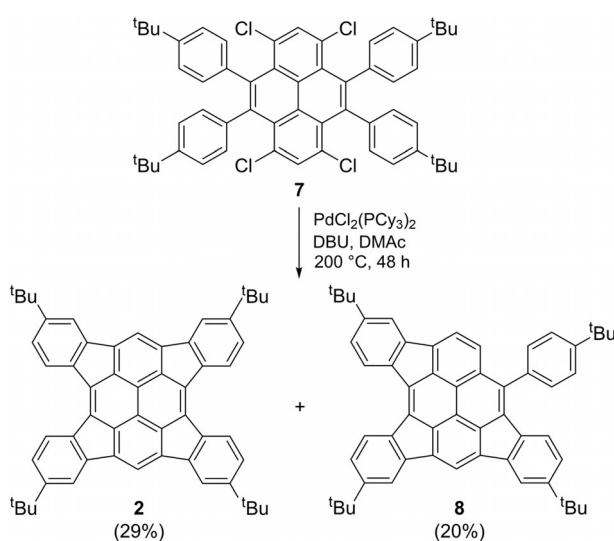


Figure 2. Single-crystal X-ray structures of tetrabromohexahydropyrene **5** (top) and tetraarylhexahydropyrene **6** (bottom) as stick models.

riperipheral *tert*-butyl groups with the central naphthyl subunits (Figure 2 e).

For the final cyclization by palladium-catalyzed direct arylation under C–H activation, typical reaction conditions ($\text{PdCl}_2(\text{PCy}_3)_2$, DMAc, 200 °C, 48 h)^[22] were used to give the targeted TIP **2** in 29% yield, along with the threefold-cyclized product **8** in 20% yield (Scheme 2). We also performed the cyclization using a wide range of conditions (e.g., various concentrations, solvents, temperatures, duration, alternative Pd sources, alternative bases), but did not obtain greater than 29% yields for **2** nor a higher ratio between the yields for **2** and **8**.



Scheme 2. Synthesis of tetraindenopyrene **2** by C–H activation.

The two compounds can be distinguished by ^1H NMR spectroscopy. Whereas TIP **2** shows four clearly defined signals between $\delta = 7.0$ and 7.5 ppm (corresponding exactly to the previous report^[13]), trindenopyrene **8** shows a more complex signal pattern consisting of 14 signals (two signals overlap at 7.8 and 7.7 ppm) between $\delta = 6.9$ and 8.2 ppm (Figure 3 bottom). Mass spectrometry shows a molecular ion peak for **2** of m/z 722.495 (m/z calcd for $\text{C}_{56}\text{H}_{50}^+$: 722.391), which is two mass units smaller than that of trindenopyrene **8** (m/z calcd for $\text{C}_{56}\text{H}_{52}^+$: 724.407 found: 724.484), consistent with the missing C–C bond.

TIP **2** showed a strong concentration dependence ($c = 0.10$ –3.08 mM) of the chemical shifts in the ^1H NMR spectra in CD_2Cl_2 (Figure 4), which is indicative of strong π – π -stacking.^[23] At room temperature, protons H^{b} ($\Delta\delta = 0.37$ ppm) and H^{c} ($\Delta\delta = 0.19$ ppm) are more weakly influenced than H^{a} ($\Delta\delta = 0.92$ ppm) and H^{d} ($\Delta\delta = 0.63$ ppm), because H^{b} and H^{c} are sterically shielded by the adjacent *tert*-butyl group against stacking.

Assuming infinite π -stacks, the averaged association K_E was determined to be $2.45 \times 10^3 \pm 0.77 \times 10^3 \text{ M}^{-1}$ ($\Delta G = -19.0 \text{ kJ mol}^{-1}$) at 293 K by a least-squares curve fitting of the infinite (isodesmic) association model (for details see the Supporting Information).^[23a, 24] This association constant is much

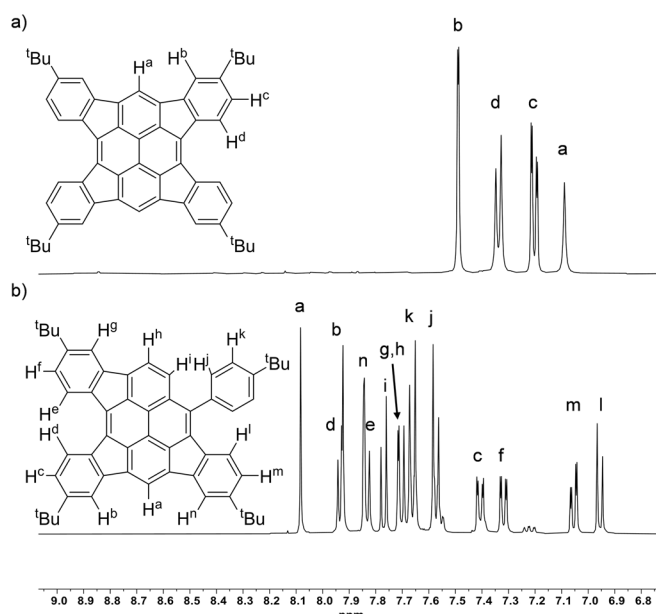


Figure 3. ^1H NMR spectra (400 MHz) of a) TIP **2** and b) trindenopyrene **8** in CD_2Cl_2 at room temperature.

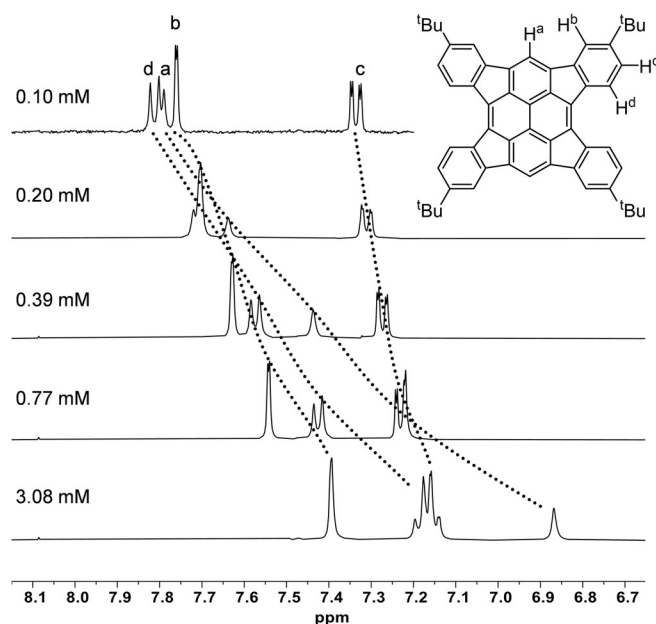


Figure 4. ^1H NMR spectra (400 MHz) of TIP **2** in CD_2Cl_2 at concentrations between 0.10 and 3.08 mM at 293 K.

higher than values reported, for example, for hexabenzocoronene-based thiophene dendrimers (K_E up to 710 M^{-1} in CDCl_3)^[25] and within an order of magnitude of values reported for various perylene- and naphthalene bisimides.^[24d] From measurements performed at temperatures ranging from 243 to 293 K, we determined $\Delta H = -15.8 \text{ kJ mol}^{-1}$ and $\Delta S = 11.9 \text{ J mol}^{-1} \text{ K}^{-1}$ from a van't-Hoff plot; this suggested that the aggregation in solution is driven by both enthalpy and entropy.^[26] The strong aggregation tendency is also reflected by a moderate solubility of **2** in CH_2Cl_2 of $(4.00 \pm 0.63) \text{ mg mL}^{-1}$. At-

tempts to grow single crystals from various solvents produced needle-shaped crystals, which unfortunately could not be structurally refined by X-ray diffraction.

TIP **2** was revisited by theoretical calculations. Scott mentioned that the TIP has a bowl-shaped structure.^[12,13] However, only the bowl-to-bowl inversion barrier calculated by DFT (B3LYP/6-31G*) was discussed, and no further details, such as geometrical parameters or energy levels of frontier molecular orbitals, were provided (see also the Discussion below).^[14] To obtain further insights into the structural details of TIP **2**, dispersion-corrected (D3)^[27] DFT methods (B3LYP/6-311G(d,p)) were used to calculate molecular properties. It was found that the input geometry (MM2 optimized models) is crucial to the outcome of the DFT optimization. Starting from a planar input, the DFT optimization using ultra-tight convergence criteria also produced a planar geometry. A frequency analysis of the result shows an imaginary frequency with $15.5\text{i}\text{ cm}^{-1}$, which is indicative of a transition state. A second optimization, this time performed with an already contorted input, resulted in a bowl-shaped structure that no longer shows an imaginary frequency; this indicates that it is a realistic energy minimum (Figure 5). The bowl depth is 0.69 \AA (if measured to the original 2,7-positions of the pyrene) or 1.44 \AA (maximum bowl depth) and thus similar to the bowl depth of dibenzorubicene (1.68 \AA).^[10b] The dispersion-corrected calculations gave a greater bowl depth than those performed without the D3 correction term (1.18 \AA); this result deviates by about 20%(!), thus indicating that dispersion has a significant effect in stabilizing a contorted structure. The *tert*-butyl groups do not contribute substantially to the curving by dispersion interactions (see the Supporting Information).

Based on the dispersion-corrected model, the bowl-to-bowl inversion barrier was calculated to be 6.47 kJ mol^{-1} ($\Delta G =$

11.9 kJ mol^{-1} , Figure 6). This is substantially higher than without dispersion correction (2.99 kJ mol^{-1}) and even higher than the previously published value (1.38 kJ mol^{-1}).^[13] Although the estimated inversion barrier is higher, it still means that TIP **2** fluctuates 51 billion times per second between the bowl-shaped minima, much too fast to be determined by variable-temperature NMR measurements. In comparison, corannulene shows an experimentally determined inversion rate of 200 000 per second at room temperature with a corresponding inversion barrier of $\Delta^{\ddagger}G = 43 \pm 1\text{ kJ mol}^{-1}$ ($10.2 \pm 0.2\text{ kcal mol}^{-1}$).^[2]

Additional information on the electronic structure of TIP **2** were obtained by AICD^[28] and NICS calculations (HF/6-31 + G(d), Figure 5). The outer benzene rings (A) show typical aromatic character with comparable NICS(-1) and NICS($+1$) values of -8.8 and -8.7 . NICS(-1) is the concave and NICS($+1$) the convex side of the bowl. Aromaticity is also observed for the D-rings (NICS(-1) = -11.7 and NICS($+1$) = -7.3 ,

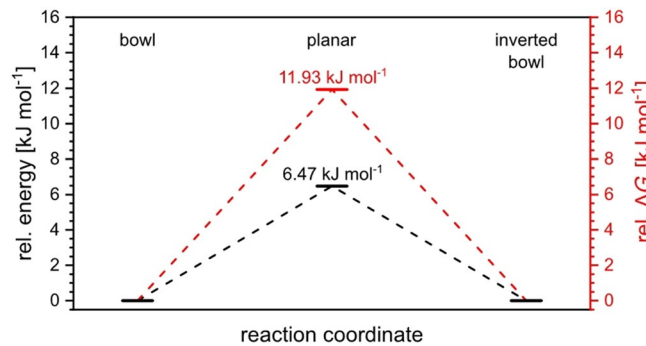


Figure 6. Inversion process of **2** via a planar transition state with the calculated difference in energy (black) and free enthalpy (red) derived from DFT calculations (B3LYP/6-311G(d,p)).

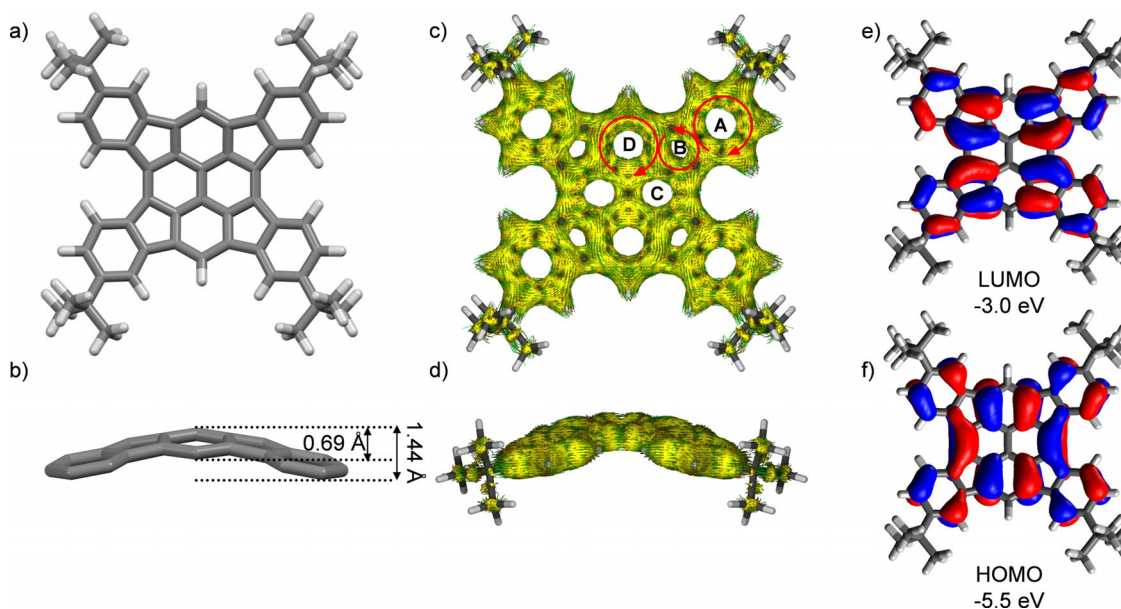


Figure 5. Geometry-optimized model (B3LYP/6-311G(d,p)) of the bowl-shaped TIP **2**. a) Top view. b) side view. AICD plots (HF/6-31 + G(d)) of **2** from c) the top/concave side with the magnetic field pointing out of the paper plane and red arrows indicating the direction of the ring current. d) Side view. Canonical MOs of **2** (B3LYP/6-311G(d,p)) with the corresponding orbital energy. e) LUMO; f) HOMO. All calculations were corrected for dispersion (D3).

due to the higher electron density on the bowl's concave side. As known from unsubstituted pyrene,^[12] the C-ring shows smaller aromaticity, with NICS(-1) = -5.3 , and here the curvature has by far the greatest influence on the virtual chemical shift, with NICS($+1$) = -0.6 . The five-membered B-rings are nearly nonaromatic, with NICS(-1) = 1.3 and NICS($+1$) = 3.7 , and with a tendency toward antiaromatic character, similar to PAHs with fused five-membered rings such as corannulene^[29] or others.^[30] The ring currents derived by AICD calculations (see red arrows in Figure 5c) are in accordance with the trends observed by the NICS calculations.

The DFT-calculated energies of the FMOs are $E_{\text{HOMO, DFT}} = -5.5$ eV and $E_{\text{LUMO, DFT}} = -3.0$ eV (Figure 5e and f). Although no oxidation was recorded within the redox window of the solvents employed (CH_2Cl_2 and *o*-DCB) at anodic potentials, two quasireversible reduction potentials were found in both these solvents (Figure 7). In CH_2Cl_2 , the reduction potentials are $E_{\text{red, 1}}^{1/2} = -1.41$ V and $E_{\text{red, 2}}^{1/2} = -1.74$ V. In *o*-DCB the two reduction peaks were found at slightly lower potentials ($E_{\text{red, 1}}^{1/2} = -1.48$ V and $E_{\text{red, 2}}^{1/2} = -1.84$ V). The first reduction potentials are higher by about 0.3–0.4 V compared to [60]PCBM ($E_{\text{red, 1}}^{1/2} = -1.08$ V) and [70]PCBM ($E_{\text{red, 1}}^{1/2} = -1.09$ V).^[31] Making a commonly used assumption, the electron affinity can be estimated as $EA = -E_{\text{red, 1}}^{1/2} + 4.8$ eV,^[32] corresponding to $EA = -3.46$ eV in CH_2Cl_2 and $EA = -3.42$ eV in *o*-DCB.

The calculated and experimentally determined FMOs suggest that TIP **2** is potentially interesting for organic electronics applications, both as an electron- and as a hole-conducting semiconductor. Initial experiments using **2** in thin-film transistors (TFTs) indicate hole mobilities of 4×10^{-4} $\text{cm}^2\text{V}^{-1}\text{s}^{-1}$ in TFTs fabricated on silicon substrates and 1×10^{-4} $\text{cm}^2\text{V}^{-1}\text{s}^{-1}$ in TFTs on flexible polyethylene naphthalate (PEN) substrates and on/off current ratios up to 10^3 measured under ambient conditions (for details, see the Supporting Information).

In summary, we have introduced an alternative synthetic approach to achieve TIP **2** in five consecutive steps and with a 50-fold higher yield both for the final cyclization step (29 vs. 0.5%)^[13] and for the overall synthesis (13 vs. 0.25%). TIP **2** was

revisited by dispersion-corrected DFT calculations, revealing that the bowl-to-bowl inversion barrier is substantially higher than previously estimated. Furthermore, TIP **2** was used to fabricate p-channel TFTs, indicating charge-carrier mobilities up to 4×10^{-4} $\text{cm}^2\text{V}^{-1}\text{s}^{-1}$ and on/off current ratios of up to 10^3 . To the best of our knowledge, this is the first example of a transistor based on a nonfunctionalized hydrocarbon buckybowl.^[33–35] The possibility of easily scaling up the synthesis of precursor **3** without the necessity for purification by column chromatography will allow us to provide TIP **2** in sufficiently high amounts to explore its chemistry and physics; this is ongoing in our laboratory.

Experimental Section

For experimental details, see the Supporting Information.

Acknowledgements

Support from the state of Baden-Württemberg through bwHPC and from the German Research Foundation (DFG) through grant no. INST 40/467-1 FUGG (JUSTUS cluster) is acknowledged. We thank the DFG for funding this project within the collaborative research center SFB1249 on "N-heteropolycycles as functional materials" (TP A04 & C01). We are grateful to Laura Weber for synthesizing starting materials.

Conflict of interest

The authors declare no conflict of interest.

Keywords: C–H activation · organic thin film transistors · polycyclic aromatic hydrocarbons · pyrene · tetraindenopyrene

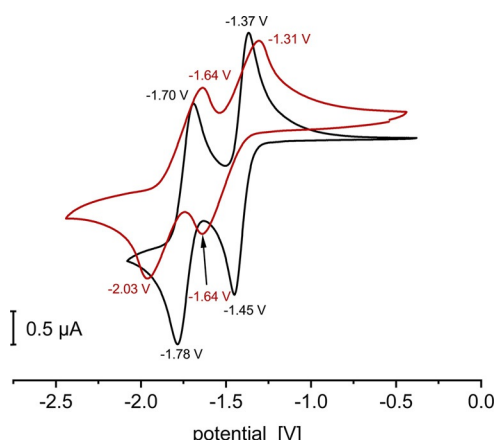


Figure 7. Cyclic voltammograms of TIP **9** in CH_2Cl_2 (black) and *o*-DCB (red), measured at room temperature with a Pt electrode, $n\text{Bu}_4\text{NPF}_6$ (0.1 M) as electrolyte, and Fc/Fc^+ as internal reference (scanning speed: 100 mVs^{-1}).

- [1] H. W. Kroto, J. R. Heath, S. C. O'Brien, R. F. Curl, R. E. Smalley, *Nature* **1985**, *318*, 162–163.
- [2] L. T. Scott, M. M. Boorum, B. J. McMahon, S. Hagen, J. Mack, J. Blank, H. Wegner, A. de Meijere, *Science* **2002**, *295*, 1500–1503.
- [3] a) Y.-T. Wu, J. S. Siegel, *Chem. Rev.* **2006**, *106*, 4843–4867; b) V. M. Tsefrikas, L. T. Scott, *Chem. Rev.* **2006**, *106*, 4868–4884.
- [4] M. M. Boorum, Y. V. Vasil'ev, T. Drewello, L. T. Scott, *Science* **2001**, *294*, 828–831.
- [5] a) X. Li, F. Kang, M. Inagaki, *Small* **2016**, *12*, 3206–3223; b) R. G. Lawton, W. E. Barth, *J. Am. Chem. Soc.* **1971**, *93*, 1730–1745; c) A. M. Butterfield, B. Gilomen, J. S. Siegel, *Org. Process Res. Dev.* **2012**, *16*, 664–676.
- [6] a) H. Sakurai, T. Daiko, T. Hirao, *Science* **2003**, *301*, 1878; b) T. Amaya, T. Hirao, *Chem. Commun.* **2011**, *47*, 10524–10535.
- [7] a) C. Thilgen, A. Herrmann, F. Diederich, *Angew. Chem. Int. Ed. Engl.* **1997**, *36*, 2268–2280; *Angew. Chem.* **1997**, *109*, 2362–2374; b) K. Hedberg, L. Hedberg, M. Bühl, D. S. Bethune, C. A. Brown, R. D. Johnson, *J. Am. Chem. Soc.* **1997**, *119*, 5314–5320; c) D. R. McKenzie, C. A. Davis, D. J. H. Cockayne, D. A. Muller, A. M. Vassallo, *Nature* **1992**, *355*, 622–624.
- [8] T.-C. Wu, M.-K. Chen, Y.-W. Lee, M.-Y. Kuo, Y.-T. Wu, *Angew. Chem. Int. Ed.* **2013**, *52*, 1289–1293; *Angew. Chem.* **2013**, *125*, 1327–1331.
- [9] a) S. Hishikawa, Y. Okabe, R. Tsuruoka, S. Higashibayashi, H. Ohtsu, M. Kawano, Y. Yakiyama, H. Sakurai, *Chem. Lett.* **2017**, *46*, 1556–1559; b) Y. Zou, W. Zeng, T. Y. Gopalakrishna, Y. Han, Q. Jiang, J. Wu, *J. Am. Chem. Soc.* **2019**, *141*, 7266–7270; c) G. Gao, M. Chen, J. Roberts, M. Feng, C. Xiao, G. Zhang, S. Parkin, C. Risko, L. Zhang, *J. Am. Chem. Soc.* **2020**, *142*, 2460–2470.

- [10] a) J. Liu, A. Narita, S. Osella, W. Zhang, D. Schollmeyer, D. Beljonne, X. Feng, K. Müllen, *J. Am. Chem. Soc.* **2016**, *138*, 2602–2608; b) J. Liu, S. Osella, J. Ma, R. Berger, D. Beljonne, D. Schollmeyer, X. Feng, K. Müllen, *J. Am. Chem. Soc.* **2016**, *138*, 8364–8367; c) H.-H. Hseuh, M.-Y. Hsu, T.-L. Wu, R.-S. Liu, *J. Org. Chem.* **2009**, *74*, 8448–8451.
- [11] X. Gu, X. Xu, H. Li, Z. Liu, Q. Miao, *J. Am. Chem. Soc.* **2015**, *137*, 16203–16208.
- [12] a) R. W. A. Havenith, J. H. van Lenthe, F. Dijkstra, L. W. Jenneskens, *J. Phys. Chem. A* **2001**, *105*, 3838–3845; b) R. W. A. Havenith, H. Jiao, L. W. Jenneskens, J. H. van Lenthe, M. Sarobe, P. v. R. Schleyer, M. Kataoka, A. Necula, L. T. Scott, *J. Am. Chem. Soc.* **2002**, *124*, 2363–2370.
- [13] a) H. A. Wegner, H. Reisch, K. Rauch, A. Demeter, K. A. Zachariasse, A. de Meijere, L. T. Scott, *J. Org. Chem.* **2006**, *71*, 9080–9087; b) H. A. Wegner, H. Reisch, K. Rauch, A. Demeter, K. A. Zachariasse, A. de Meijere, L. T. Scott, *J. Org. Chem.* **2007**, *72*, 1870.
- [14] V. Akhmetov, M. Feofanov, O. Papaianina, S. Troyanov, K. Amsharov, *Chem. Eur. J.* **2019**, *25*, 11609–11613.
- [15] S. Seifert, D. Schmidt, K. Shoyama, F. Würthner, *Angew. Chem. Int. Ed.* **2017**, *56*, 7595–7600; *Angew. Chem.* **2017**, *129*, 7703–7708.
- [16] L. Zöphel, R. Berger, P. Gao, V. Enkelmann, M. Baumgarten, M. Wagner, K. Müllen, *Chem. Eur. J.* **2013**, *19*, 17821–17826.
- [17] a) L. Zöphel, V. Enkelmann, R. Rieger, K. Müllen, *Org. Lett.* **2011**, *13*, 4506–4509; b) L. Zöphel, D. Beckmann, V. Enkelmann, D. Chercka, R. Rieger, K. Müllen, *Chem. Commun.* **2011**, *47*, 6960–6962.
- [18] Compound 5 was mentioned earlier, but the compound was never isolated or fully characterized: D. Zhao, Q. Wu, Z. Cai, T. Zheng, W. Chen, J. Lu, L. Yu, *Chem. Mater.* **2016**, *28*, 1139–1146.
- [19] J. Hu, D. Zhang, F. W. Harris, *J. Org. Chem.* **2005**, *70*, 707–708.
- [20] a) G. R. Desiraju, R. Parthasarathy, *J. Am. Chem. Soc.* **1989**, *111*, 8725–8726; b) G. R. Desiraju, *Angew. Chem. Int. Ed.* **2011**, *50*, 52–59; *Angew. Chem.* **2011**, *123*, 52–60; c) T. T. Bui, S. Dahoui, C. Lecomte, G. R. Desiraju, E. Espinosa, *Angew. Chem. Int. Ed.* **2009**, *48*, 3838–3841; *Angew. Chem.* **2009**, *121*, 3896–3899.
- [21] a) O. Hassel, K. O. Strømme, *Acta Chem. Scand.* **1958**, *12*, 1146; b) L. C. Gilday, S. W. Robinson, T. A. Barendt, M. J. Langton, B. R. Mullaney, P. D. Beer, *Chem. Rev.* **2015**, *115*, 7118–7195.
- [22] a) Y. Wang, O. Allemand, T. S. Balaban, N. Vanthuyne, A. Linden, K. K. Baldridge, J. S. Siegel, *Angew. Chem. Int. Ed.* **2018**, *57*, 6470–6474; *Angew. Chem.* **2018**, *130*, 6580–6584; b) X. Tian, L. M. Roch, K. K. Baldridge, J. S. Siegel, *Eur. J. Org. Chem.* **2017**, 2801–2805; c) S. Liu, L. M. Roch, O. Allemand, J. Xu, N. Vanthuyne, K. K. Baldridge, J. S. Siegel, *J. Org. Chem.* **2018**, *83*, 3979–3986; d) S. Lampart, L. M. Roch, A. K. Dutta, Y. Wang, R. Warshamanager, A. D. Finke, A. Linden, K. K. Baldridge, J. S. Siegel, *Angew. Chem. Int. Ed.* **2016**, *55*, 14648–14652; *Angew. Chem.* **2016**, *128*, 14868–14872; e) T. Kubo, S. Miyazaki, T. Kodama, M. Aoba, Y. Hirao, H. Kurata, *Chem. Commun.* **2015**, *51*, 3801–3803; f) Y.-C. Hsieh, T.-C. Wu, J.-Y. Li, Y.-T. Chen, M.-Y. Kuo, P.-T. Chou, Y.-T. Wu, *Org. Lett.* **2016**, *18*, 1868–1871; g) W. Hagui, H. Doucet, J.-F. Soulé, *Chem.* **2019**, *5*, 2006–2078.
- [23] a) D. Zhao, J. S. Moore, *J. Org. Chem.* **2002**, *67*, 3548–3554; b) J. Wu, A. Fechtenkötter, J. Gauss, M. D. Watson, M. Kastler, C. Fechtenkötter, M. Wagner, K. Müllen, *J. Am. Chem. Soc.* **2004**, *126*, 11311–11321; c) C. Shao, M. Grüne, M. Stolte, F. Würthner, *Chem. Eur. J.* **2012**, *18*, 13665–13677; d) J. A. A. W. Elemans, A. E. Rowan, R. J. M. Nolte, *J. Am. Chem. Soc.* **2002**, *124*, 1532–1540.
- [24] a) Y. Tobe, N. Utsumi, K. Kawabata, A. Nagano, K. Adachi, S. Araki, M. Sonoda, K. Hirose, K. Naemura, *J. Am. Chem. Soc.* **2002**, *124*, 5350–5364; b) Y. Nakamura, T. Nakazato, T. Kamatsuka, H. Shinokubo, Y. Miyake, *Chem. Eur. J.* **2019**, *25*, 10571–10574; c) R. B. Martin, *Chem. Rev.* **1996**, *96*, 3043–3064; d) Z. Chen, A. Lohr, C. R. Saha-Möller, F. Würthner, *Chem. Soc. Rev.* **2009**, *38*, 564–584.
- [25] W. W. H. Wong, C.-Q. Ma, W. Pisula, C. Yan, X. Feng, D. J. Jones, K. Müllen, R. A. J. Janssen, P. Bäuerle, A. B. Holmes, *Chem. Mater.* **2010**, *22*, 457–466.
- [26] M. Rekharsky, Y. Inoue, S. Tobey, A. Metzger, E. Anslyn, *J. Am. Chem. Soc.* **2002**, *124*, 14959–14967.
- [27] S. Grimme, S. Ehrlich, L. Goerigk, *J. Comput. Chem.* **2011**, *32*, 1456–1465.
- [28] a) D. Geuenich, K. Hess, F. Köhler, R. Herges, *Chem. Rev.* **2005**, *105*, 3758–3772; b) R. Herges, D. Geuenich, *J. Phys. Chem. A* **2001**, *105*, 3214–3220.
- [29] J. C. Dobrowolski, P. F. J. Lipiński, *RSC Adv.* **2016**, *6*, 23900–23904.
- [30] a) K. K. Laali, T. Okazaki, S. E. Galembbeck, *J. Chem. Soc. Perkin Trans. 2* **2002**, 621–629; b) K. Yamamoto, Y. Ie, N. Tohnai, F. Kakiuchi, Y. Aso, *Scientific Reports* **2018**, *8*, 17663; c) X. Yang, F. Rominger, M. Mastalerz, *Angew. Chem. Int. Ed.* **2019**, *58*, 17577–17582; *Angew. Chem.* **2019**, *131*, 17741–17746.
- [31] F. B. Kooistra, V. D. Mihailescu, L. M. Popescu, D. Kronholm, P. W. M. Blom, J. C. Hummelen, *Chem. Mater.* **2006**, *18*, 3068–3073.
- [32] N. Kulisic, S. More, A. Mateo-Alonso, *Chem. Commun.* **2011**, *47*, 514–516.
- [33] K. Shi, T. Lei, X.-Y. Wang, J.-Y. Wang, J. Pei, *Chem. Sci.* **2014**, *5*, 1041–1045.
- [34] R.-Q. Lu, Y.-N. Zhou, X.-Y. Yan, K. Shi, Y.-Q. Zheng, M. Luo, X.-C. Wang, J. Pei, H. Xia, L. Zoppi, K. K. Baldridge, J. S. Siegel, X.-Y. Cao, *Chem. Commun.* **2015**, *51*, 1681–1684.
- [35] a) M. Stępień, *Synlett* **2013**, *24*, 1316–1321; b) M. Saito, H. Shinokubo, H. Sakurai, *Mater. Chem. Front.* **2018**, *2*, 635–661; c) X.-Q. Hou, Y.-T. Sun, L. Liu, S.-T. Wang, R.-L. Geng, X.-F. Shao, *Chin. Chem. Lett.* **2016**, *27*, 1166–1174.

Manuscript received: March 31, 2020

Revised manuscript received: April 20, 2020

Accepted manuscript online: April 21, 2020

Version of record online: July 20, 2020

Chemistry—A European Journal

Supporting Information

2,7,11,16-Tetra-*tert*-Butyl Tetraindenopyrene Revisited by an “Inverse” Synthetic Approach

Sven M. Elbert,^[a] Anika Haidisch,^[a] Tobias Kirschbaum,^[a] Frank Rominger,^[a]
Ute Zschieschang,^[b] Hagen Klauk,^[b] and Michael Mastalerz*^[a]

1. General Remarks

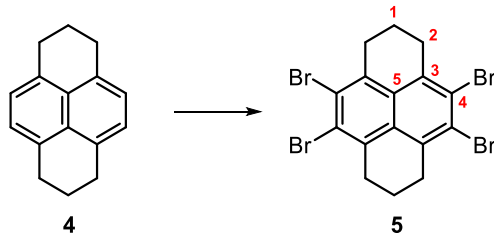
Experimental Details: Commercially available reagents were obtained from Sigma-Aldrich and have been used without further purification unless otherwise mentioned. Flash column chromatography was performed using Silica Gel with a particle size of 0.040-0.063 mm. (Macherey-Nagel & Co. KG, Düren). The eluents were light petroleum ether and dichloromethane or mixtures of them. For thin layer chromatography fluorescent labelled silica coated aluminium plates (60 F254, Merck) were used. The spots were detected by using UV-light irradiation with wavelengths of $\lambda_{\text{ex}} = 254$ and 366 nm. Melting points were measured on a Büchi B-540 and are not corrected. The melting points were measured in open glass capillaries. NMR-spectra (^1H , ^{13}C , 2D spectra) were recorded in CDCl_3 or $\text{DCM}-d_2$ using a Bruker Avance III 400 (^1H NMR: 400 MHz; ^{13}C NMR: 101 MHz) spectrometer at 298 K or Brucker Avance III 600 (^1H : 600 MHz, ^{13}C : 151 MHz) spectrometer at 295 K, unless otherwise mentioned. Chemical shifts are reported in parts per million (ppm) relative to traces of CHCl_3 ($\delta = 7.26$ ppm, $\delta_{\text{C}} = 77.2$ ppm)^[S1] or CH_2Cl_2 ($\delta_{\text{H}} = 5.32$ ppm, $\delta_{\text{C}} = 53.8$ ppm)^[S1] in the corresponding deuterated solvent, unless otherwise mentioned. IR spectra were recorded on a Fourier transform spectrophotometer (Bruker Lumos) equipped with a Zn/Se ATR crystal. The signal intensity was described with s (strong), m (medium), w (weak) an br (broad). MALDI-TOF-mass spectra were carried out on a Bruker AutoFlex Speed time-of-flight with DCTB (trans-2-[3-(4-tert-butylphenyl)-2-methyl-2-propenylidene]malo-nonitrile) as matrix. Elemental analyses to determine the amount of C, N and H were performed by the Microanalytical Laboratory at the University of Heidelberg using an Elementar Vario EL machine. Absorption spectra were recorded on a Jasco UV-VIS V-730 spectrophotometer and fluorescence spectra were recorded on a Jasco FP-8300 spectrofluorometer. For the calculation of molar extinction coefficients at least five solutions of different concentration were prepared by standard addition method. Cyclic voltammograms were obtained at a scan rate of 100 mVs⁻¹ with a Pt working electrode (0.78 mm²), a Pt counter electrode, and an Ag reference electrode using an Autolab PGSTAT 101 potentiostat from Deutsche Metrohm with *n*-Bu₄NClO₄ (0.1 M) as electrolyte in dichloromethane or o-DCB.

Computational Details: All quantum-chemical calculations were performed by employing the Gaussian09 program package.^[S2] The theoretical approach is based on Kohn-Scham density functional methodologies^[S3] using the B3LYP functional.^[S4] As basis set the triple- ζ -bases (6-311G(d,p))^[S5] was used. As dispersion correction

Grimme's D3 dispersion including Becke-Johnson damping was applied.^[S6] The geometries of the regarded species were fully optimized using ultra-tight convergence criteria of the representative computational method. Ground states were confirmed by using frequency calculations to not exhibit any imaginary frequency. Prediction of excited state properties were performed using time-depended DFT methods with the cam-B3LYP functional^[S7] and convoluted with GaussSum.^[S8] NICS(0) and NICS(1) values were calculated from the optimized geometries by adding a ghost atom in the centroid or 1 Å above/below of the corresponding ring and performing a single-point calculation based on Hartree-Fock methods^[S9] using the augmented double- ζ -basis (6-31+G(d))^[S5, S10] with the GIAO method.^[S11] Ring-current analysis was accomplished by performing a single-point calculation with the CSGT method^[S11b, S11c, S12] on the HF/6-31+G(d) level and using the AICD program package.^[S13]

2. Syntheses and Characterization

4,5,9,10-Tetrabromo-1,2,3,6,7,8-hexahydropyrene 5

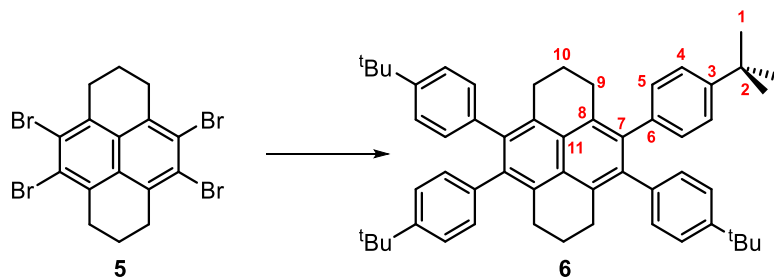


Hexahydropyrene **4** (2.10 g, 10.0 mmol, 1 eq.) was dissolved in CH₂Cl₂ (60 mL) and iron powder (426.7 mg, 7.65 mmol, 0.77 eq.) was added. While stirring, bromine (2.2 mL, 43.0 mmol, 4.3 eq.) was added and the mixture stirred for additional 30 min at 80 °C, whereby a solid precipitated. The mixture was cooled to room temperature and poured on water (100 mL). The precipitate was collected by filtration, washed with CHCl₃ (10 mL) and MeOH (20 mL) to give 4.4 g (84%) of tetrabromide **5** as colorless solid. M.p. = 253°C-256°C (dec.). ¹H-NMR (400 MHz, CDCl₃): δ = 3.20 (t, *J* = 6.3 Hz, 8H, H-2), 2.03 (q, *J* = 6.3 Hz, 4H, H-1) ppm. ¹³C-NMR (101 MHz, CDCl₃): δ = 135.8 (C 3), 130.6 (C 5), 125.3 (C 4), 34.4 (C 2), 23.2 (C 1) ppm. IR (neat, ATR): $\tilde{\nu}$ = 3422 (br), 2945 (w), 2927 (m), 2858 (m), 1652 (br), 1529 (m), 1454 (m), 1429 (w), 1416 (w), 1343 (w), 1289 (s), 1194 (s), 1165 (w), 1068 (m), 945 (m), 901 (s), 849.21 (m), 787 (w), 746 (m), 696 (w), 665 (w), 609 (w) cm⁻¹. HRMS (MALDI-TOF+, DCTB): [M]⁺: *m/z* calcd. for

$C_{16}H_{12}Br_4^+$: 523.767, found 523.781. Anal. Calcd. for $C_{16}H_{12}Br_4$: C 36.68, H 2.31, found: C 36.76, H 2.50.

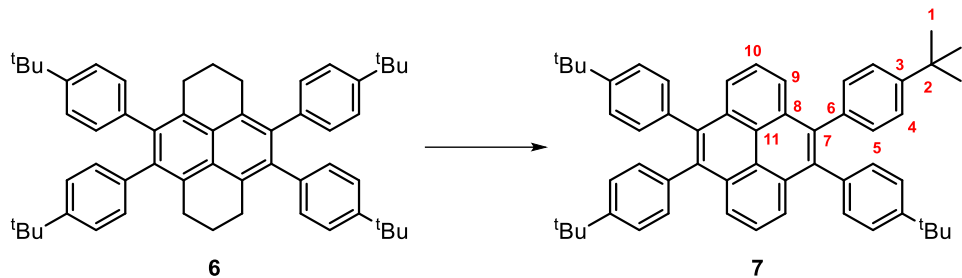
Compound **5** was mentioned in literature but neither isolated nor fully characterized.^[S14]

4,5,9,10-Tetrakis(4-(*tert*-butyl)phenyl)-1,2,3,6,7,8-hexahydropyrene **6**



Compound **5** (2.62 g, 5 mmol, 1 eq.) and 4-*tert*-butylphenyl-boronic acid (4.45 g, 25.0 mmol, 5 eq.) were dissolved in dry THF (20 mL) and 1 M K_2CO_3 -solution (20 mL) under an argon atmosphere. Pd_2dba_3 (366 mg, 0.4 mmol, 8 mol%) and $HP^tBu_3BF_4$ (435 mg, 1.5 mmol, 30 mol%) were added and the mixture refluxed while vigorous stirring overnight at 80 °C. After cooling to room temperature the solid was collected by filtration and washed with cold $CHCl_3$ (8 mL). The obtained greyish solid was dissolved in boiling $CHCl_3$, filtered over a pad of Celite while hot and the solvent was removed under reduced pressure to give 2.98 g (80%) of **6** as colorless solid. M.p. = >400°C. 1H -NMR (300 MHz, $CDCl_3$): δ = 7.10 (d, J = 8.3 Hz, 8H, H-4), 6.87 (d, J = 8.3 Hz, 8H, H-5), 2.85 (t, J = 5.9 Hz, 8H, H-9), 1.86 (s, 1H), 1.22 (s, 36H, H-1) ppm. ^{13}C -NMR (101 MHz, $CDCl_3$): δ = 148.5 (C-3), 138.4 (C-6), 138.0 (C-7), 131.7 (C-8), 130.1 (C-5), 129.4 (C-11), 124.0 (C-4), 34.4 (C-2), 31.5 (C-1), 30.6 (C-9), 23.5 (C 10) ppm. IR (neat, ATR): $\tilde{\nu}$ = 2961 (m), 2930 (m), 2901 (m), 2867 (m), 2832 (m), 1512 (m), 1473 (w), 1456 (m), 1428 (m), 1391 (m), 1363 (m), 1324 (w), 1268 (m), 1195 (w), 1129 (m), 1118 (m), 1104 (m). 1069 (w), 1017 (m), 959 (w), 947 (w), 925 (w), 849 (s), 836 (s), 832 (s), 787 (s), 731 (w), 694 (m), 680 (w), 647 (m), 638 (w), 619 (w), 615 (w), 604 (w) cm^{-1} . HRMS (MALDI-TOF+, DCTB): [M] $^+$: m/z calcd. for $C_{56}H_{64}^+$: 736.501, found: 736.467. Anal. calcd. for $C_{56}H_{64}\cdot H_2O$: C 89.07, H 8.81 found: C 89.23, H 8.84.

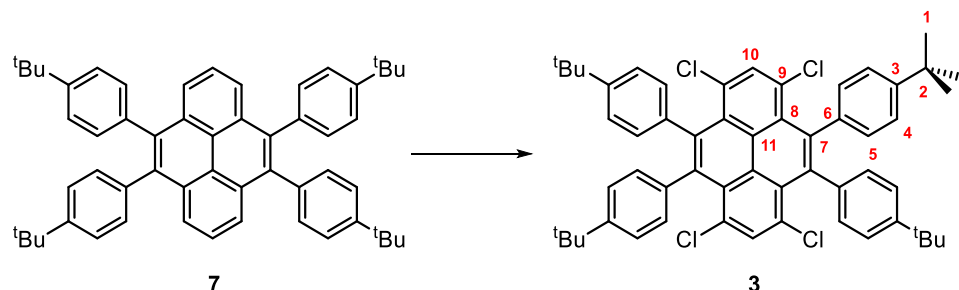
4,5,6,10-Tetrakis(4-(*tert*-butyl)phenyl)pyrene **7**



Hexahydriopyrene **6** (2.83 g, 3.84 mmol, 1 eq.) and DDQ (2.61 g, 11.5 mmol, 3 eq.) were dissolved in dry toluene (62 mL) under argon atmosphere. The mixture was stirred for 4 h at 130 °C, whereby the color changed from red to brown and a solid precipitated. After cooling to room temperature, the solid was filtrated and washed with cold CHCl₃ (30 mL) and MeOH (15 mL) until the washing solution was colorless. After drying in a stream of air, 1.96 g (70%) of pyrene **7** was isolated as colorless solid. M.p. >400°C. ¹H-NMR (600 MHz, CDCl₃): δ = 7.99 (d, J = 7.8 Hz, 4H, H-9), 7.82 (t, J = 7.8 Hz, 2H, H 10), 7.27 (d, J = 8.3 Hz, 8 H, H-4), 7.17 (d, J = 8.1 Hz, 8H, H-5), 1.29 (s, 36 H, H 1) ppm. ¹³C-NMR (151 MHz, CDCl₃): δ = 149.2 (C-3), 138.2 (C-7), 136.9 (C-6), 131.4 (C-8), 131.0 (C-5), 125.8 (C-10), 125.0 (C-9), 124.4 (C-4), 123.9 (C-11), 34.6 (C-2), 31.5 (C-1) ppm. IR (neat, ATR): ν = 3200 (bw), 2954 (m), 2899 (w), 2860 (w), 2362 (w), 2334 (w), 1579 (w), 1510 (w), 1452 (s), 1398 (w), 1359 (w), 1311 (w), 1269 (s), 1192 (s), 1109 (m), 1074 (w), 1022 (w), 987 (w), 968 (w), 946 (vw), 889 (m), 858 (w), 835 (m), 802 (s), 776 (w), 727 (s), 702 (w), 626 (s) cm⁻¹. UV/Vis (CH₂Cl₂): λ_{max} (log ε) = 380 (3.34), 352 (4.43), 336 (4.34), 289 (4.80), 278 (4.53) nm. HRMS (MALDI-TOF+, DCTB): [M]⁺: m/z calcd. for C₅₆H₅₈⁺: 730.454, found: 730.534.

The analytical data is in accordance to the data published before.^[S15]

4,5,6,10-Tetrakis(4-(*tert*-butyl)phenyl)-1,3,6,8-tetrachloropyrene **3**

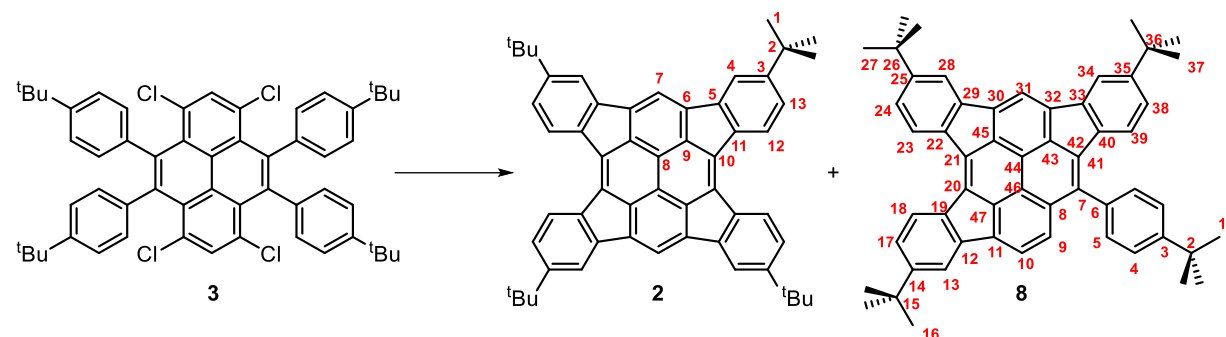


Pyrene **7** (4.98 g, 6.8 mmol,) and N-chlorosuccinimide (4.09 g, 30.6 mmol, 4.5 equiv.) were dissolved in CHCl₃ (70 mL) and stirred for 42 h at 80 °C. The obtained suspension

was cooled to room temperature and washed with water (2×200 mL) and brine (2×200 mL), dried over magnesium sulfate, filtered and the solvent was removed under reduced pressure to give 5.58 g (94%) of tetrachloropyrene **3** as a bright yellow solid. M.p.: 340°C (dec.). **3** can be further purified by recrystallization from ethanol/chloroform. $^1\text{H-NMR}$ (600 MHz, CDCl_3): $\delta = 7.89$ (s, 2H , H-10), 7.09 (d, $J = 8.2$ Hz, 8H , H-4), 7.01 (d, $J = 8.2$ Hz, 8H , H 5), 1.24 (s, 36H , H 1) ppm. $^{13}\text{C-NMR}$ (151 MHz, CDCl_3): $\delta = 149.4$ (C-3), 138.8 (C-7), 137.4 (C-6), 134.6 (C 10), 131.6 (C 5), 131.0 (C 8/9), 128.5 (C 11), 126.7 (C 8/9), 123.4 (C 4), 34.5 (C 2), 31.5 (C 1) ppm. IR (neat, ATR): $\tilde{\nu} = 3084$ (bs), 2956 (w), 2900 (w), 1901 (w), 1763 (w), 1568 (m), 1511 (m), 1456 (m), 1420 (m), 1396 (m), 1360 (m), 1289 (m), 1268 (m), 1202 (m), 1169 (m), 1108 (s), 1072 (m), 1023 (s), 998 (m), 936 (m), 883 (m), 857 (m), 829 (s), 793 (w), 749 (w), 729 (w), 701 (w), 630 (w) cm^{-1} . UV/VIS (CH_2Cl_2): λ_{max} ($\log \epsilon$) = 418 (3.69), 381 (4.48), 365 (4.39), 305 (4.77), 262 (4.64) nm. HRMS (MALDI-TOF+, DCTB): [M] $^+$: m/z calcd. for $\text{C}_{56}\text{H}_{54}\text{Cl}_4^+$: 866.298 , found: 866.299 . Anal. calcd. for $\text{C}_{56}\text{H}_{54}\text{Cl}_4$: C 77.41 , H 6.26 , found: C 77.08 , H 6.43 .

The analytical data is in accordance to the data published before.^[S15]

2,7,11,16-Tetra-*tert*-butyltetraindeno[1,2,3-cd:1',2',3'-fg:1'',2'',3''-jk:1'',2'',3''-mn]pyrene **2**



Tetrachloropyrene **3** (86.7 mg, 100 μmol) and $\text{PdCl}_2(\text{PCy}_3)_2$ (30.0 mg, 40.6 μmol , 40.6 mol%) were dissolved in dry *N,N*-dimethylacetamide (1 mL) under argon atmosphere. To the solution DBU (0.24 mL, 1.61 mmol, 16.1 equiv.) was added dropwise. The reaction mixture was stirred for 48 h at 200°C . After cooling the mixture to room temperature, the solution was diluted with CH_2Cl_2 (100 mL) and washed with water (2×100 mL) and brine (2×100 mL), dried over MgSO_4 and the solvent was removed under reduced pressure. The crude product was purified by column chromatography (SiO_2 , $\text{CH}_2\text{Cl}_2/\text{PE}$ 1:15, $R_f = 0.86$, 0.84 (**8**), 0.28 (**2**), 0.00 detected

with $\text{CH}_2\text{Cl}_2/\text{PE}$ 2:1) to give as first fraction 14.5 mg (20%) of triindenopyrene **8** as red solid. M.p. >400 °C. $^1\text{H-NMR}$ (600 MHz, CDCl_3): δ = 8.18 (s, 1H, H-31), 8.01 (d, J = 8.0 Hz, 1H, H-23), 7.94 (d, J = 1.7 Hz, 1H, H-28), 7.92 (d, J = 7.9 Hz, 1H, H-18), 7.86 (d, J = 1.6 Hz, 1H, H-34), 7.79 (d, J = 7.9 Hz, 1H, H-9), 7.74 (d, J = 7.9 Hz, 1H, H-10), 7.70 (d, J = 1.7 Hz, 1H, H-13), 7.63 (d, J = 8.2 Hz, 2H, H-4), 7.59 (d, J = 8.1 Hz, 2H, H-5), 7.40 (dd, J = 7.9, 1.8 Hz, 1H, H-24), 7.31 (dd, J = 7.9, 1.7 Hz, 1H, H-17), 7.07 (dd, J = 8.0, 1.8 Hz, 1H, H-38), 7.00 (d, J = 8.0 Hz, 1H, H-39), 1.52 (s, 9H, H-27), 1.51 (s, 9H, H-1), 1.45 (s, 9H, H-16), 1.42 (s, 9H, H-37) ppm. $^{13}\text{C-NMR}$ (151 MHz, CDCl_3): δ = 152.3 (C-25), 152.3 (C-14), 151.4 (C-3), 151.1 (C-37), 144.5 (Cq), 143.4 (Cq), 143.4 (Cq), 138.6 (Cq), 138.7 (Cq), 138.4 (Cq), 137.3 (Cq), 137.2 (Cq), 136.6 (Cq), 136.4 (Cq), 135.5 (Cq), 134.8 (Cq), 134.4 (Cq), 133.4 (Cq), 133.1 (Cq), 132.9 (Cq), 132.4 (Cq), 131.9 (Cq), 130.2 (C-5), 128.8 (C-10), 126.3 (C-23), 126.0 (C-18), 125.4 (C-4), 125.2 (C-17), 124.3 (C-39), 124.1 (C-24), 124.1 (C-38), 120.7 (Cq), 120.1 (C-9), 119.9 (Cq), 119.3 (C-28), 119.2 (C-34), 117.7, 112.8 (C-31), 35.1 (Cq-^tBu), 35.2 (Cq-^tBu), 35.1 (Cq-^tBu), 35.0 (Cq-^tBu), 31.7 (C-1), 31.6 (C-27), 31.6 (C-37), 31.5 (C-16) ppm. IR (neat, ATR): $\tilde{\nu}$ = 2955 (s), 2900 (m), 2862 (m), 1608 (m), 1461 (m), 1441 (m), 1388 (m), 1359 (m), 1319 (w), 1298 (w), 1273 (w), 1251 (m), 1199 (w), 1161 (vw), 1109 (w), 1093 (w), 1022 (w), 997 (w), 869 (s), 842 (m), 817 (vs), 646 (s) cm^{-1} . HRMS (MALDI-TOF+, DCTB): [M]⁺: m/z calcd. for $\text{C}_{56}\text{H}_{52}^+$: 724.407 found: 724.484.

Second fraction gave tetraindenopyrene **2** (21.3 mg, 29%) as dark red solid. M.p. >400 °C. $^1\text{H-NMR}$ (400 MHz, CD_2Cl_2): δ = 7.49 (d, J = 1.6 Hz, 4H, H-4), 7.34 (d, J = 8.0 Hz, 4H, H-12), 7.20 (dd, J = 7.9, 1.8 Hz, 4H, H-13), 7.09 (s, 2H, H-7), 1.55 (s, 36H, H-1) ppm. $^{13}\text{C-NMR}$ (101 MHz, CD_2Cl_2): δ = 151.9 (C-3), 144.1 (C-5/6/9), 139.3 (C-5/6/9), 138.2 (C-11), 136.8 (C-5/6/9), 133.1 (C-10), 126.5 (C-12), 124.6 (C-13), 119.5 (C-4), 113.2 (C-7), 35.4 (C-2), 31.7 (C-1) ppm. Note: The signal of C-8 was not resolved. IR (neat, ATR): $\tilde{\nu}$ = 2955 (s), 2904 (m), 2866 (w), 1608 (m), 1561 (w), 1505 (w), 1473 (m), 1458 (m), 1435 (s), 1390 (m), 1360 (m), 1323 (w), 1286 (m), 1251 (s), 1198 (w), 1095 (m), 1072 (m), 887 (w), 864 (s), 814 (s), 678 (w), 646 (s) cm^{-1} . HRMS (MALDI-TOF+, DCTB): [M]⁺: m/z calcd. for $\text{C}_{56}\text{H}_{50}^+$: 722.391 found: 722.495. UV/Vis (DCM): $\lambda_{\text{max}} (\log \epsilon)$ = 546 (3.94), 466 (4.04), 419 (4.27), 398 (4.18), 362 (4.55), 332 (4.72), 311 (4.90), 298 (4.82), 288 (4.80), 277 (4.86) nm. Anal. calcd. for $\text{C}_{56}\text{H}_{50}$: C 93.03, H 6.97, found: C 92.82, H 6.84.

The analytical data is in accordance to the data published before.^[S16]

3. NMR-Spectra

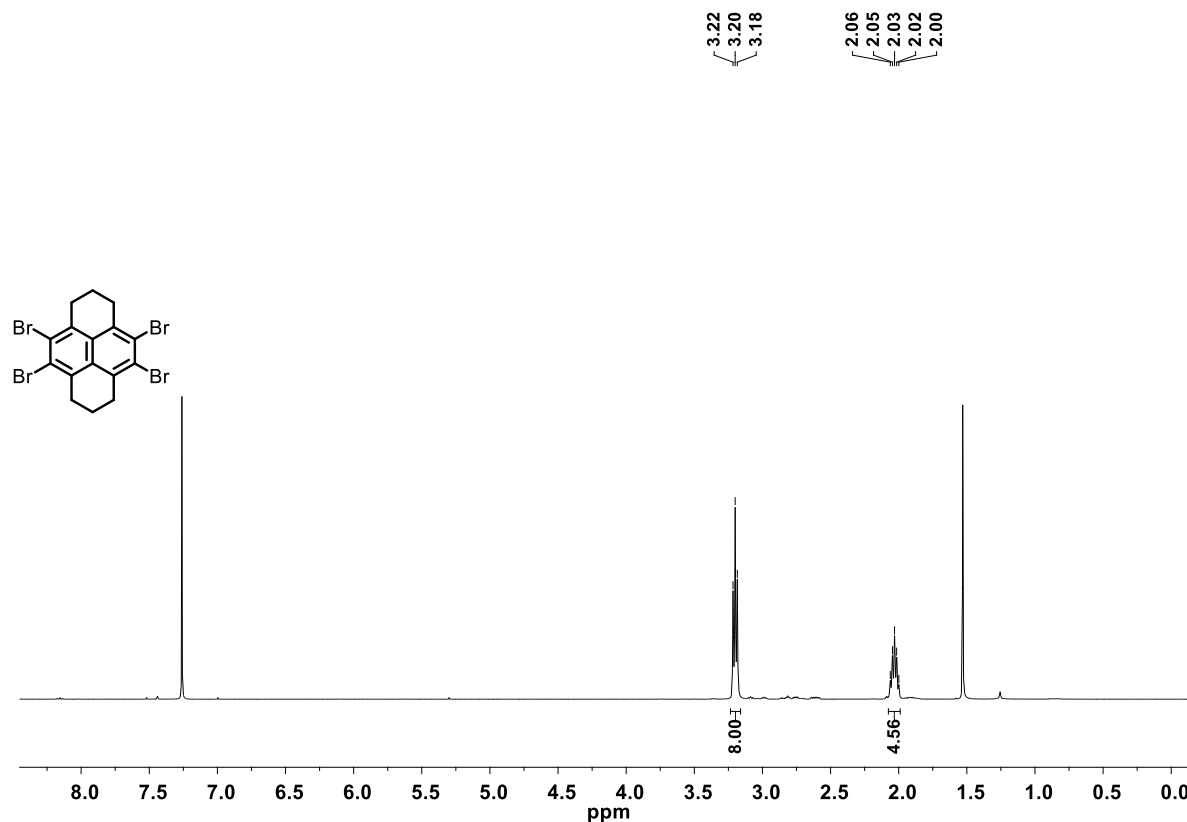


Figure S1: ¹H-NMR spectrum of compound 5 (CDCl_3 , 295 K, 400 MHz).

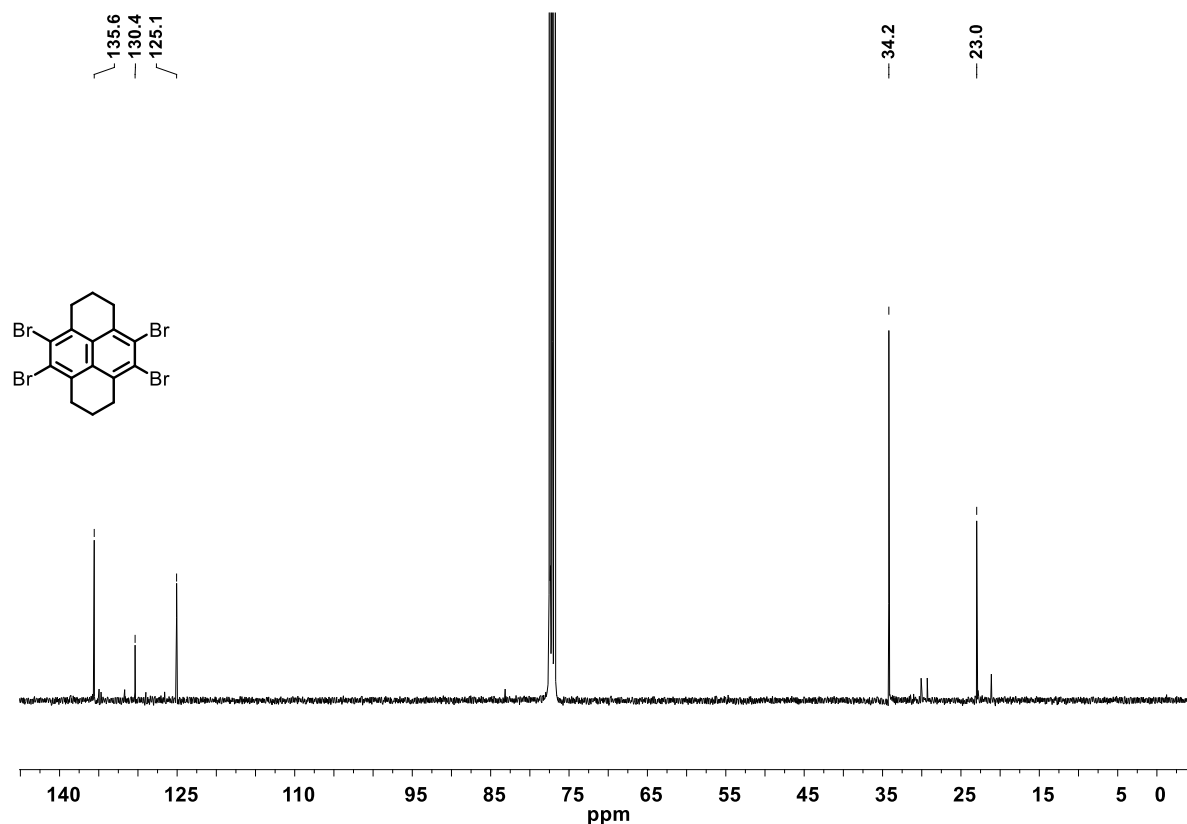


Figure S2: ¹³C-NMR spectrum of compound 5 (CDCl_3 , 295 K, 101 MHz).

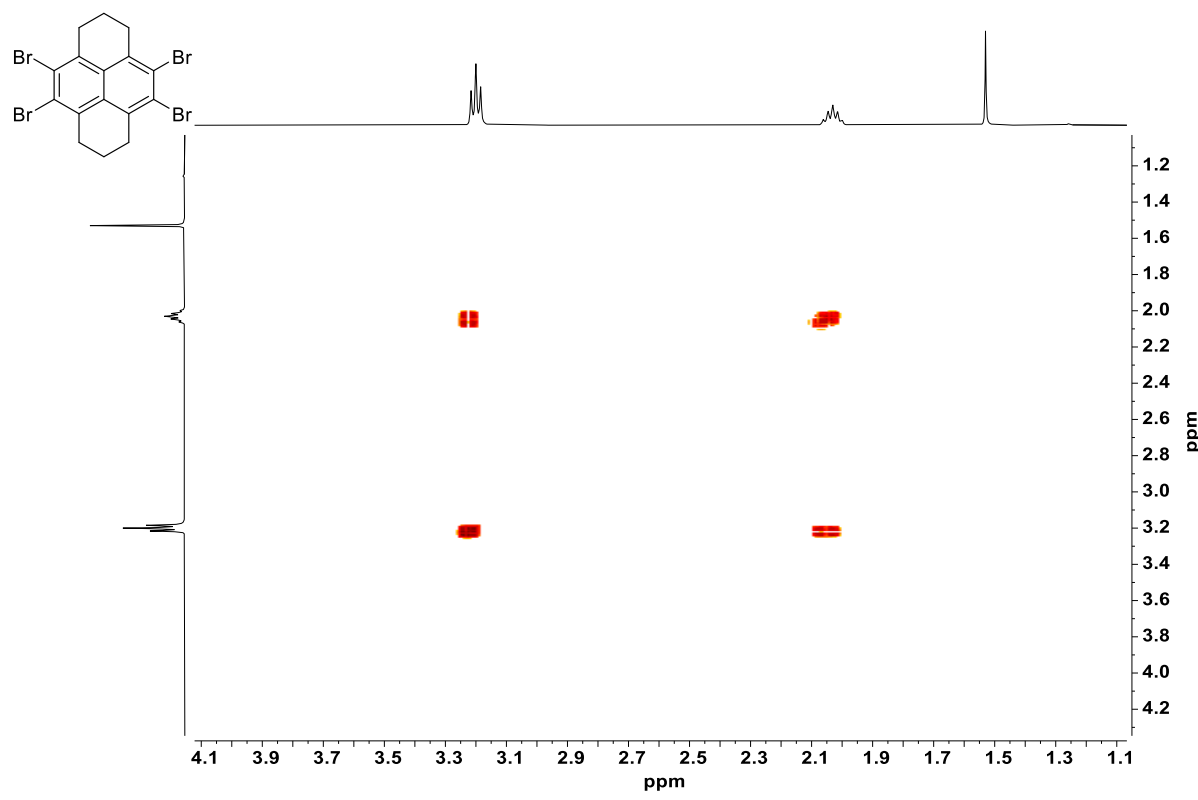


Figure S3: ^1H , ^1H -COSY-NMR spectrum of compound 5 (CDCl_3 , 295 K, 400/400 MHz).

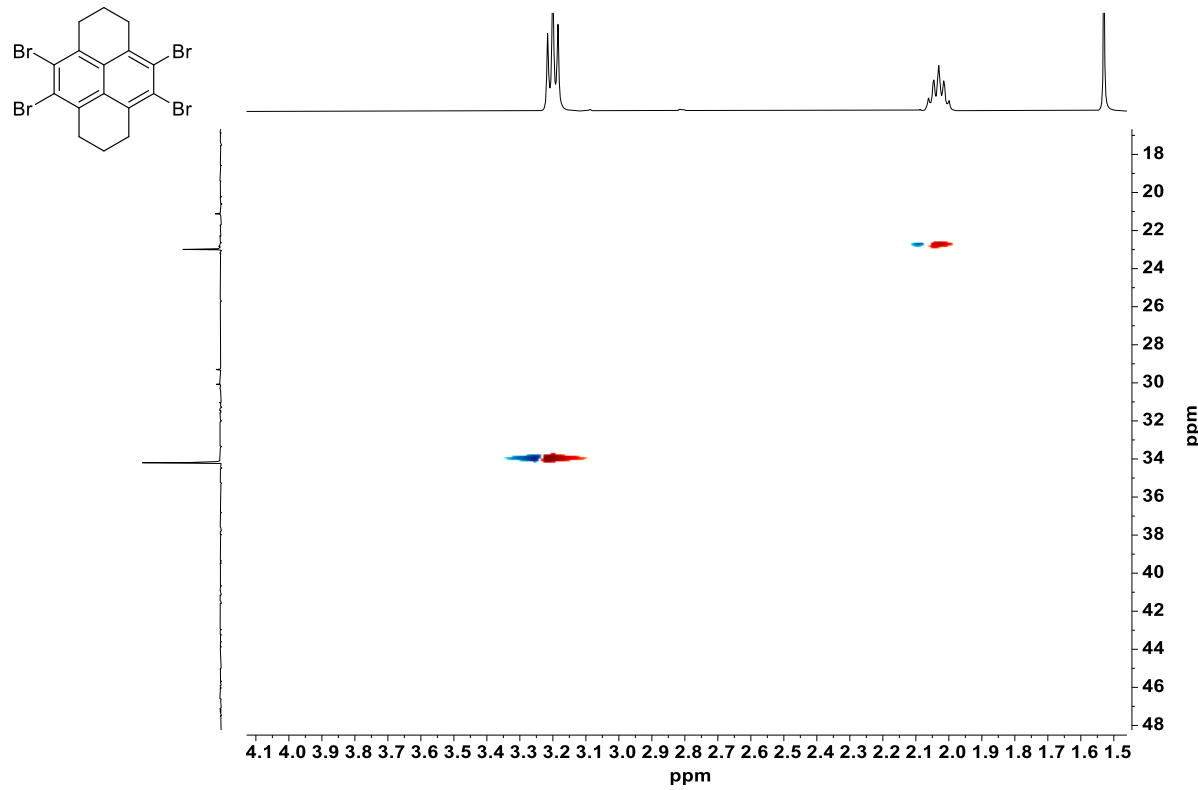


Figure S4: ^1H , ^{13}C -HSQC-NMR spectrum of compound 5 (CDCl_3 , 295 K, 400/100 MHz).

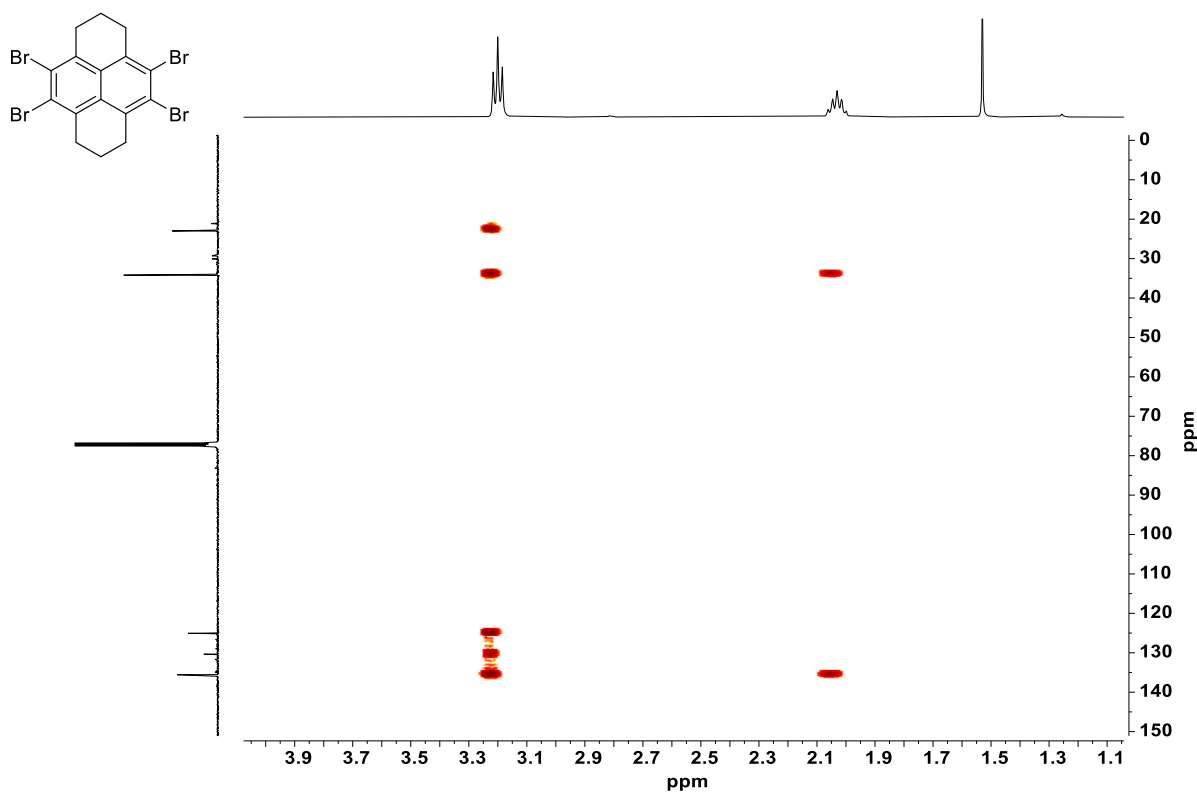


Figure S5: ^1H , ^{13}C -HMBC-NMR spectrum of compound 5 (CDCl_3 , 295 K, 400/100 MHz).

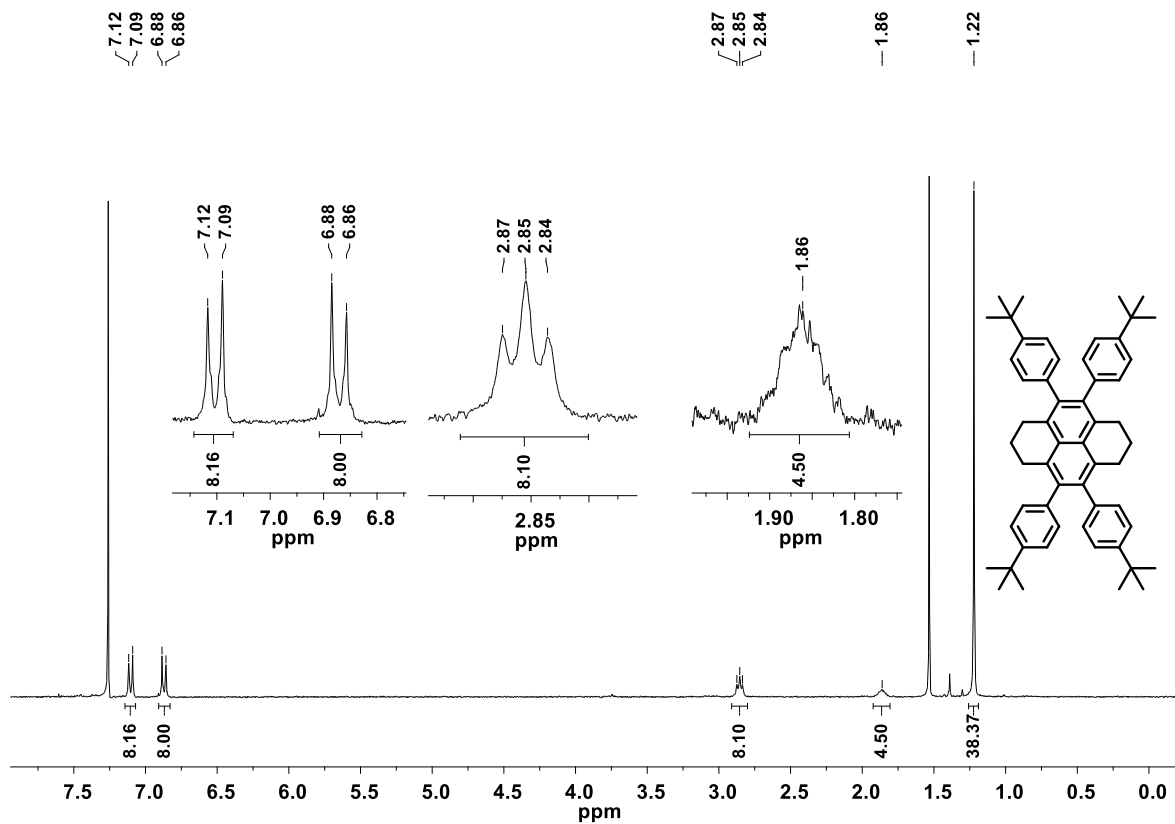


Figure S6: ^1H -NMR spectrum of compound 6 (CDCl_3 , 300 MHz, 300 K).

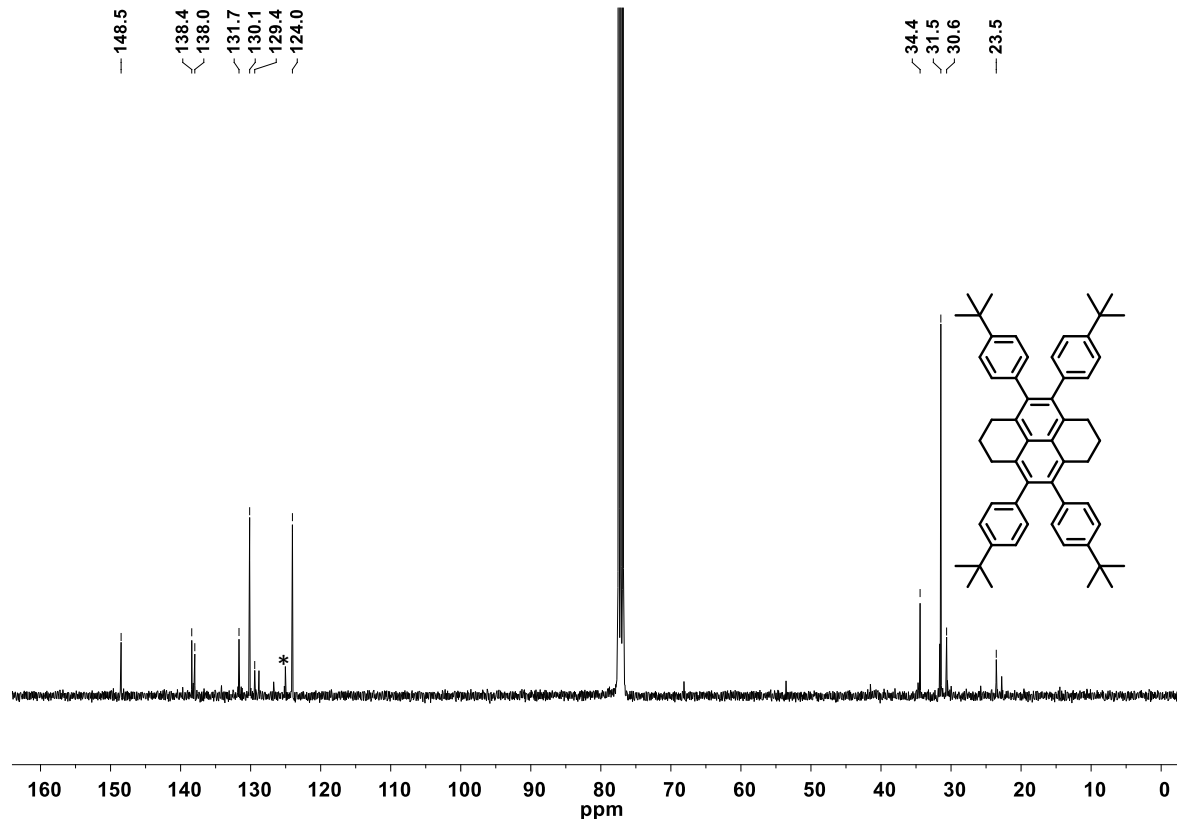


Figure S7: ¹³C-NMR spectrum of compound **6** (CDCl_3 , 100 MHz, 300 K). The *-symbol marks partially oxidized pyrene **7**. Compound **6** oxidized to **7** completely within 7 d in CDCl_3 solution at r.t.

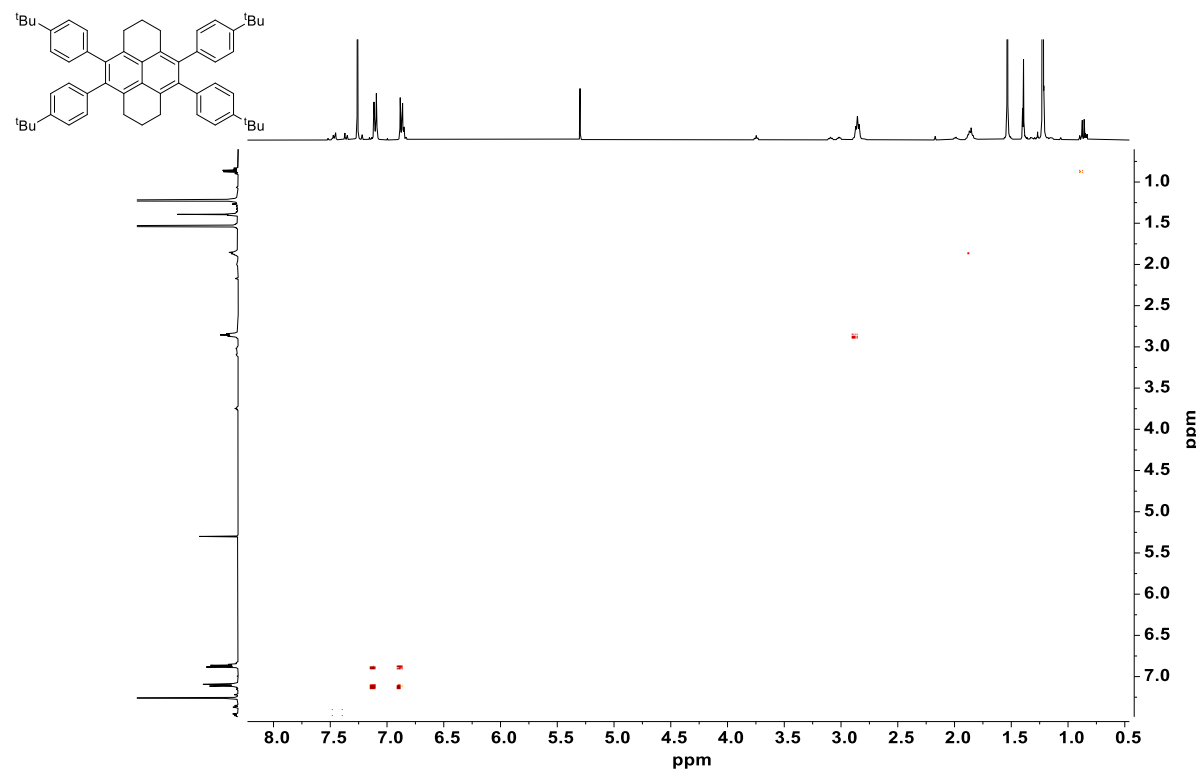


Figure S8: ¹H,¹H-COSY-NMR spectrum of compound **6** (CDCl_3 , 295 K, 400/400 MHz).

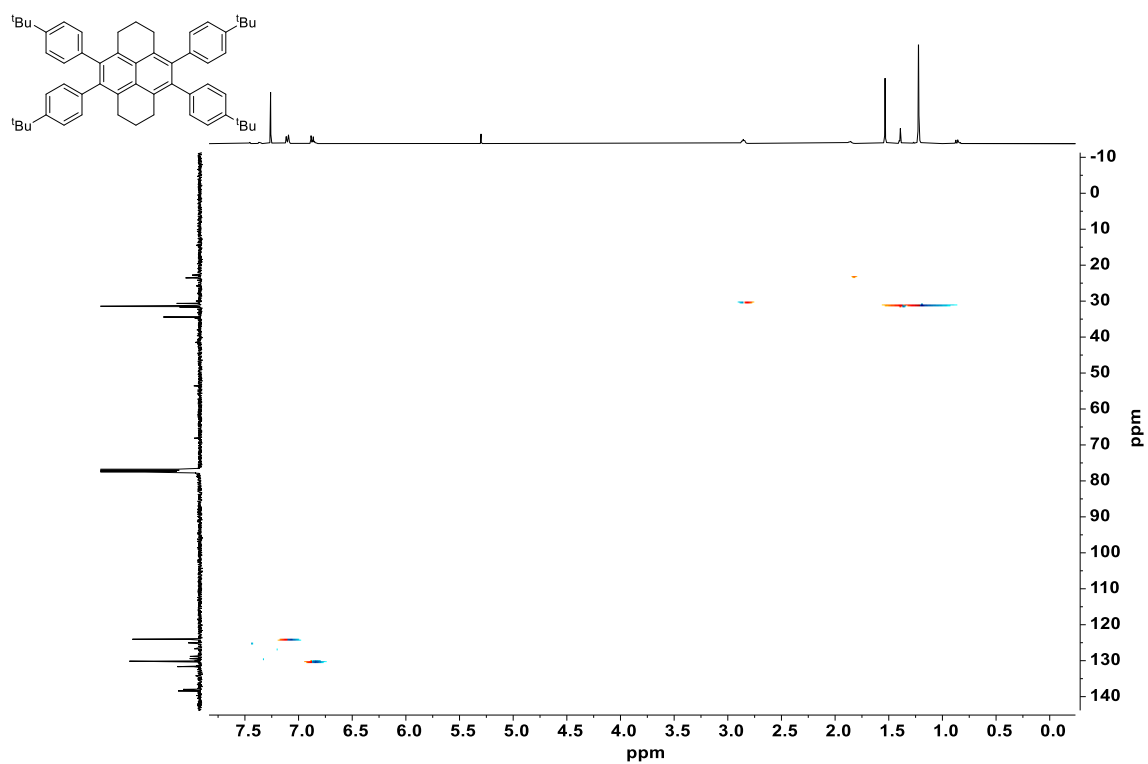


Figure S9: $^1\text{H}, ^{13}\text{C}$ -HSQC-NMR spectrum of compound **6** (CDCl_3 , 295 K, 400/100 MHz).

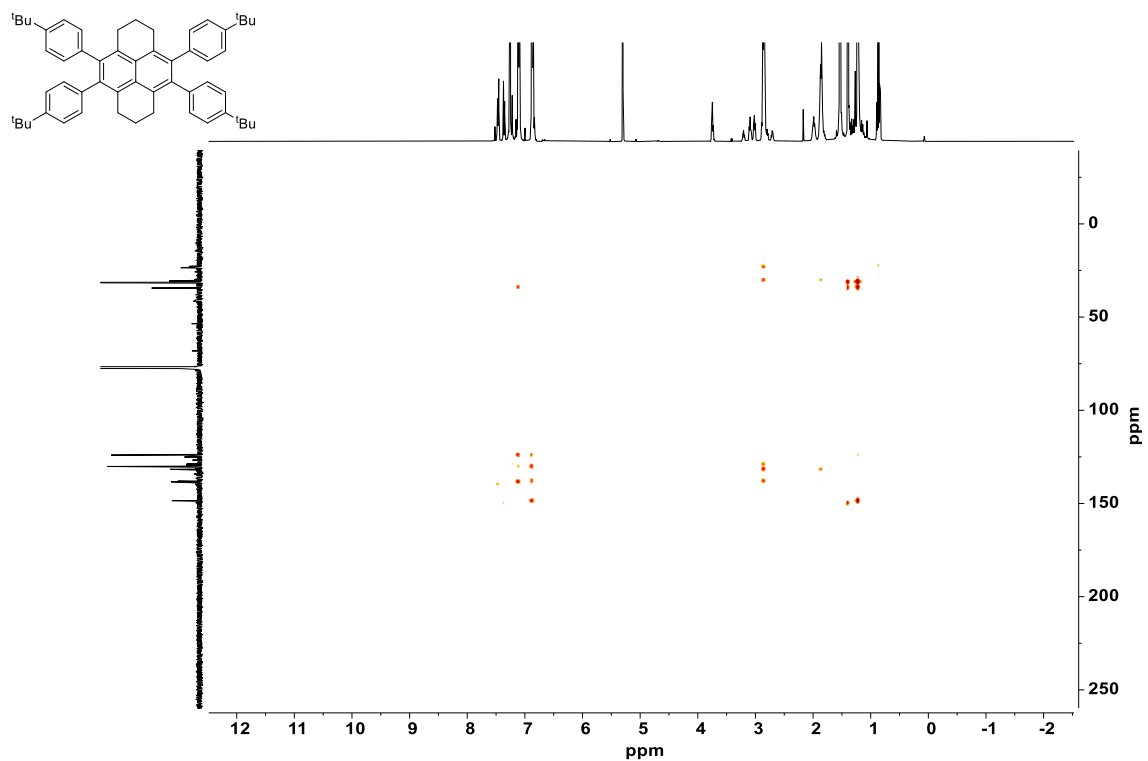


Figure S10: $^1\text{H}, ^{13}\text{C}$ -HMBC-NMR spectrum of compound **6** (CDCl_3 , 295 K, 400/100 MHz).

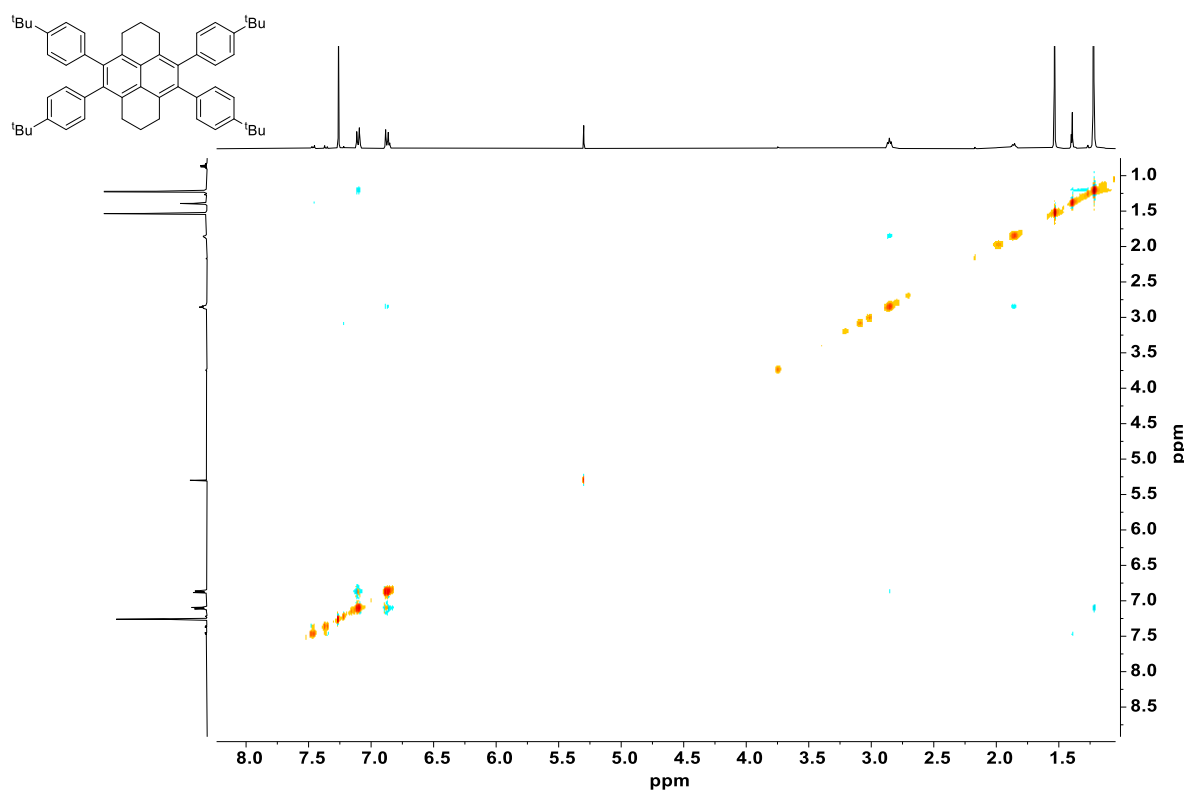


Figure S11: ¹H, ¹H-NOESY-NMR spectrum of compound 6 (CDCl_3 , 295 K, 400/400 MHz).

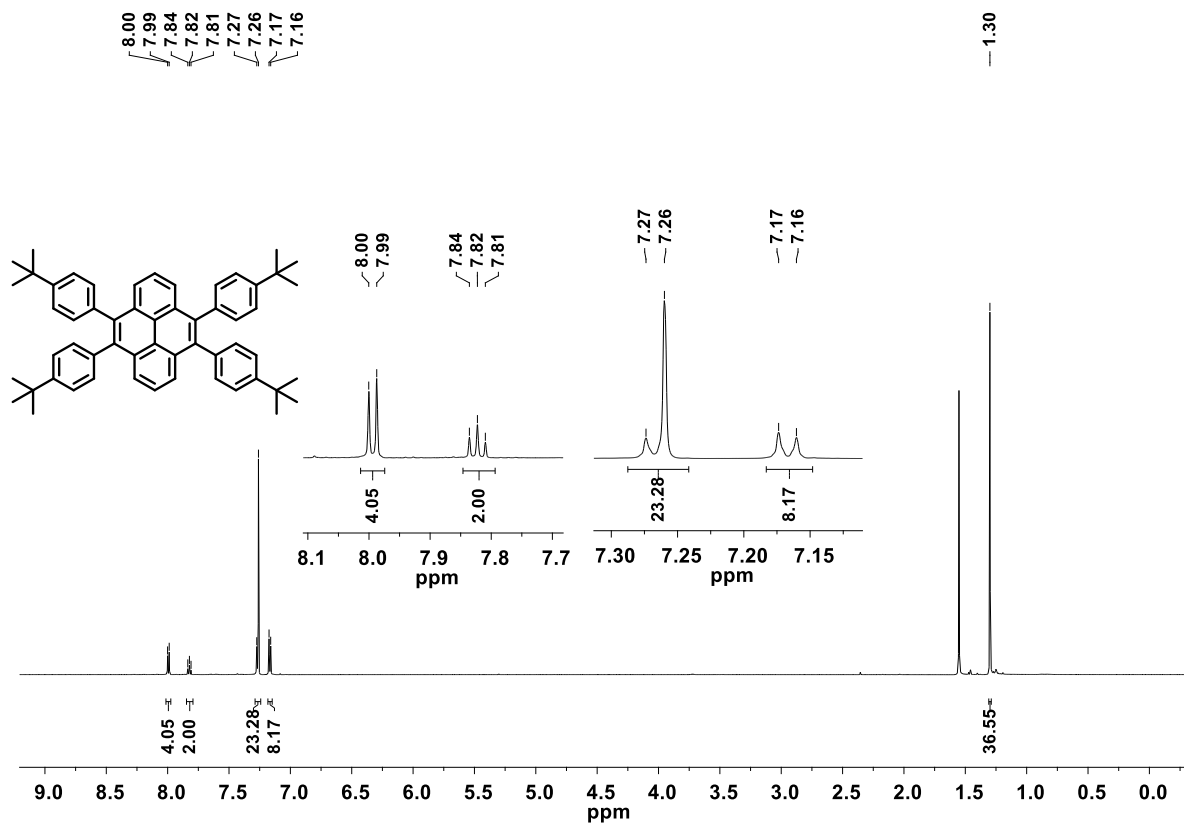


Figure S12: ¹H-NMR spectrum of compound 7 (CDCl_3 , 600 MHz, 295 K).

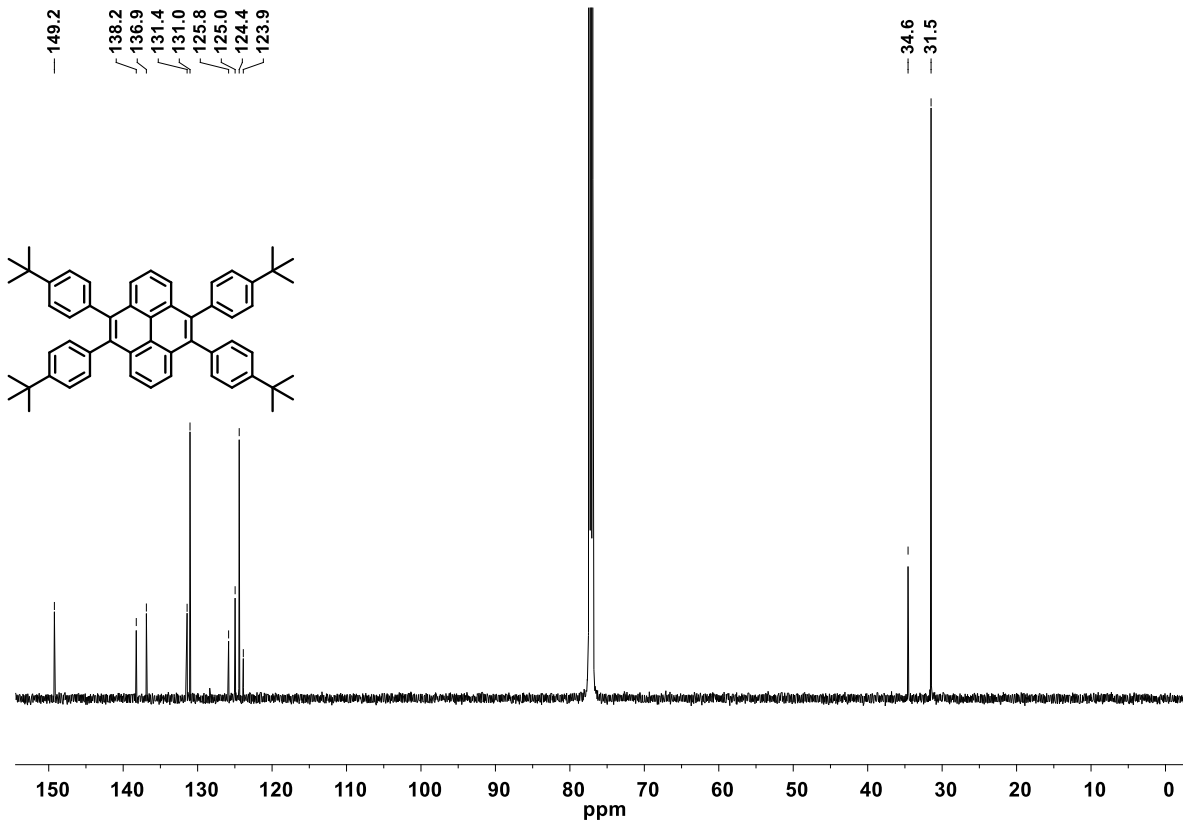


Figure S13: ^{13}C -NMR spectrum of compound 7 (CDCl_3 , 151 MHz, 295 K).

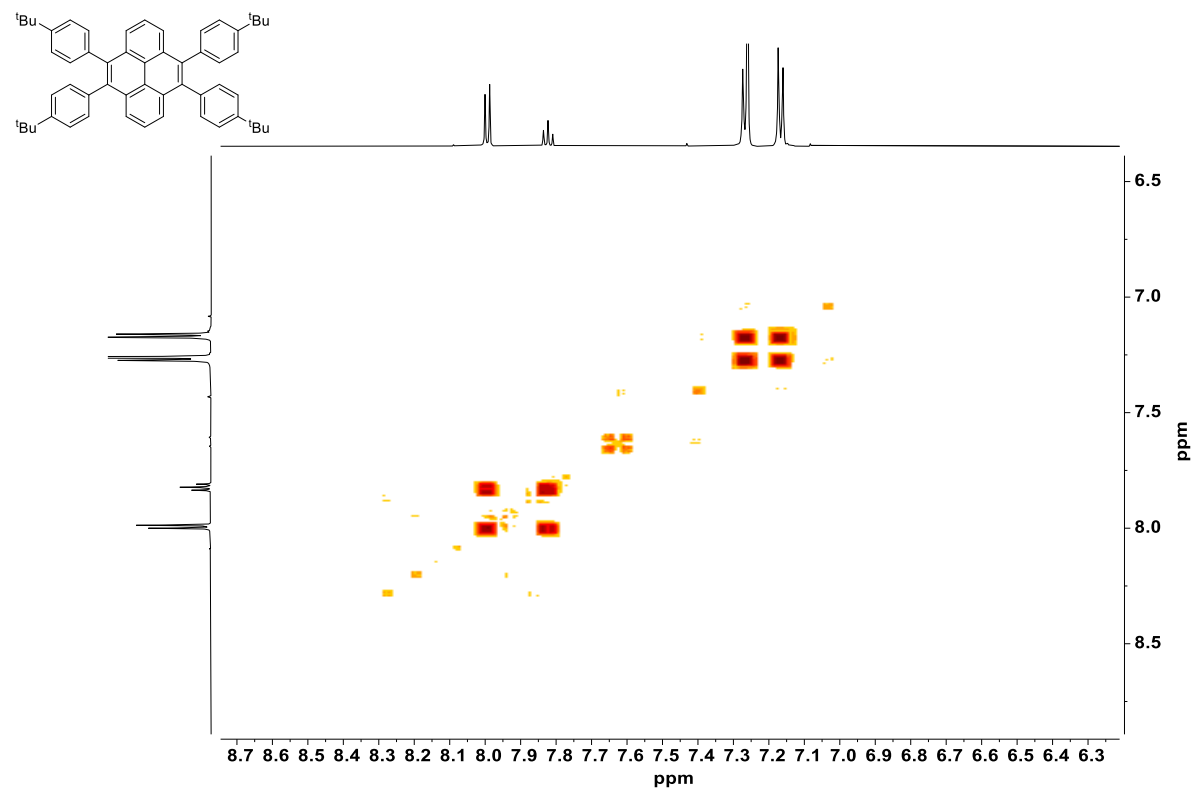


Figure S14: $^1\text{H},^1\text{H}$ -COSY-NMR spectrum of compound 7 (CDCl_3 , 295 K, 600/600 MHz).

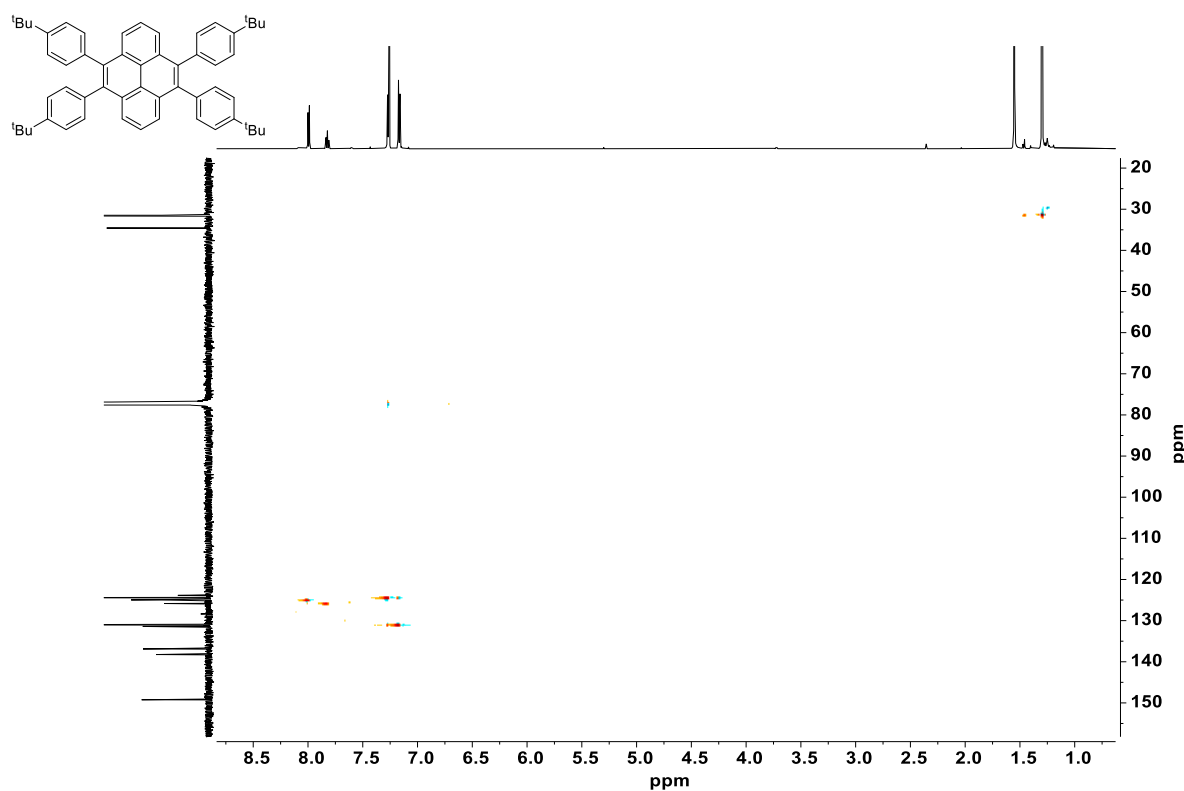


Figure S15: ¹H, ¹³C-HSQC-NMR spectrum of compound 7 (CDCl_3 , 295 K, 600/151 MHz).

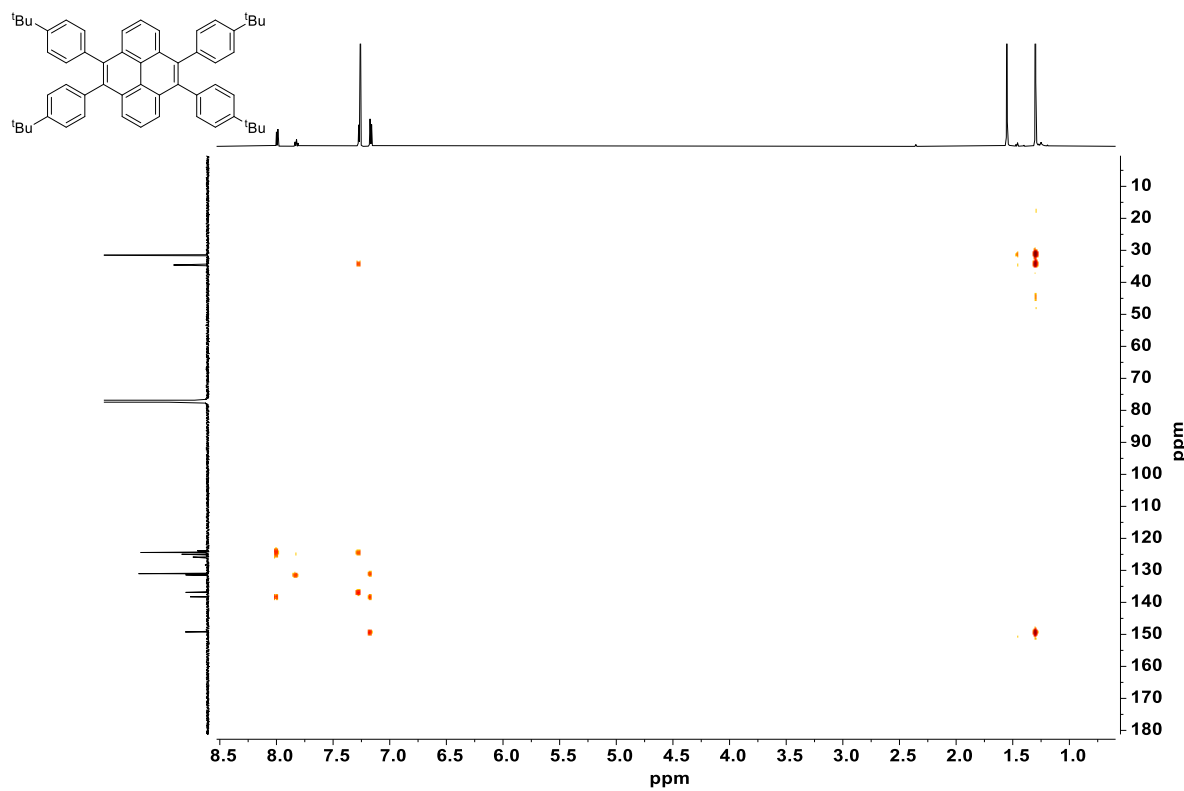


Figure S16: ¹H, ¹³C-HMBC-NMR spectrum of compound 7 (CDCl_3 , 295 K, 600/151 MHz).

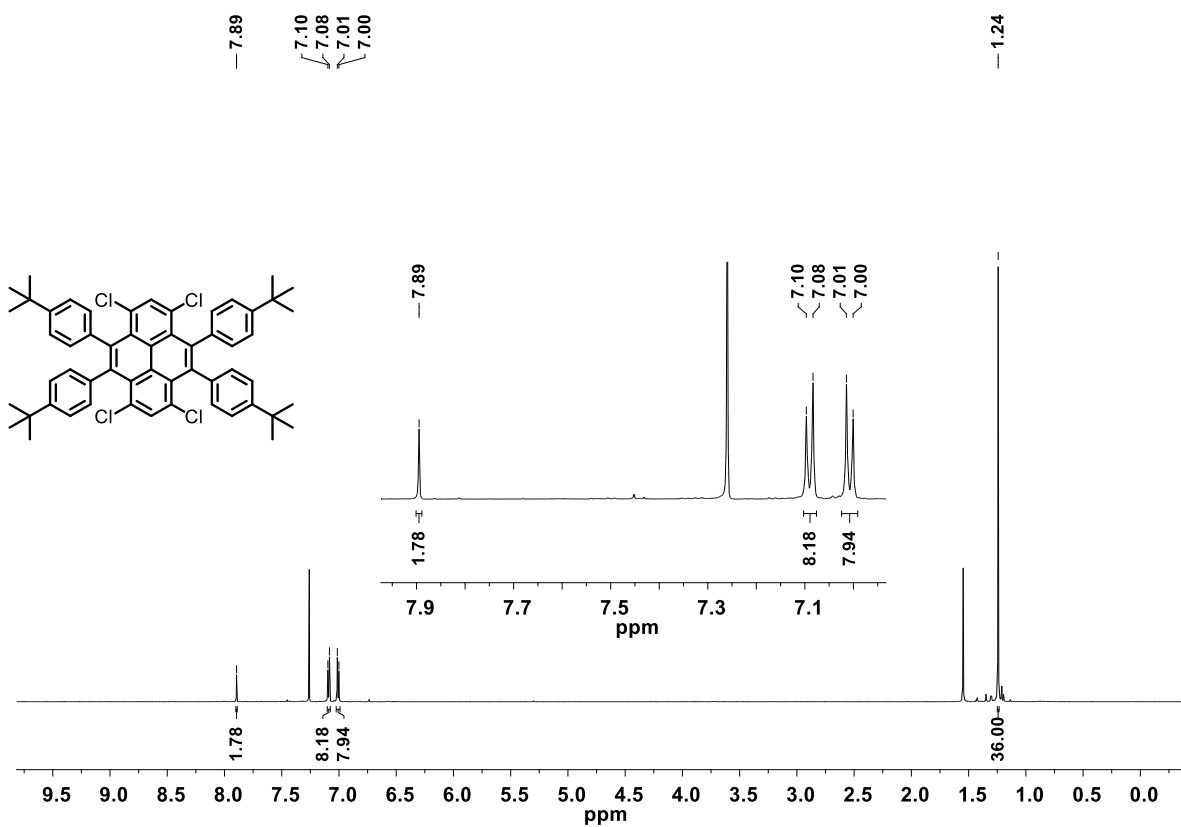


Figure S17: ¹H-NMR spectrum of compound 3 (CDCl₃, 600 MHz, 295 K).

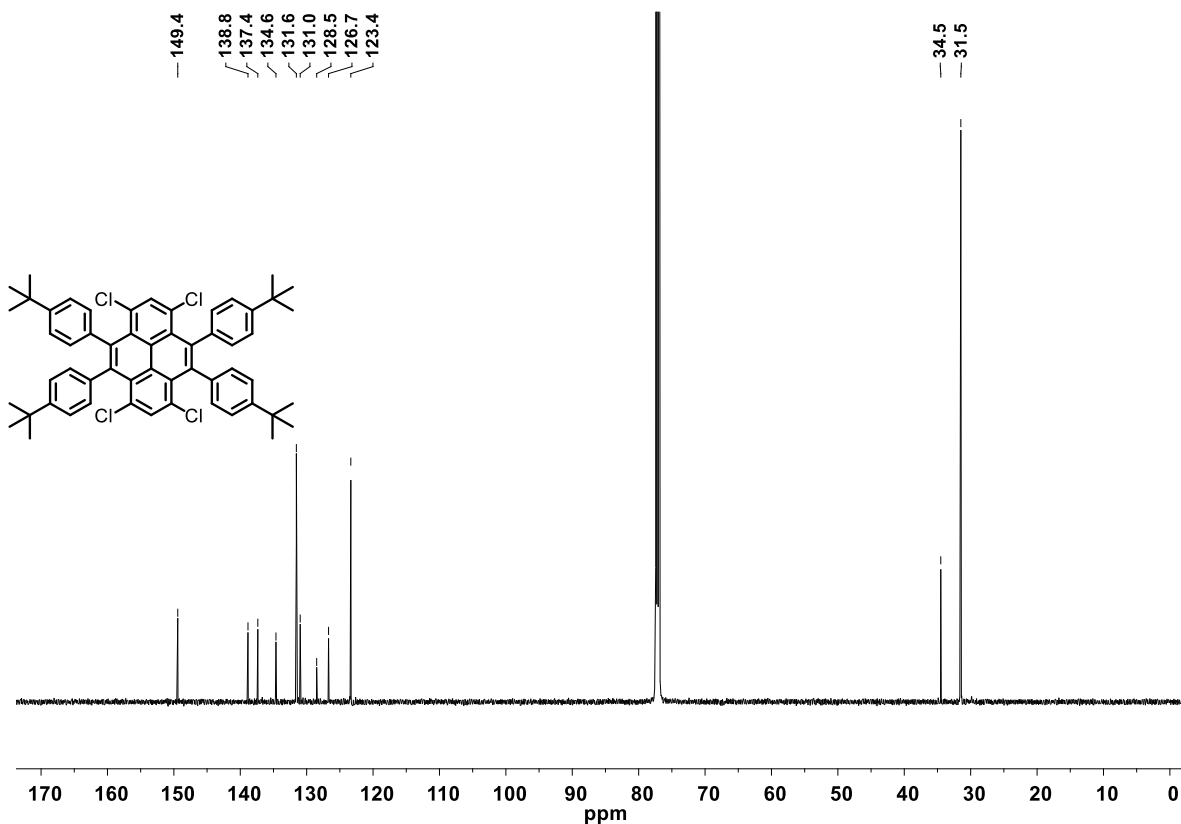


Figure S18: ¹³C-NMR spectrum of compound 3 (CDCl₃, 151 MHz, 295 K).

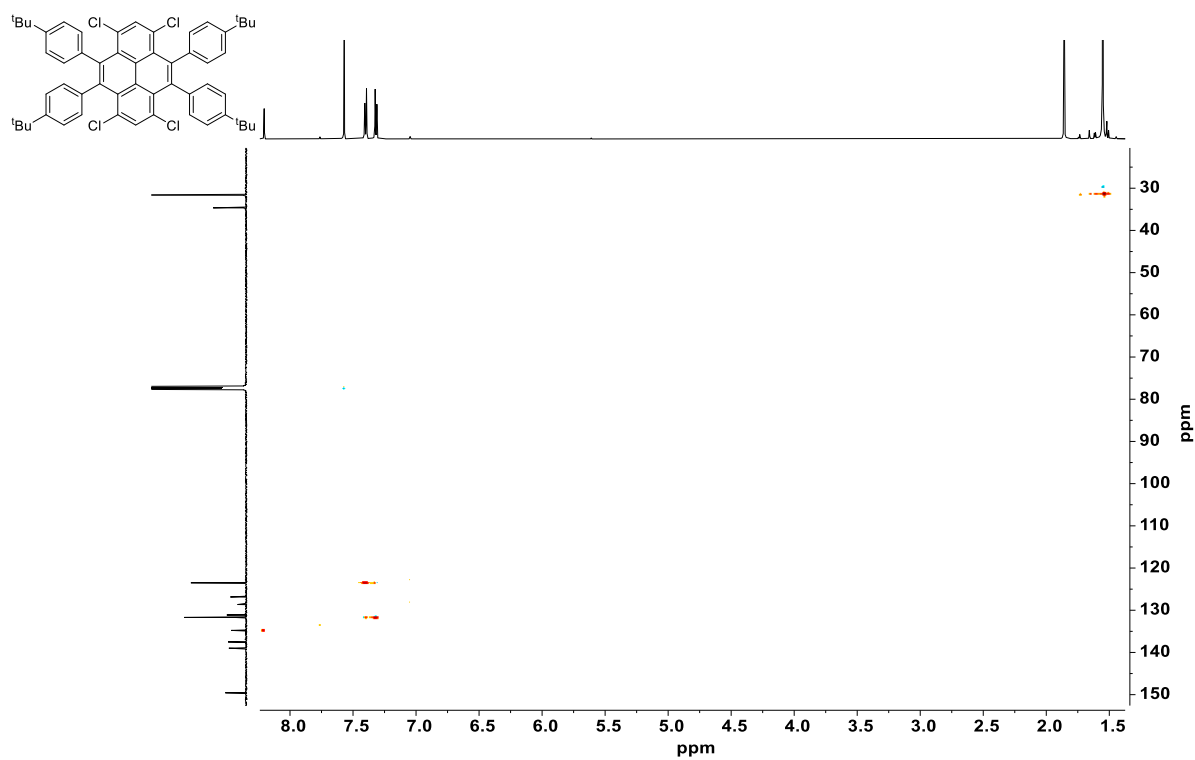


Figure S19: $^1\text{H}, ^{13}\text{C}$ -HSQC-NMR spectrum of compound 3 (CDCl_3 , 295 K, 600/151 MHz).

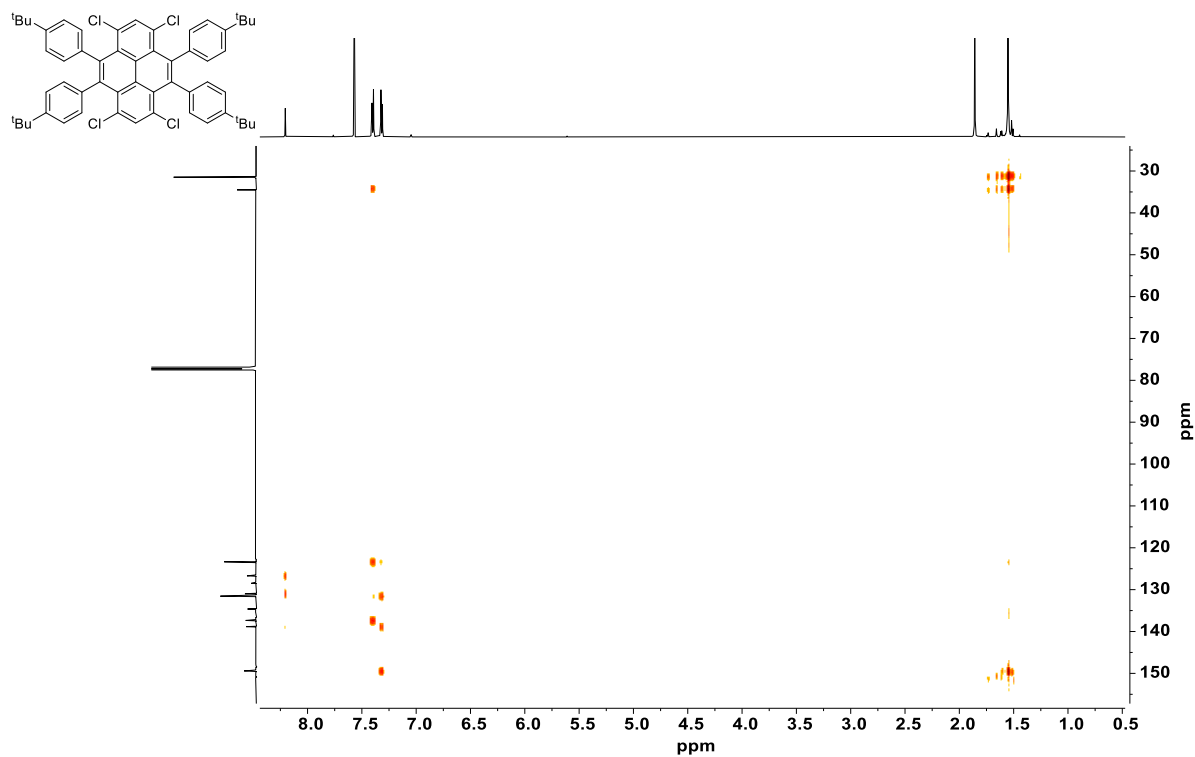


Figure S20: $^1\text{H}, ^{13}\text{C}$ -HMBC-NMR spectrum of compound 3 (CDCl_3 , 295 K, 600/151 MHz).

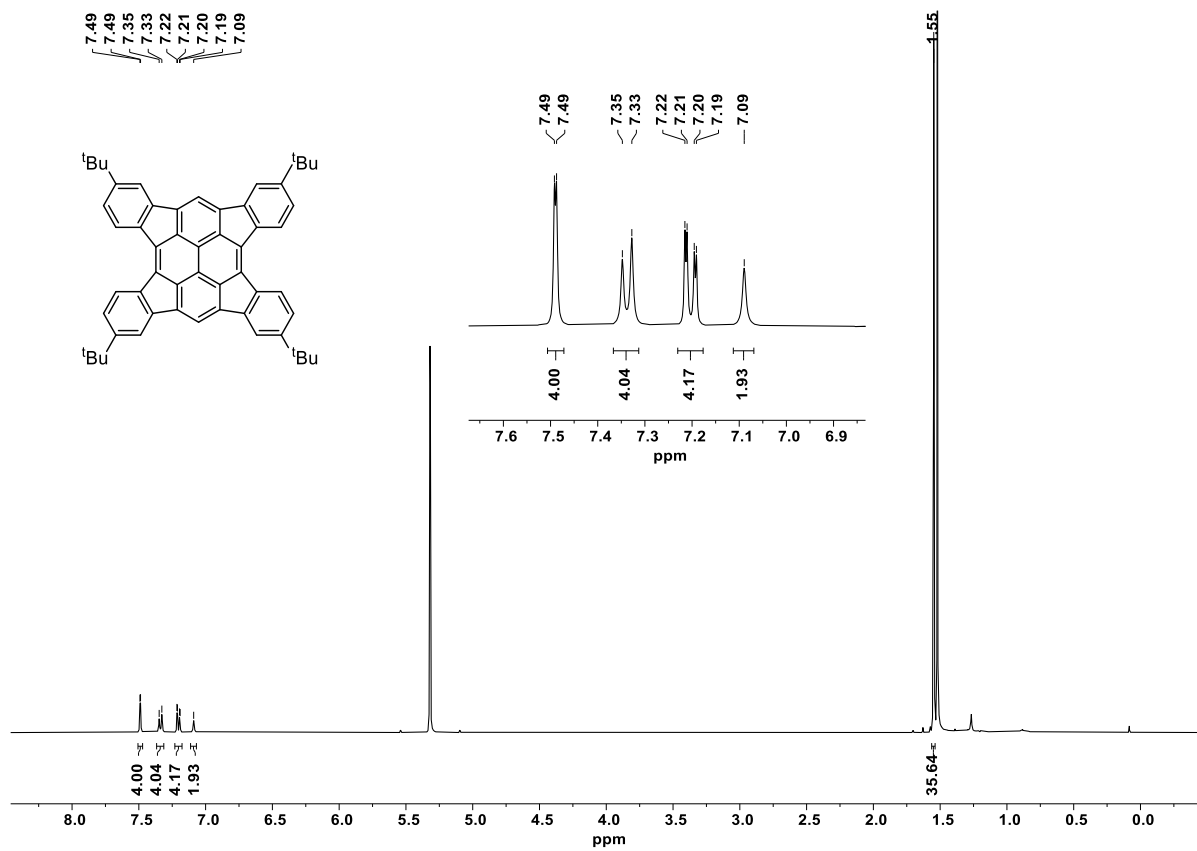


Figure S21: ¹H-NMR spectrum of compound 2 (CD₂Cl₂, 400 MHz, 295 K).

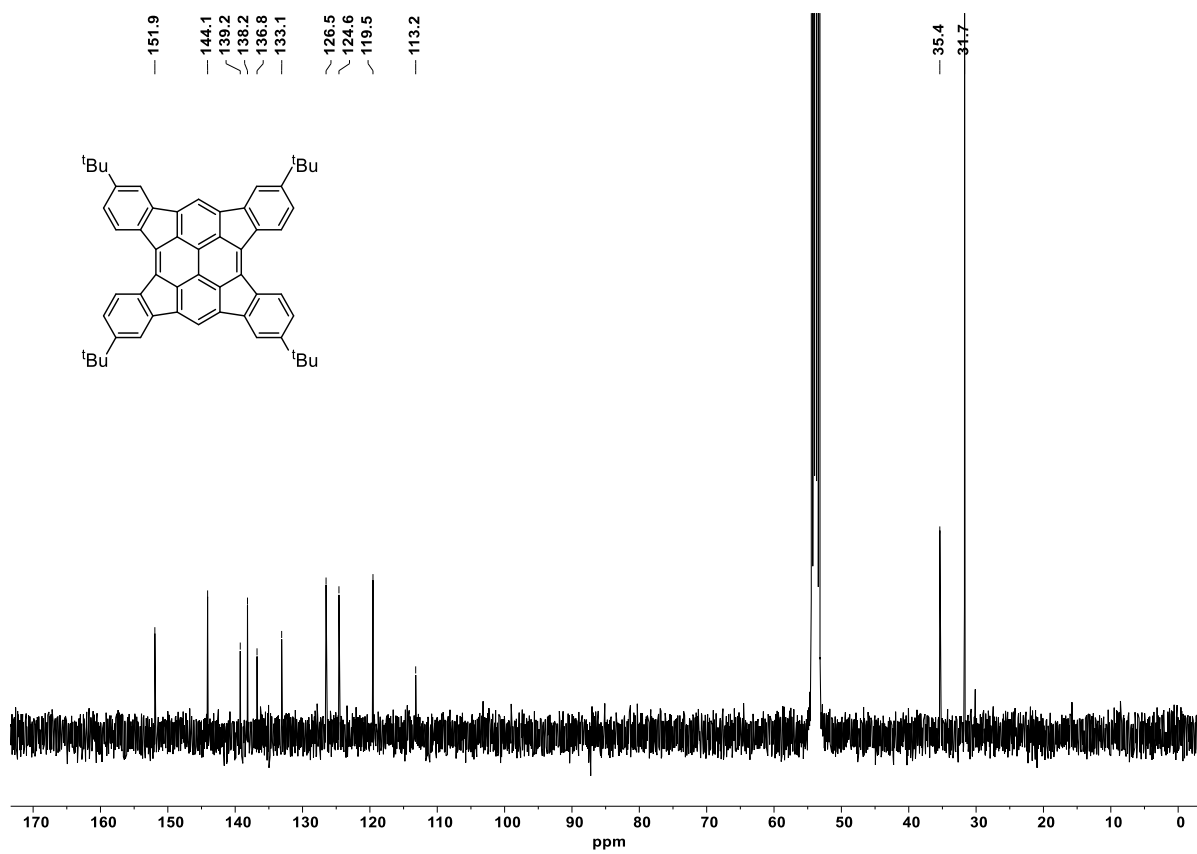


Figure S22: ¹³C-NMR spectrum of compound 2 (CD₂Cl₂, 101 MHz, 295 K).

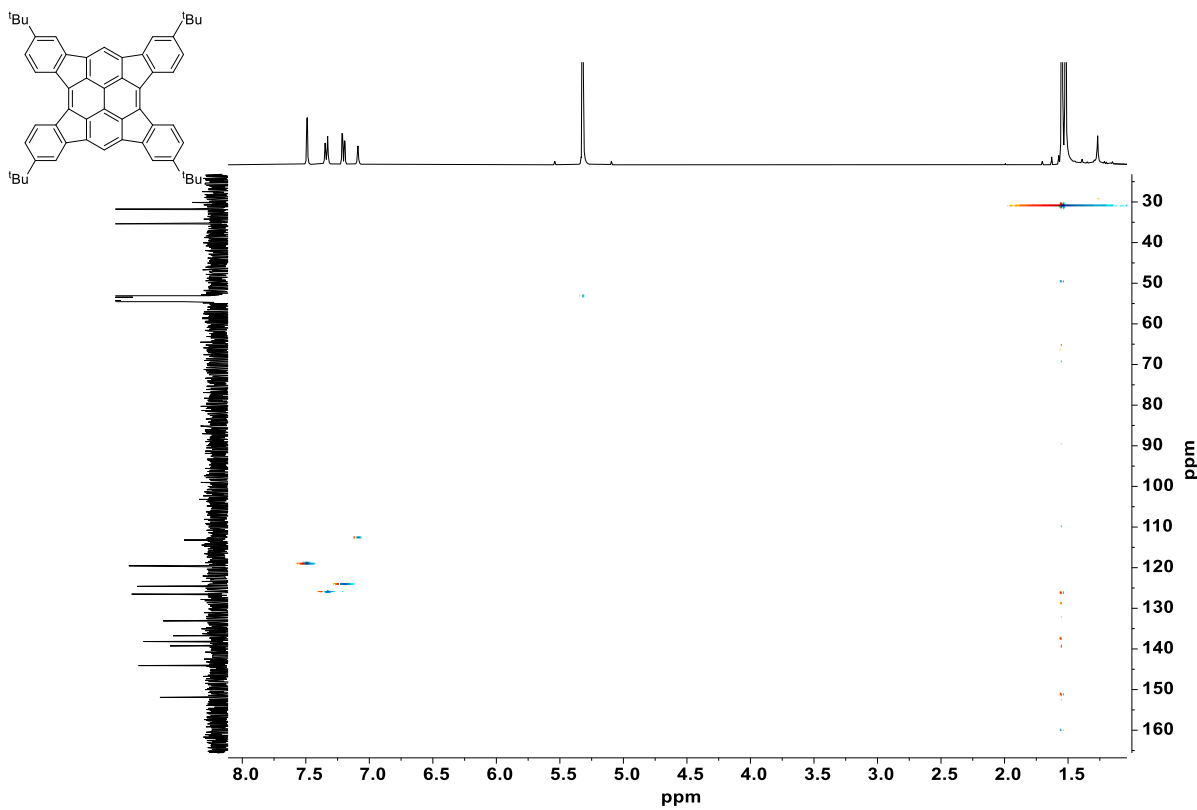


Figure S23: $^1\text{H}, ^{13}\text{C}$ -HSQC-NMR spectrum of compound **2** (CDCl_3 , 295 K, 400/101 MHz).

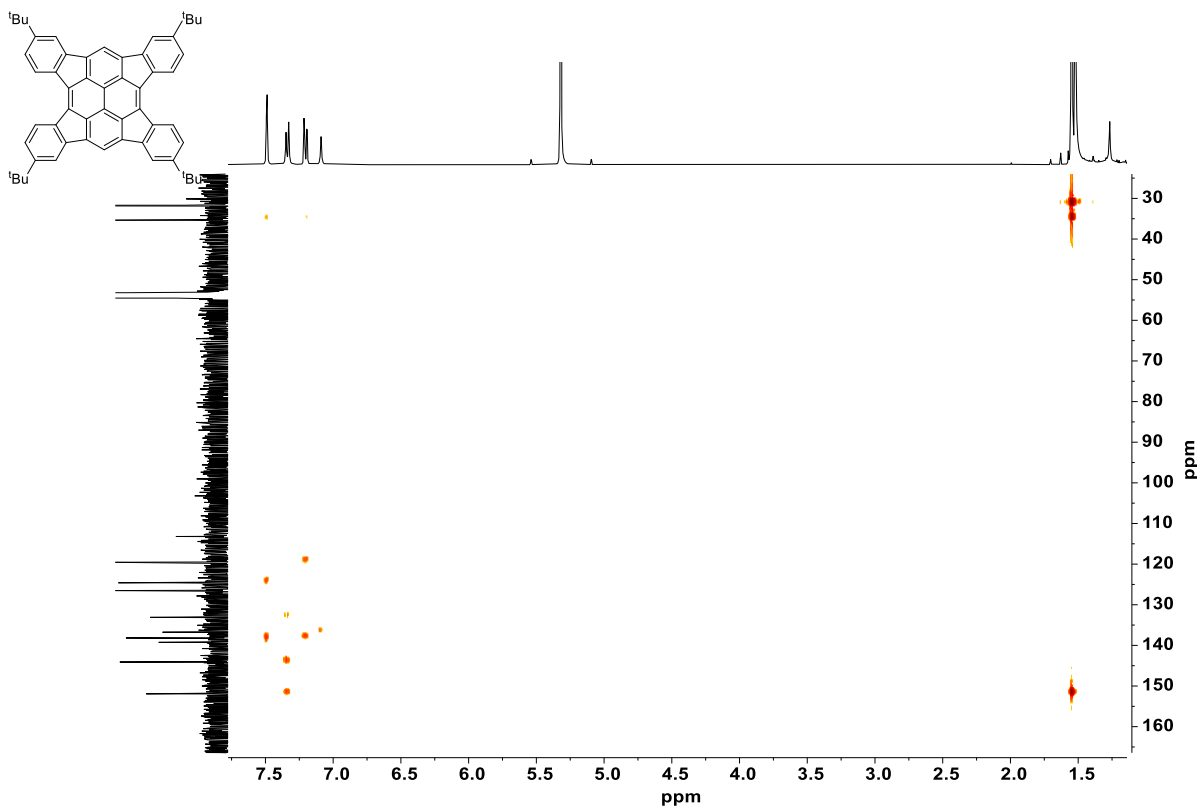


Figure S24: $^1\text{H}, ^{13}\text{C}$ -HMBC-NMR spectrum of compound **2** (CDCl_3 , 295 K, 400/101 MHz).

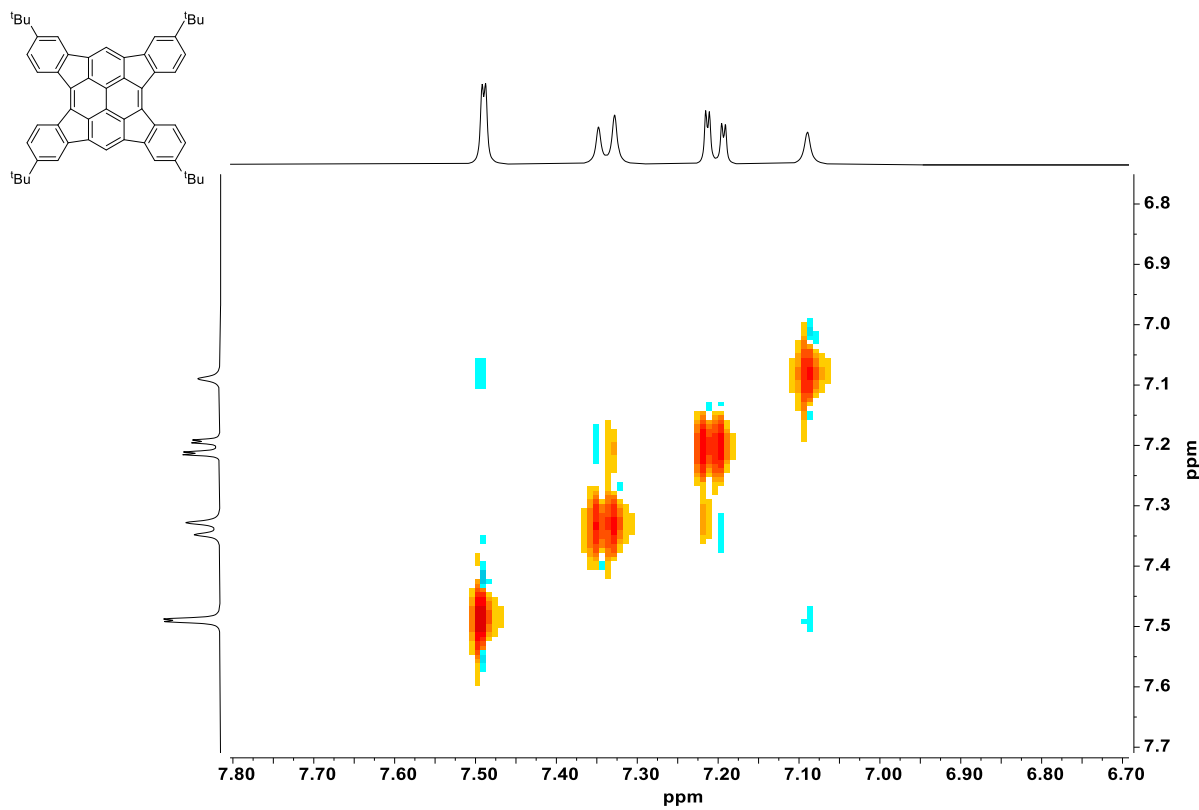


Figure S25: ^1H , ^1H -NOESY-NMR spectrum of compound **2** (CDCl_3 , 295 K, 400/400 MHz).

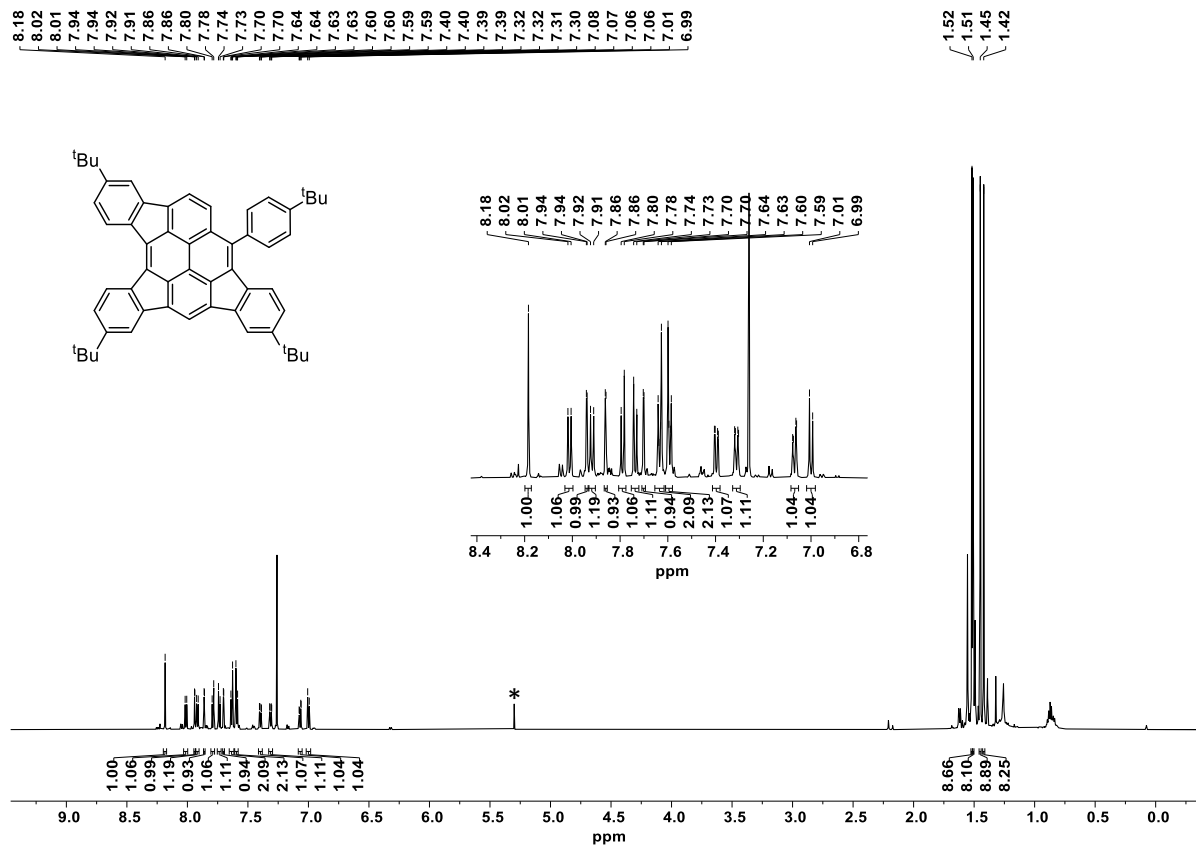


Figure S26: ^1H -NMR spectrum of compound **8** (CDCl_3 , 600 MHz, 295 K). The * marks residual CH_2Cl_2 .

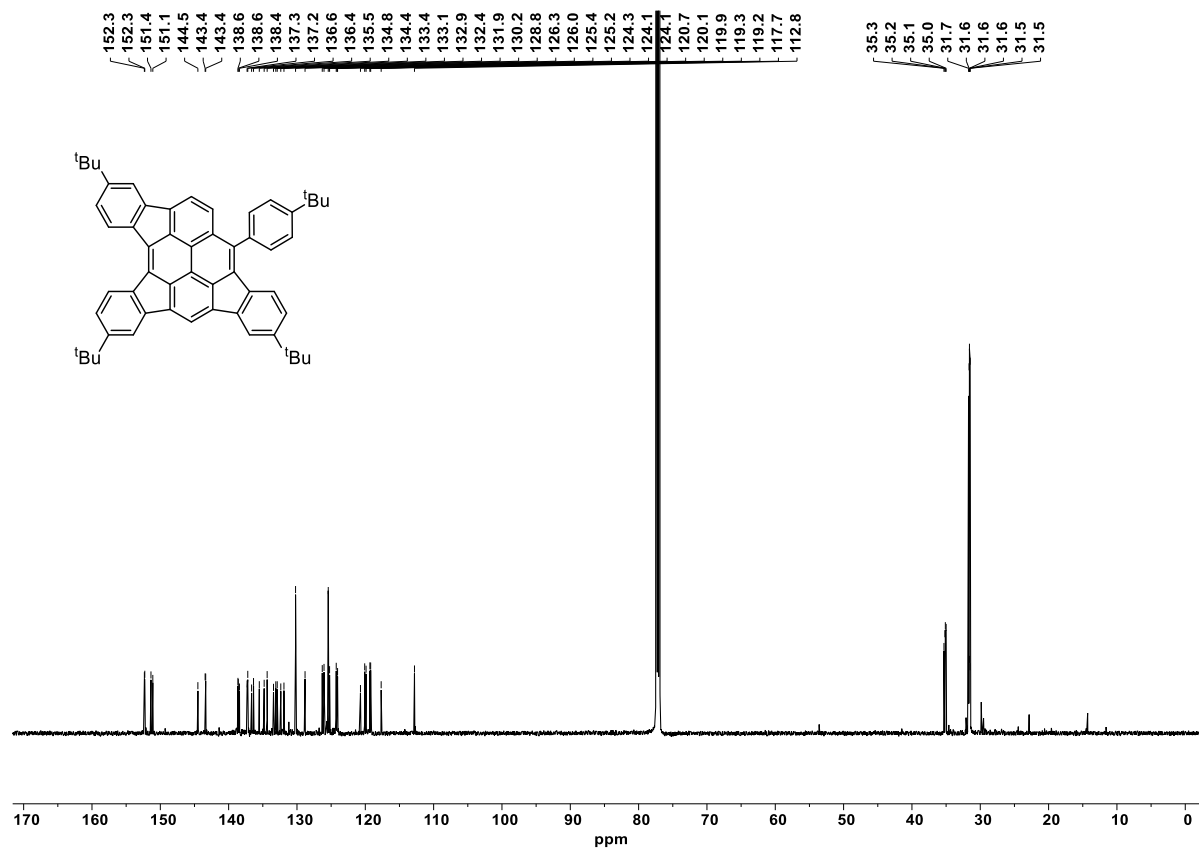


Figure S27: ^{13}C -NMR spectrum of compound 8 (CDCl_3 , 151 MHz, 295 K).

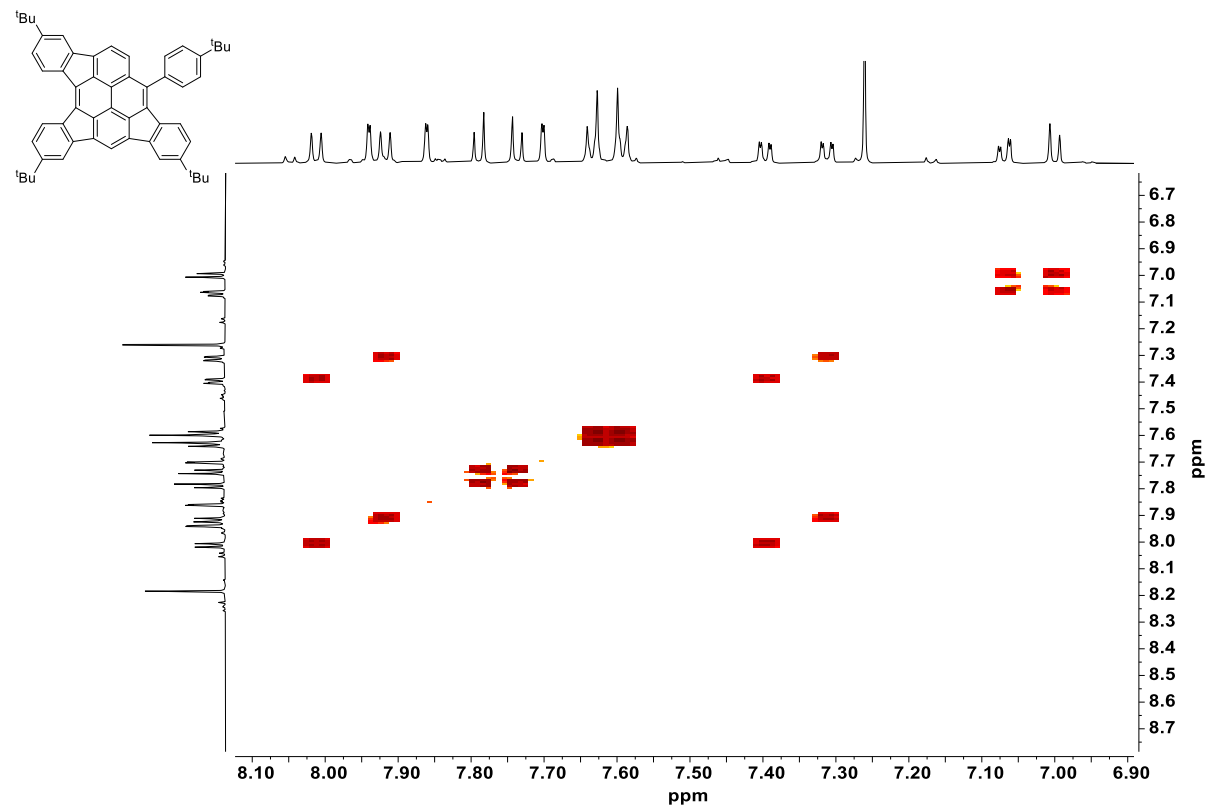
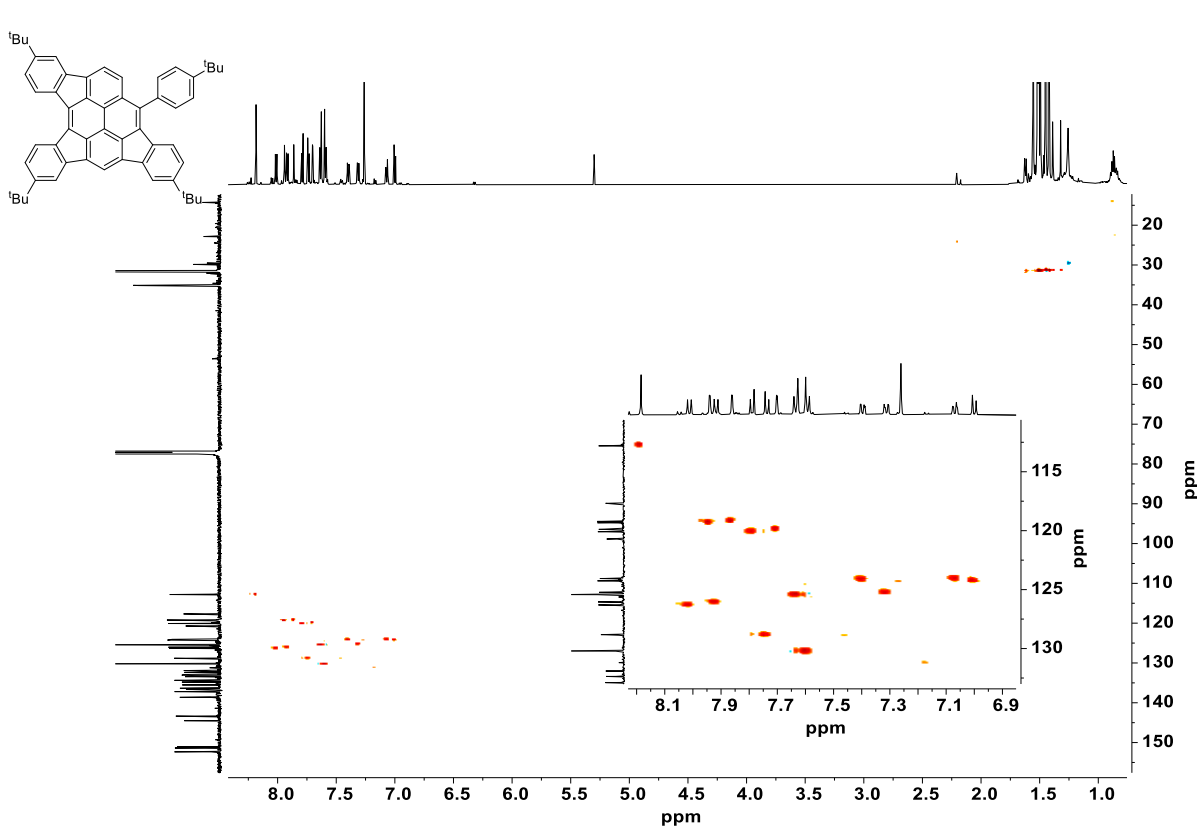
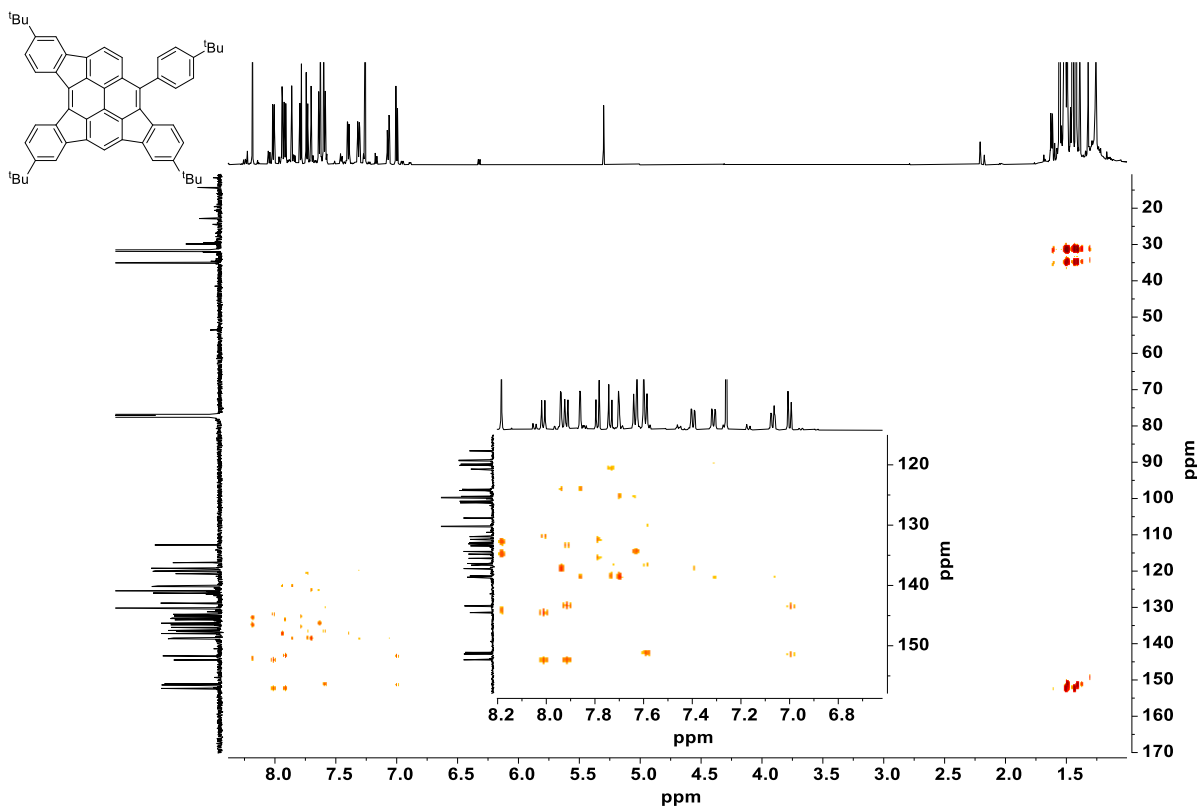


Figure S28: $^1\text{H},^1\text{H}$ -COSY-NMR spectrum of compound 8 (CDCl_3 , 295 K, 600/600 MHz).



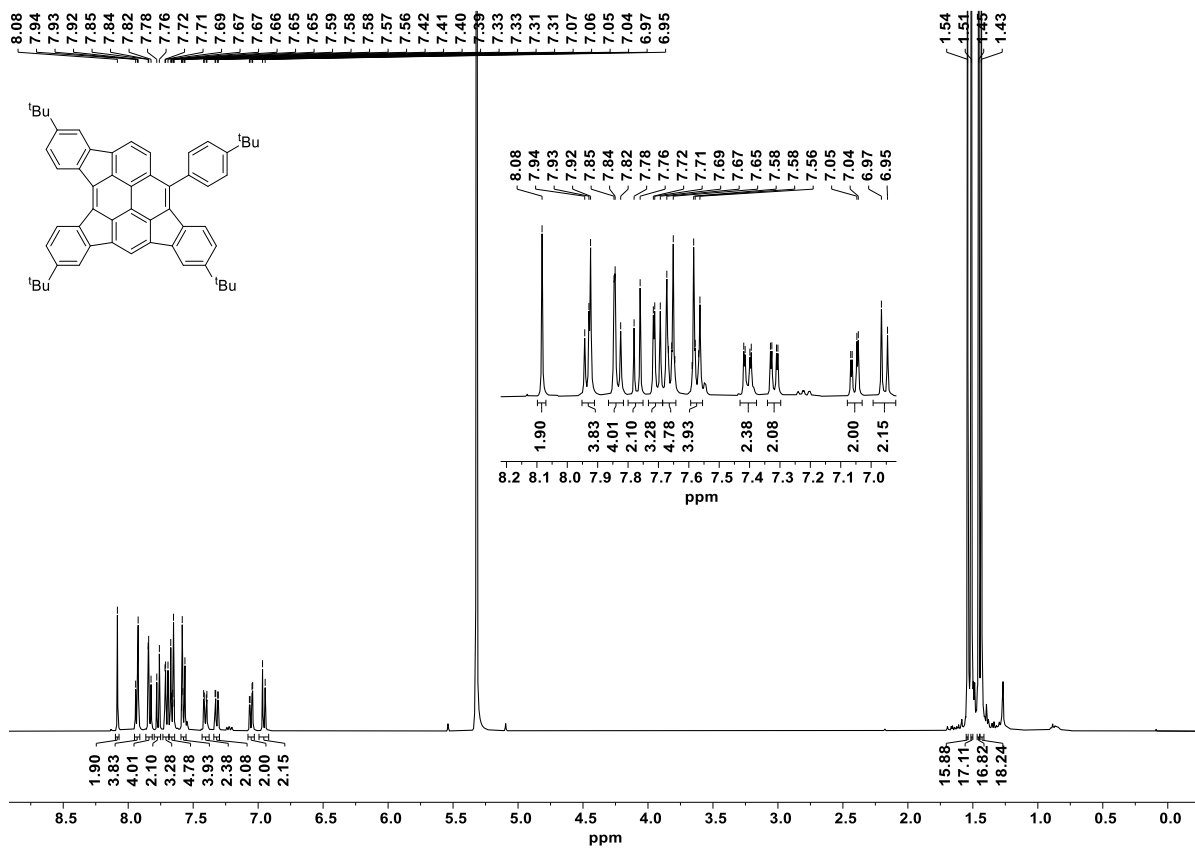


Figure S31: ^1H -NMR spectrum of compound 8 (CD_2Cl_2 , 400 MHz, 295 K).

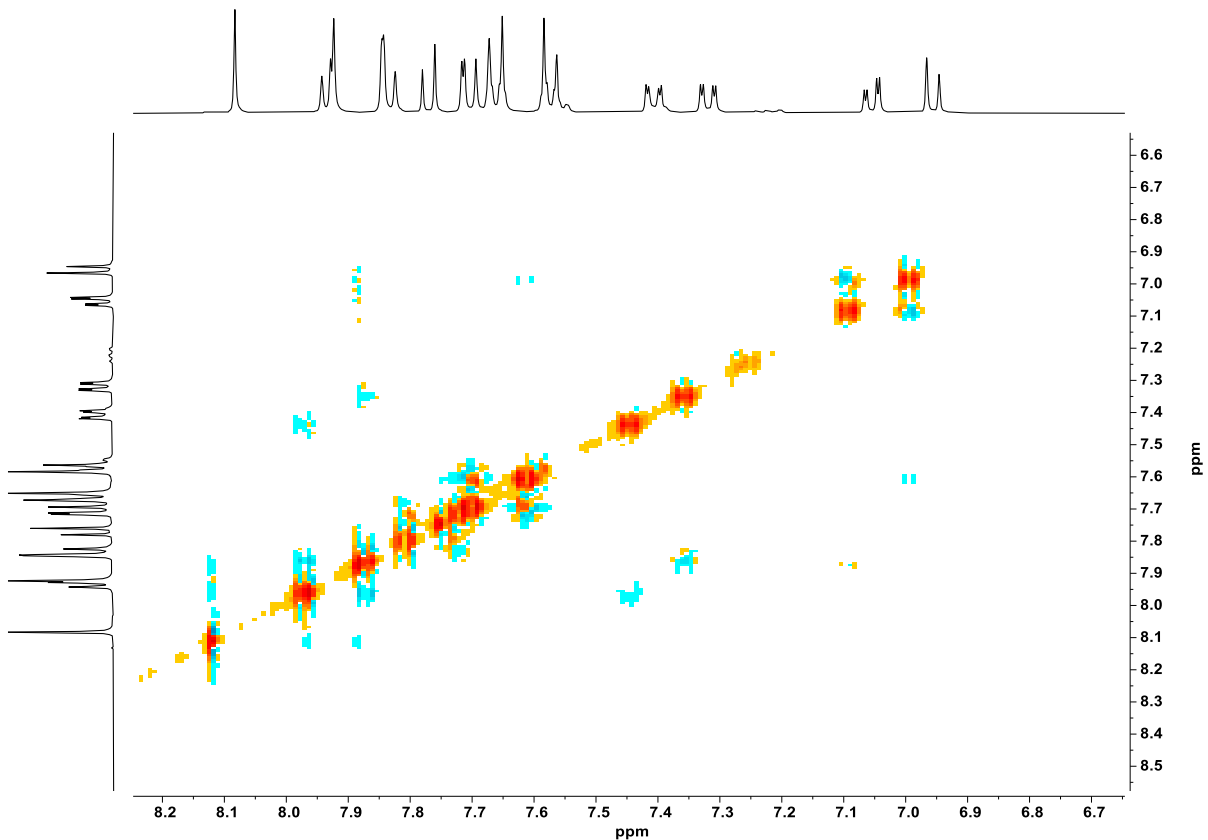


Figure S32: $^1\text{H},^1\text{H}$ -NOESY-NMR spectrum of compound 8 (CDCl_3 , 295 K, 400/400 MHz).

4. NMR-Aggregation Studies

To investigate the aggregation behavior of TIP **2** by NMR techniques, 6.67 mg (9.23 µmol) of **2** were dissolved in 3 mL of CD₂Cl₂ creating a 3.08 mM stock solution. This stock solution was diluted with CD₂Cl₂ according to the following table.

V _{stock solution}	V _{CD₂Cl₂added}	Resulting concentration
600 µL	-	3.08 mM
450 µL	150 µL	2.31 mM
300 µL	300 µL	1.54 mM
150 µL	450 µL	0.77 mM
75 µL	525 µL	0.39 mM
40 µL	560 µL	0.20 mM
20 µL	580 µL	0.10 mM

The obtained solutions were vigorously shaken and analyzed by ¹H NMR spectroscopy at 400 MHz with an equilibration time of at least 10 min at the corresponding temperature prior to the measurements.

Temperatures of 293, 283, 273, 263, 253 and 243 K have been investigated. Assuming infinite π-stacks with the association constant $K_E = K_2 = K_3 = \dots = K_n$ with the number of molecules n = 2 to infinity, K_E was determined by a least-squares curve fitting of the infinite (isodesmic) association model:^[S17]

$$\delta = \delta_m + (\delta_a - \delta_m) \left(1 + \frac{1 - \sqrt{4K_E C_t + 1}}{2K_E C_t} \right)$$

with δ as the observed chemical shift; δ_a as the chemical shift of the infinite aggregate; δ_m as the chemical shift of the monomer; C_t as the total concentration of the substrate (see above). Since the association constants K_E is calculated for every proton individually by this method, also an average value for K_E was determined.

The Gibb's energy ΔG was then calculated as

$$\Delta G = -RT \ln K_E'$$

where K_E' is the averaged K_E of the four individual protons (see below).

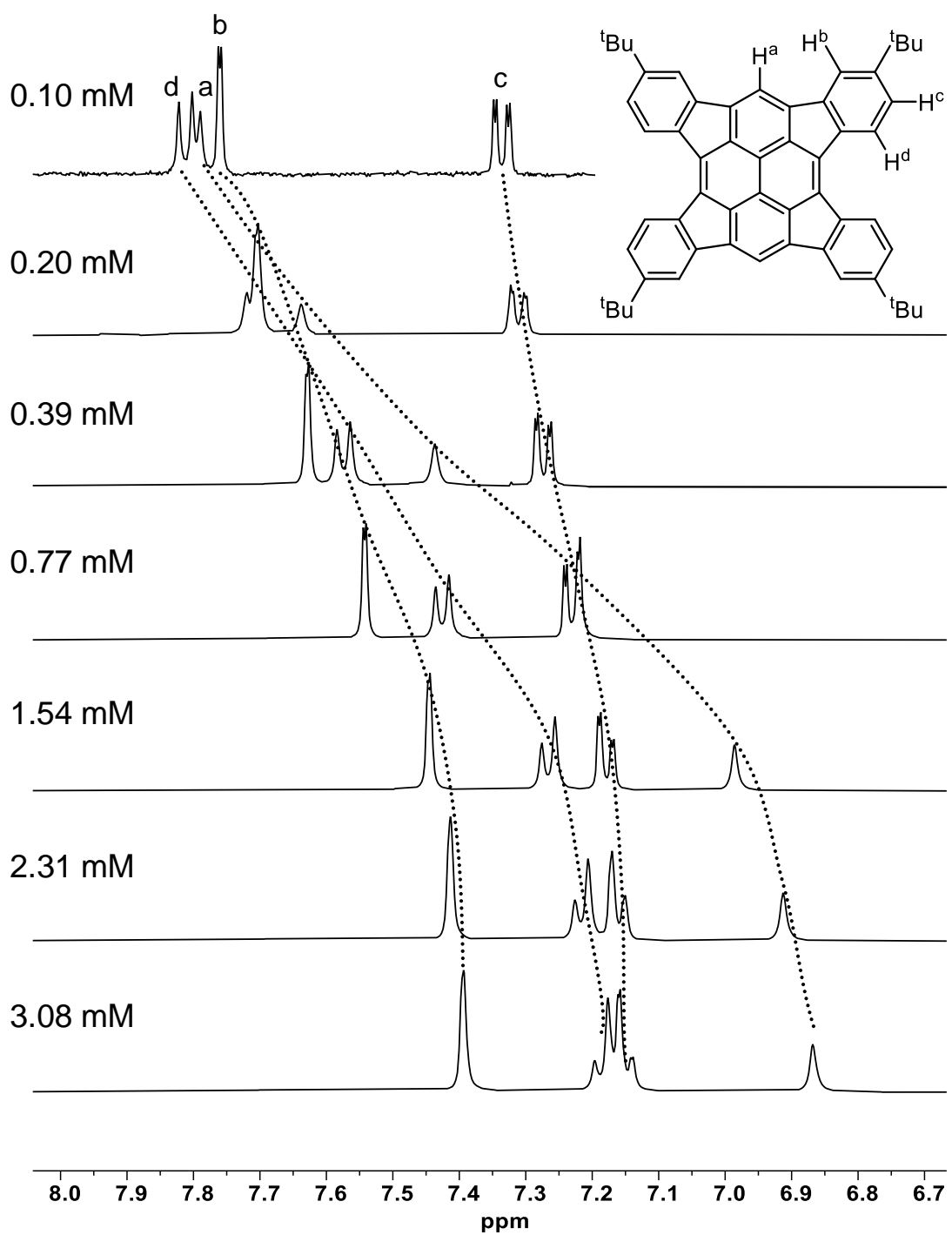


Figure S33: ¹H-NMR spectra of TIP 2 in CD₂Cl₂ (400 MHz) at concentrations between $c = 0.10\text{-}3.08\text{ mM}$ at 293 K.

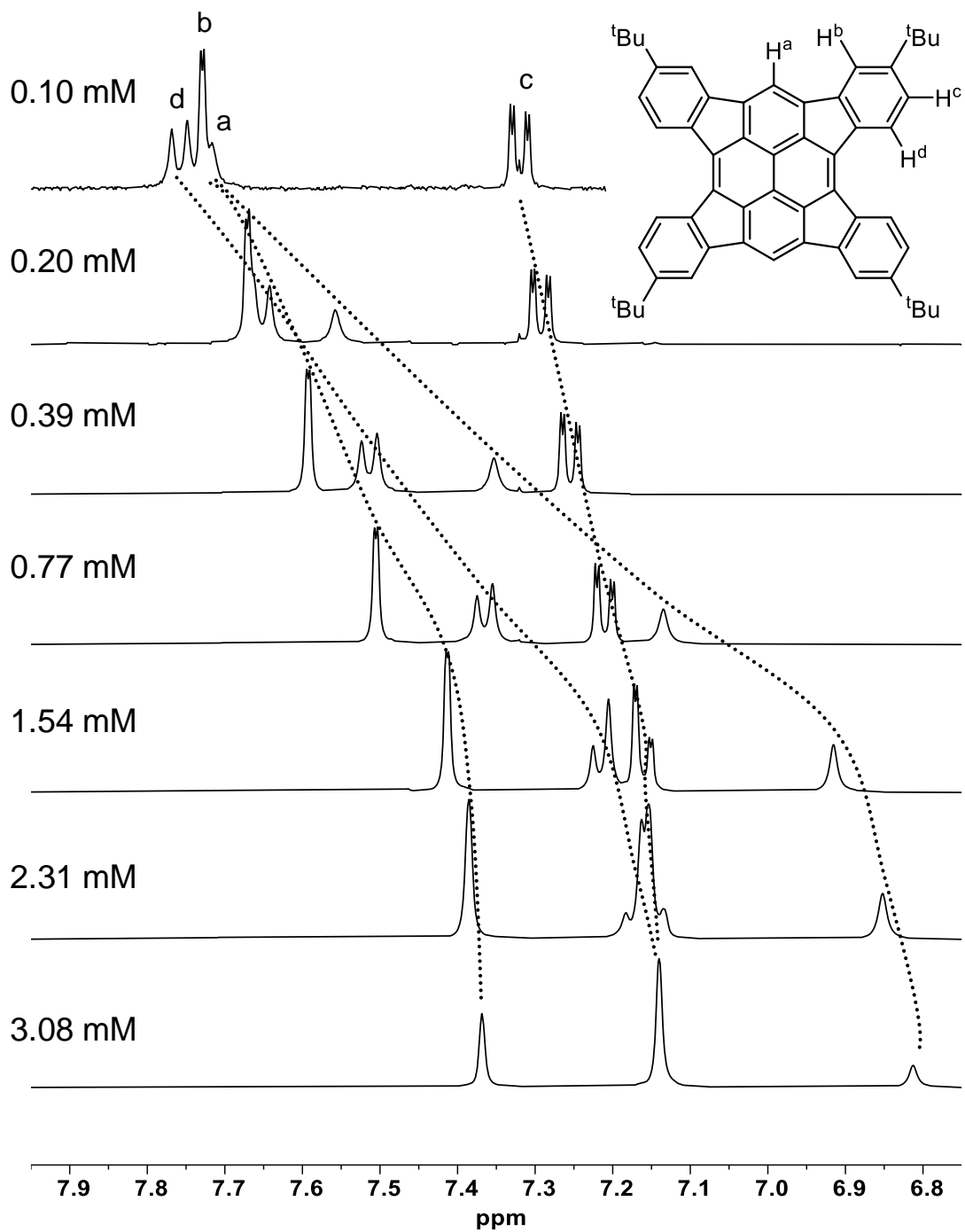


Figure S34: ¹H-NMR spectra of TIP **2** in CD₂Cl₂ (400 MHz) at concentrations between $c = 0.10\text{-}3.08\text{ mM}$ at 283 K.

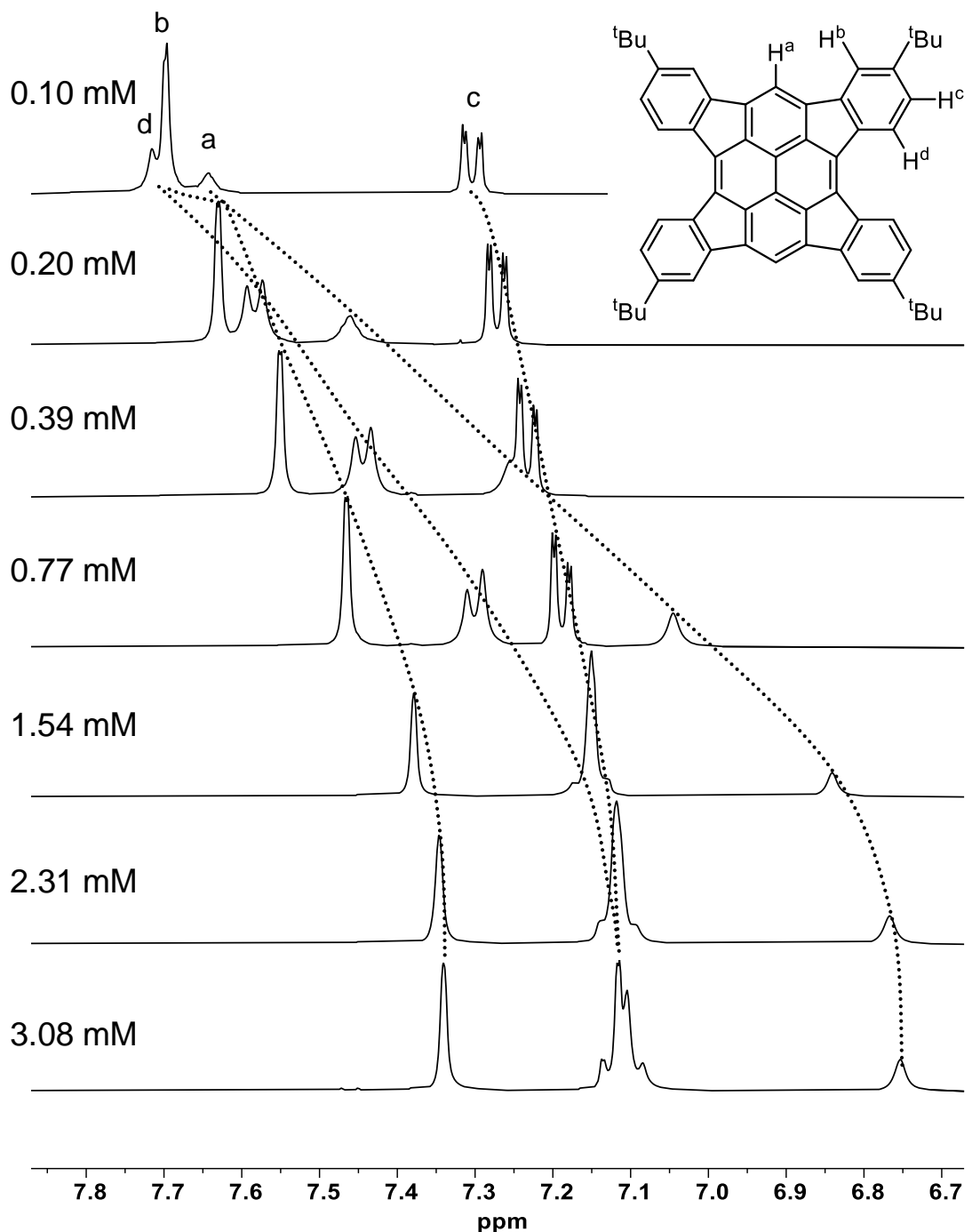


Figure S35: ¹H-NMR spectra of TIP **2** in CD₂Cl₂ (400 MHz) at concentrations between $c = 0.10\text{-}3.08\text{ mM}$ at 273 K.

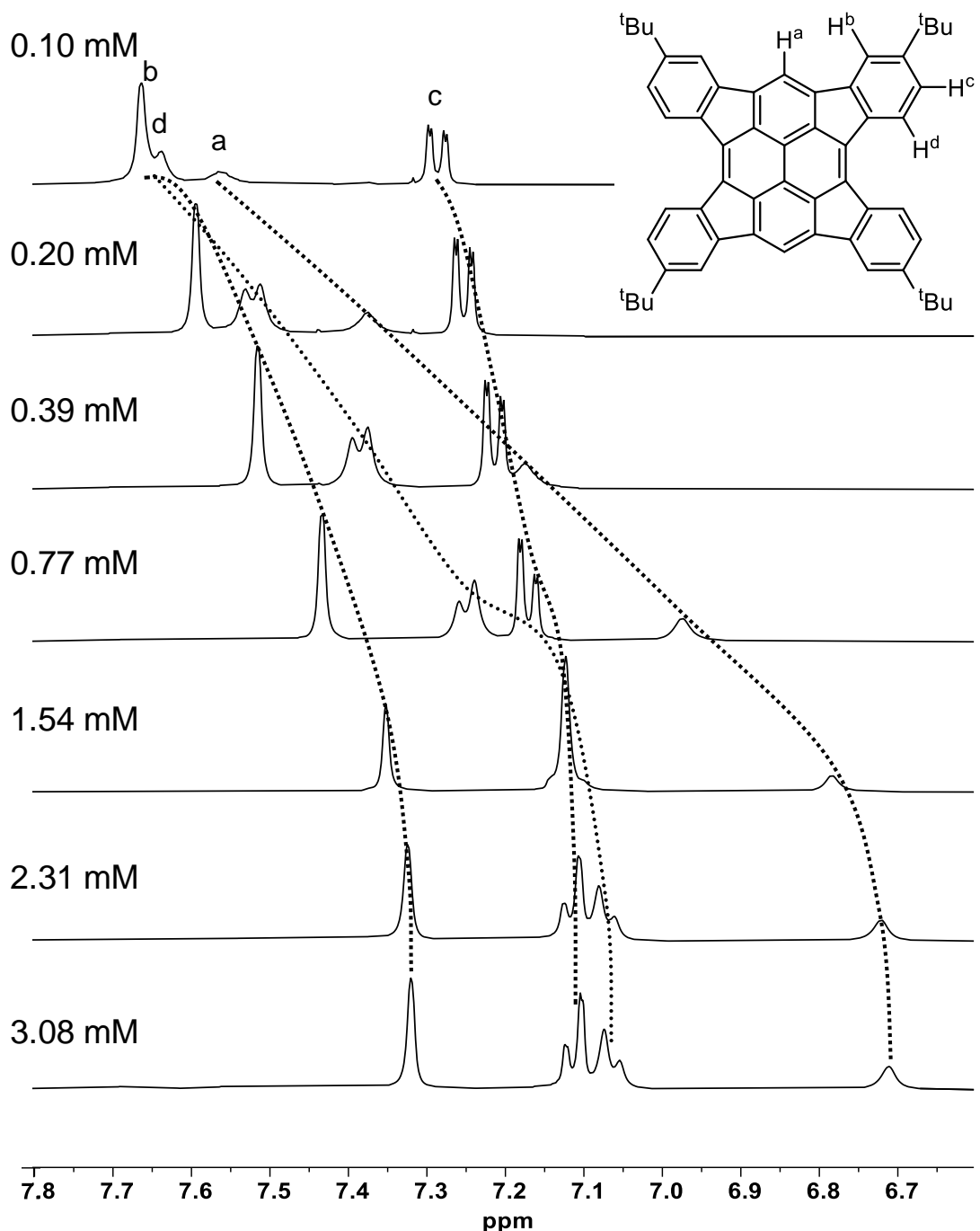


Figure S36: ¹H-NMR spectra of TIP 2 in CD_2Cl_2 (400 MHz) at concentrations between $c = 0.10\text{-}3.08 \text{ mM}$ at 263 K.

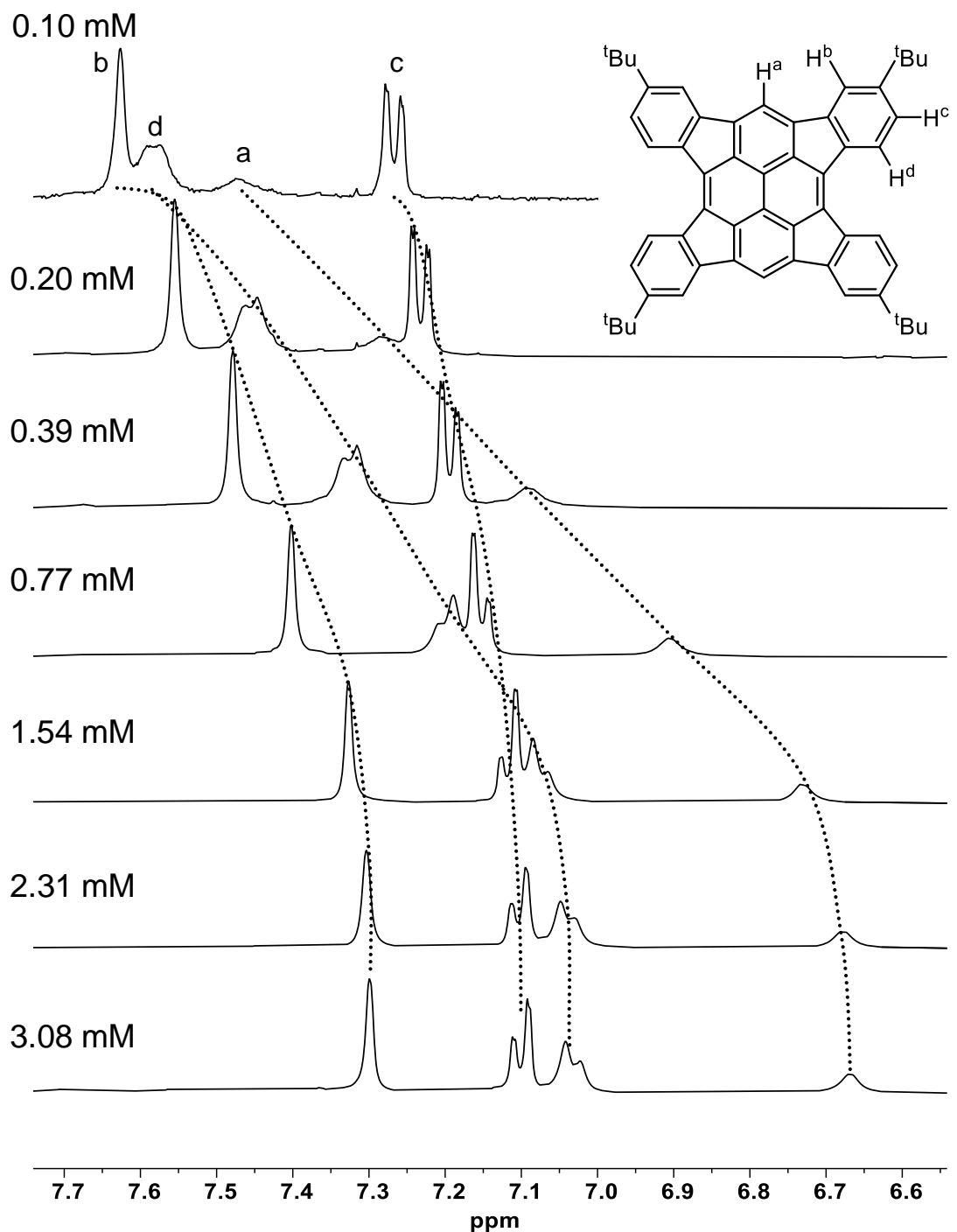


Figure S37: ^1H -NMR spectra of **TIP 2** in CD_2Cl_2 (400 MHz) at concentrations between $c = 0.10\text{-}3.08 \text{ mM}$ at 253 K.

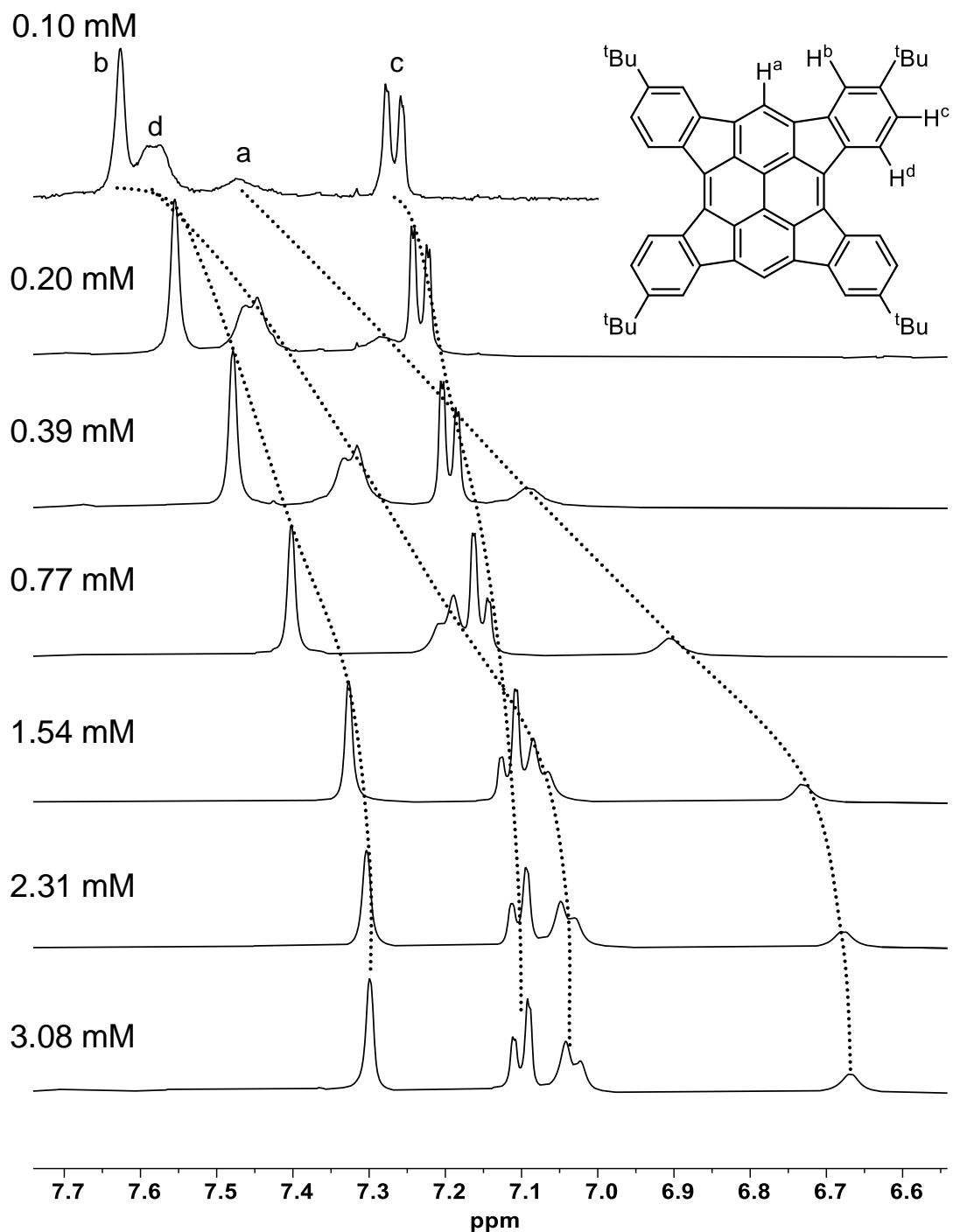


Figure S38: ^1H -NMR spectra of **TIP 2** in CD_2Cl_2 (400 MHz) at concentrations between $c = 0.10\text{-}3.08 \text{ mM}$ at 243 K.

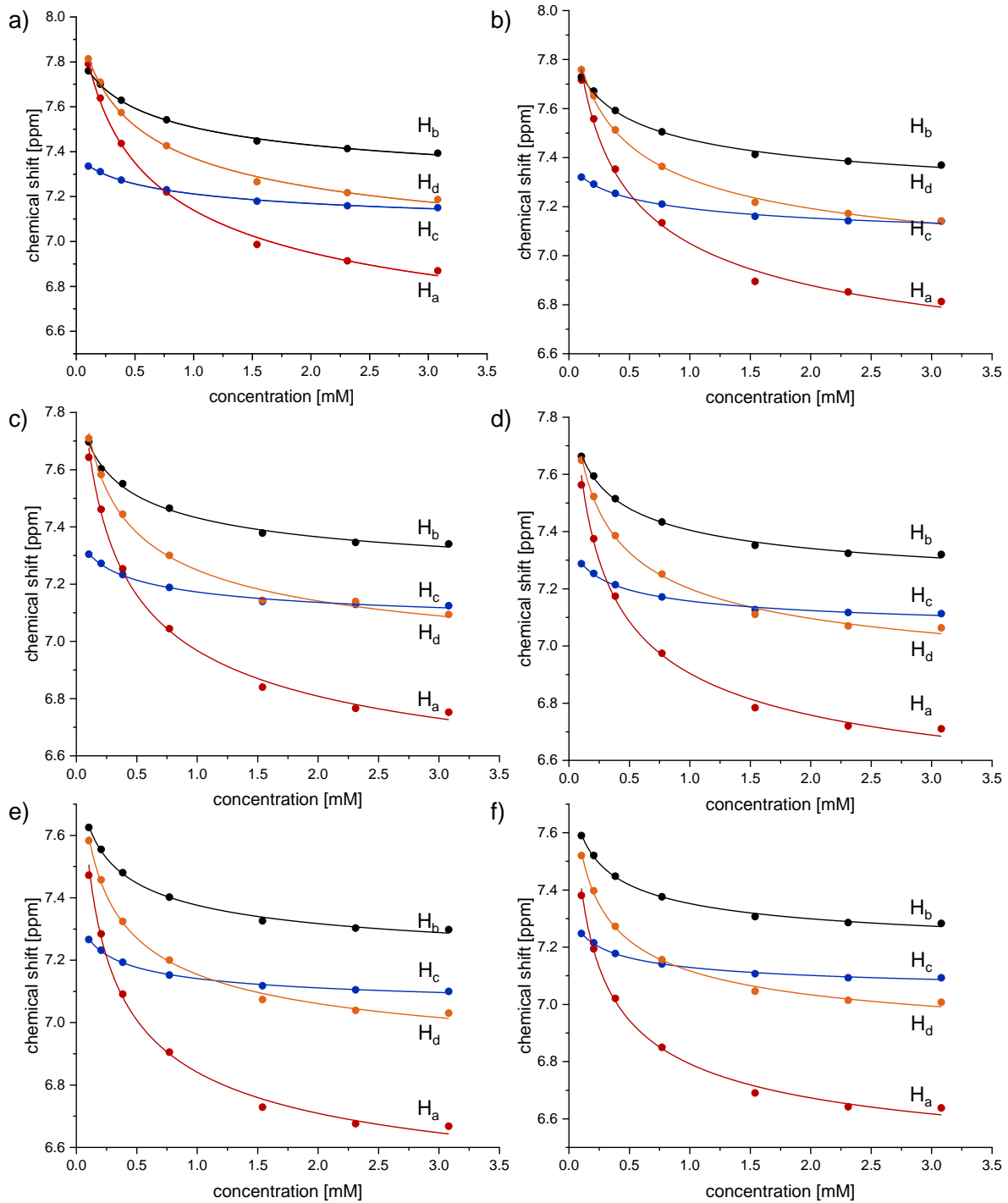


Figure S39: Fitting curves of least-squares curve fittings of the infinite (isodesmic) association model for the single protons of TIP **2** at various concentrations at a) 293 K, b) 283 K, c) 273 K, d) 263 K, e) 253 K and f) 243 K.

The following table summarizes the experimental findings described above:

293 K

conc.	δH^a	δH^b	δH^c	δH^d
0.10 mM	7.790	7.760	7.335	7.813
0.20 mM	7.638	7.700	7.311	7.710
0.39 mM	7.436	7.629	7.273	7.574
0.77 mM	7.220	7.542	7.230	7.426
1.54 mM	6.986	7.447	7.179	7.266
2.31 mM	6.913	7.413	7.159	7.217
3.08 mM	6.869	7.393	7.150	7.187
δ_m [ppm]	8.208 ± 0.153	7.875 ± 0.025	7.385 ± 0.012	8.073 ± 0.082
δ_a [ppm]	6.349 ± 0.071	7.151 ± 0.025	7.009 ± 0.018	6.821 ± 0.049
K_e [M ⁻¹]	$(3.24 \pm 1.23) \times 10^3$	$(2.03 \pm 0.46) \times 10^3$	$(1.58 \pm 0.38) \times 10^3$	$(2.94 \pm 0.98) \times 10^3$
R^2	0.99999	1	1	0.99999

$$\text{average } K_E = (2.45 \pm 0.77) \times 10^3 \text{ M}^{-1}$$

$$\Delta G = -19.0 \text{ kJ/mol}$$

283 K

conc	δH^a	δH^b	δH^c	δH^d
0.10 mM	7.716	7.729	7.320	7.758
0.20 mM	7.558	7.671	7.292	7.652
0.39 mM	7.353	7.592	7.254	7.513
0.77 mM	7.134	7.505	7.210	7.364
1.54 mM	6.895	7.413	7.160	7.217
2.31 mM	6.852	7.385	7.142	7.172
3.08 mM	6.812	7.369	7.140	7.140
δ_m [ppm]	8.274 ± 0.330	7.871 ± 0.041	7.382 ± 0.021	8.056 ± 0.090
δ_a [ppm]	6.352 ± 0.093	7.152 ± 0.030	7.017 ± 0.021	6.809 ± 0.041
K_e [M ⁻¹]	$(4.82 \pm 3.27) \times 10^3$	$(2.77 \pm 0.87) \times 10^3$	$(2.23 \pm 0.83) \times 10^3$	$(3.65 \pm 1.21) \times 10^3$
R^2	0.99998	1	1	1

$$\text{average } K_E = (3.37 \pm 1.13) \times 10^3 \text{ M}^{-1}$$

$$\Delta G = -19.1 \text{ kJ/mol}$$

273 K

conc	δH^a	δH^b	δH^c	δH^d
0.10 mM	7.643	7.697	7.304	7.709
0.20 mM	7.461	7.603	7.272	7.583
0.39 mM	7.253	7.551	7.233	7.444
0.77 mM	7.044	7.465	7.188	7.3
1.54 mM	6.84	7.378	7.139	7.143
2.31 mM	6.766	7.346	7.129	7.139
3.08 mM	6.752	7.34	7.124	7.094
δ_m [ppm]	8.286 ± 0.320	7.856 ± 0.066	7.383 ± 0.030	8.140 ± 0.270
δ_a [ppm]	6.333 ± 0.065	7.153 ± 0.033	7.018 ± 0.019	6.820 ± 0.061
K_e [M ⁻¹]	$(6.40 \pm 3.80) \times 10^3$	$(3.84 \pm 1.73) \times 10^3$	$(3.23 \pm 1.41) \times 10^3$	$(6.40 \pm 4.89) \times 10^3$
R^2	0.99999	1	1	0.99999

$$\text{average } K_E = (4.97 \pm 1.67) \times 10^3 \text{ M}^{-1}$$

$$\Delta G = -19.3 \text{ kJ/mol}$$

263 K

conc	δH^a	δH^b	δH^c	δH^d
0.10 mM	7.563	7.663	7.287	7.649
0.20 mM	7.375	7.594	7.253	7.522
0.39 mM	7.174	7.515	7.214	7.386
0.77 mM	6.974	7.433	7.171	7.251
1.54 mM	6.784	7.352	7.127	7.11
2.31 mM	6.72	7.324	7.117	7.07
3.08 mM	6.71	7.32	7.113	7.063
δ_m [ppm]	8.316 ± 0.429	7.858 ± 0.069	7.377 ± 0.032	8.067 ± 0.207
δ_a [ppm]	6.337 ± 0.061	7.144 ± 0.026	7.020 ± 0.016	6.787 ± 0.047
K_e [M ⁻¹]	$(8.69 \pm 6.24) \times 10^3$	$(4.75 \pm 2.01) \times 10^3$	$(4.19 \pm 1.81) \times 10^3$	$(6.50 \pm 3.92) \times 10^3$
R^2	0.99999	1	1	0.99999

average $K_E = (6.03 \pm 2.03) \times 10^3$ M⁻¹

$\Delta G = -19.0$ kJ/mol

253 K

conc	δH^a	δH^b	δH^c	δH^d
0.10 mM	7.472	7.625	7.266	7.583
0.20 mM	7.284	7.555	7.232	7.457
0.39 mM	7.091	7.48	7.193	7.324
0.77 mM	6.905	7.402	7.152	7.2
1.54 mM	6.729	7.326	7.118	7.074
2.31 mM	6.676	7.303	7.105	7.039
3.08 mM	6.668	7.298	7.1	7.03
δ_m [ppm]	8.338 ± 0.560	7.834 ± 0.075	7.366 ± 0.024	8.050 ± 0.222
δ_a [ppm]	6.339 ± 0.056	7.139 ± 0.023	7.021 ± 0.009	6.790 ± 0.037
K_e [M ⁻¹]	$(11.9 \pm 10.2) \times 10^3$	$(5.65 \pm 2.52) \times 10^3$	$(5.33 \pm 1.65) \times 10^3$	$(8.50 \pm 5.17) \times 10^3$
R^2	0.99999	1	1	0.99999

average $K_E = (7.85 \pm 3.06) \times 10^3$ M⁻¹

$\Delta G = -18.9$ kJ/mol

243 K

conc	δH^a	δH^b	δH^c	δH^d
0.10 mM	7.381	7.59	7.248	7.52
0.20 mM	7.194	7.521	7.215	7.397
0.39 mM	7.021	7.448	7.178	7.273
0.77 mM	6.85	7.376	7.141	7.156
1.54 mM	6.69	7.307	7.107	7.046
2.31 mM	6.642	7.286	7.093	7.014
3.08 mM	6.638	7.283	7.093	7.007
δ_m [ppm]	8.237 ± 0.577	7.819 ± 0.089	7.345 ± 0.03	8.032 ± 0.249
δ_a [ppm]	6.342 ± 0.051	7.143 ± 0.021	7.027 ± 0.011	6.797 ± 0.091
K_e [M ⁻¹]	$(13.5 \pm 12.4) \times 10^3$	$(7.16 \pm 3.56) \times 10^3$	$(5.58 \pm 2.26) \times 10^3$	$(11.0 \pm 7.19) \times 10^3$
R^2	0.99999	1	1	1

average $K_E = (9.32 \pm 3.61) \times 10^3$ M⁻¹

$\Delta G = -18.5$ kJ/mol

The calculation of K_E at different temperatures was used to determine ΔS as well as ΔH according to the van't Hoff equation:

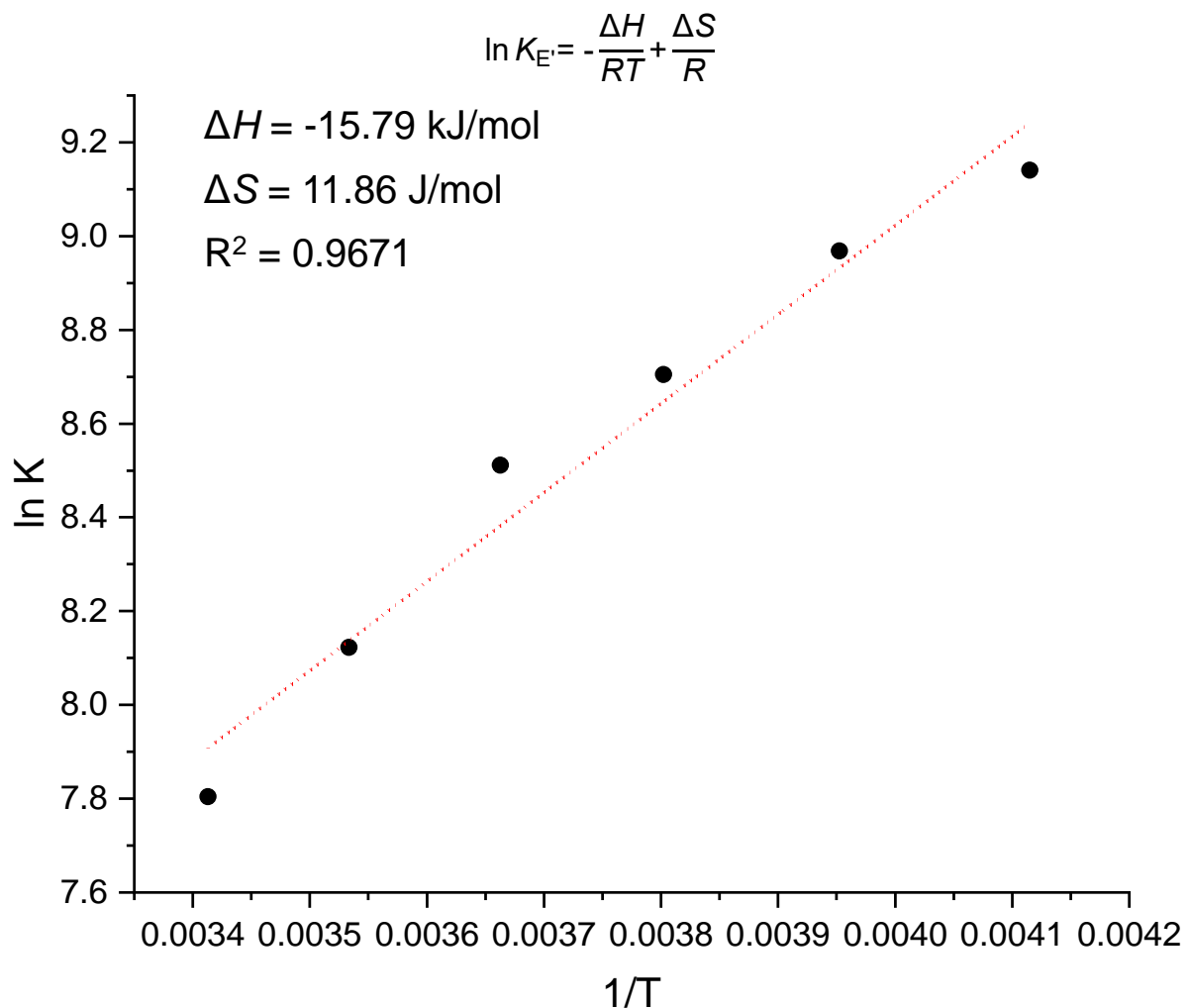


Figure S40: van't Hoff-plot of the association constancies K_E against $1/T$ of TIP **2** as described above.

5. UV/Vis-Spectroscopy

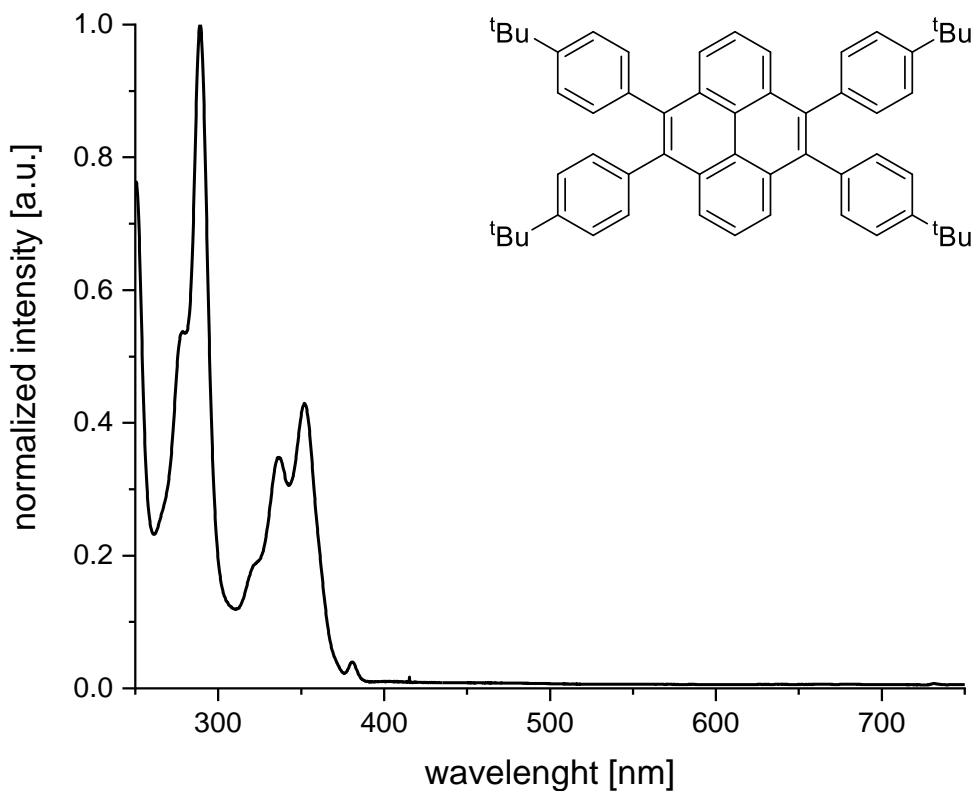


Figure S41: UV/Vis spectrum of compound **7** in CH_2Cl_2 ($c = 1.29 \cdot 10^{-5}$ M).

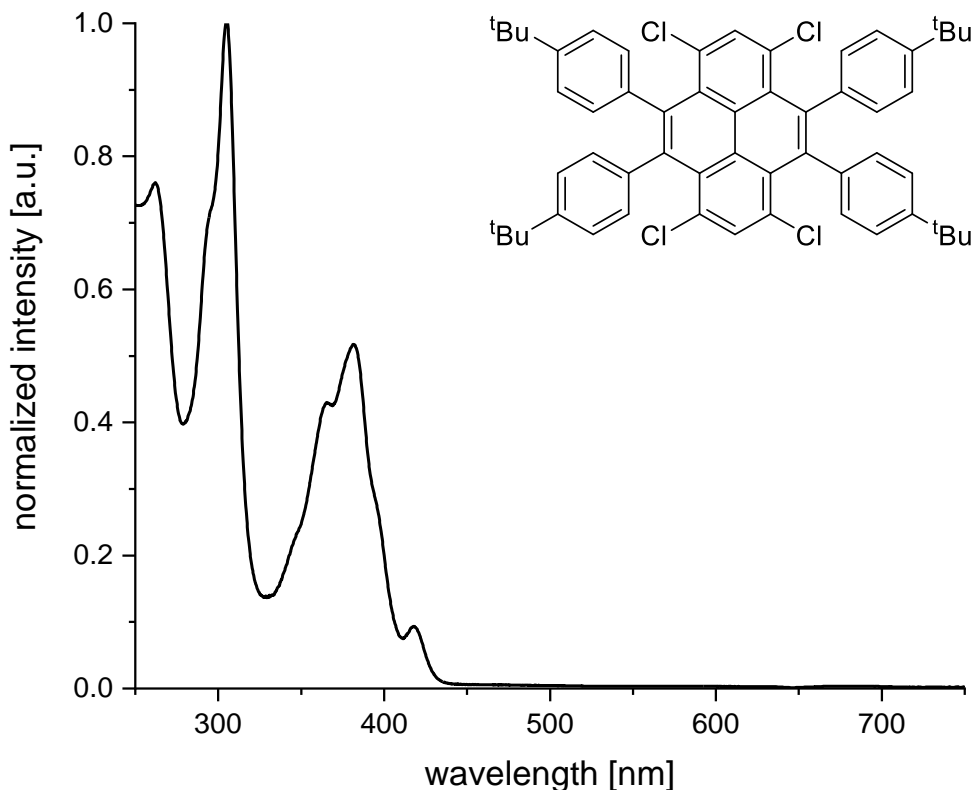


Figure S42: UV/Vis spectrum of compound **3** in CH_2Cl_2 ($c = 9.97 \cdot 10^{-6}$ M).

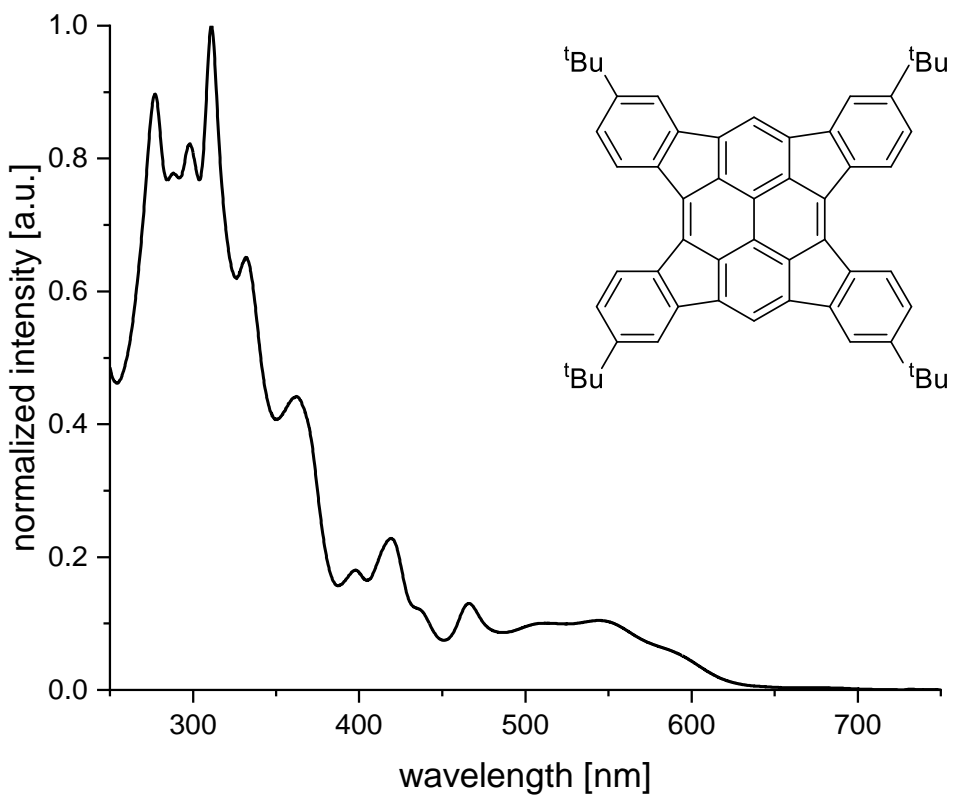


Figure S43: UV/Vis spectrum of compound **2** in CH_2Cl_2 ($c = 1.01 \cdot 10^{-5}$ M).

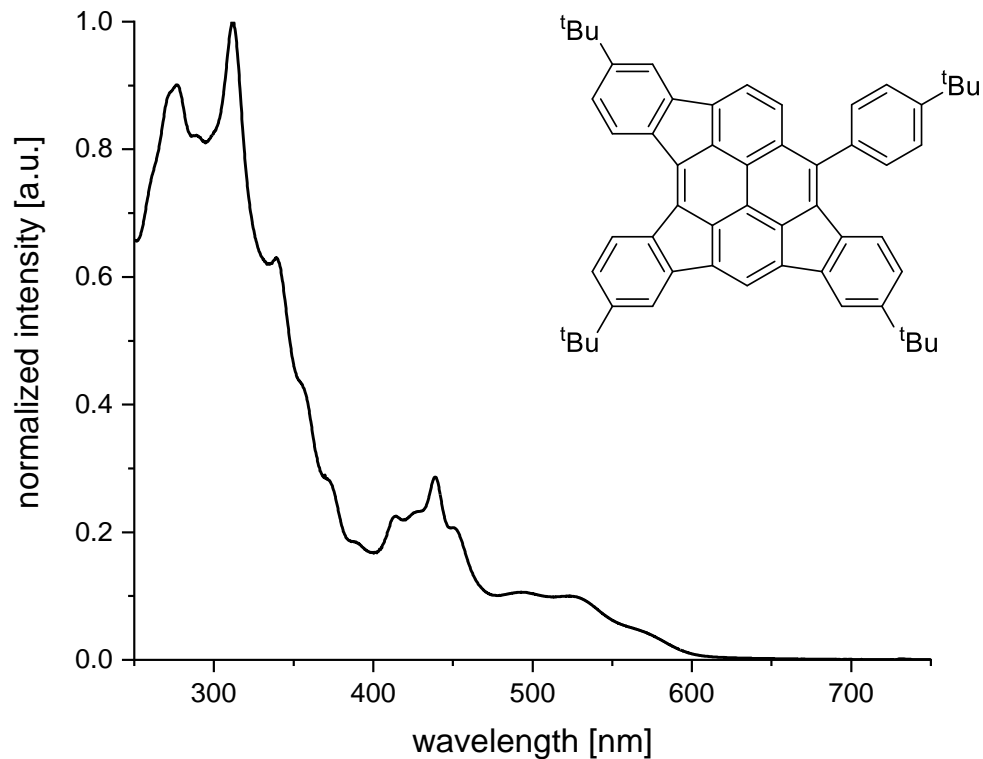


Figure S44: UV/Vis spectrum of compound **8** in CH_2Cl_2 .

6. DFT-Calculations

Geometry

After we observed the curved geometry for TIP **2**, we applied dispersion correction to the geometry optimization. Whereas there was hardly any change for the planar transition state, the bowl-shaped TIP shows an increased curvature, when dispersion correction is applied. The differences for both geometries are given in Figure S45. The *tert*-butyl groups have indeed a non-negligible influence of about 4% to the bowl depth.

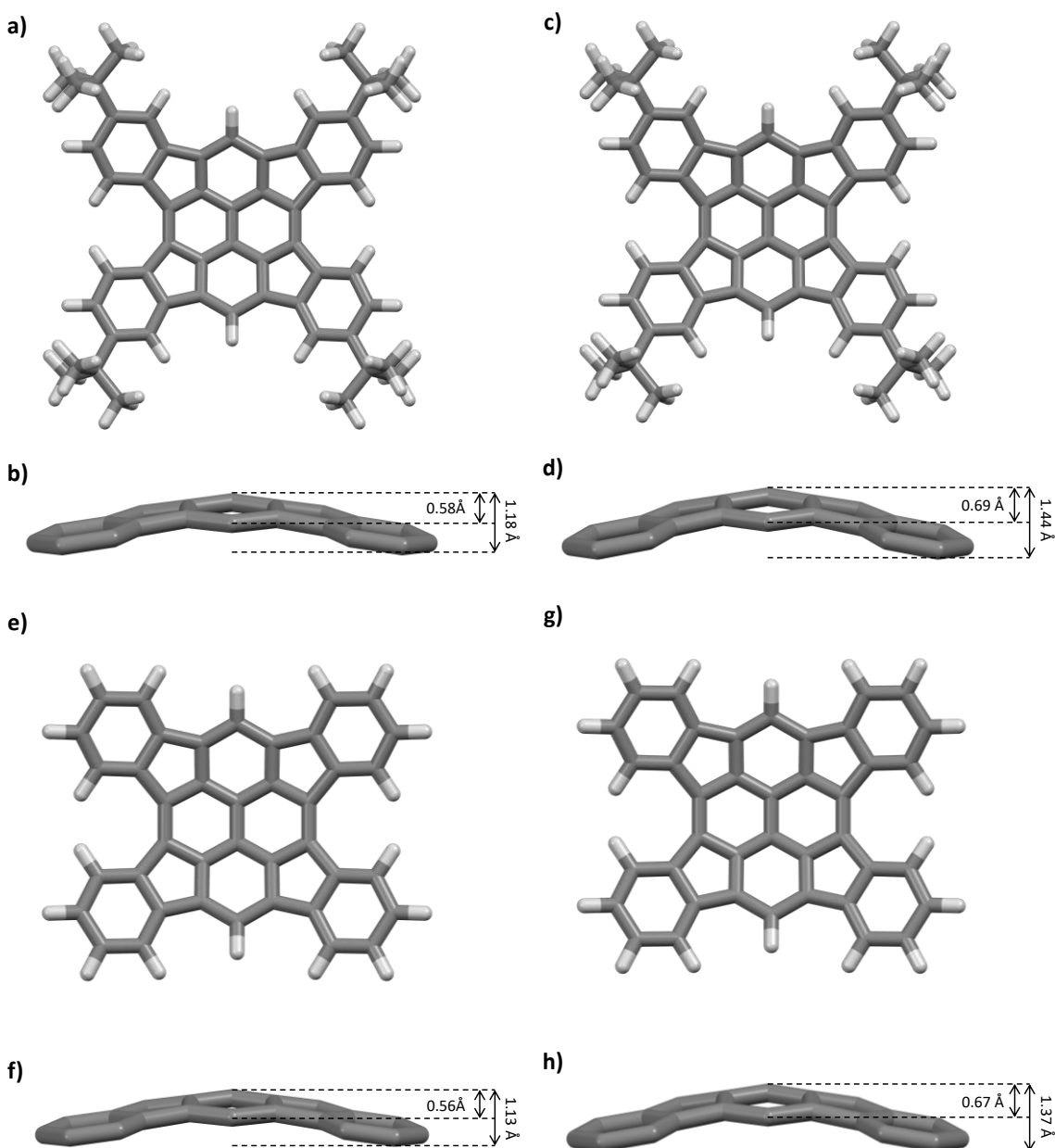


Figure S45: Geometry optimized model (B3LYP/6-311G(d,p)) of TIP **2** and TIP without *tert*-butyl groups without dispersion correction (left) and with Grimme's D3BJ dispersion correction. a), c), e) and g) Top view. b), d), f) and h) Side view with estimated bowl depths. The *tert*-butyl groups as well as hydrogen atoms are omitted for clarity.

Inversion Barrier

For the inversion process the planar transition state as well as the bowl-shaped minima were computed, and both analyzed by frequency calculations to obtain thermodynamic data. Following the Eyring equation we calculated the theoretical inversion frequency:

$$k = \frac{\kappa k_B T}{h} e^{\frac{\Delta^\ddagger G}{RT}}$$

Assuming that κ equals 1 for unimolecular reactions and using the calculated value for $\Delta^\ddagger G$ at 298.15 K, an inversion rate of $2.18 \times 10^{11} \text{ s}^{-1}$ can be calculated. This means the TIP 2 is flipping 218 billion times per second (see Figure S46). Applying dispersion correction, we obtained a larger value for $\Delta^\ddagger G$, so that $k = 5.05 \times 10^{10} \text{ s}^{-1}$ or 51 billion times per second.

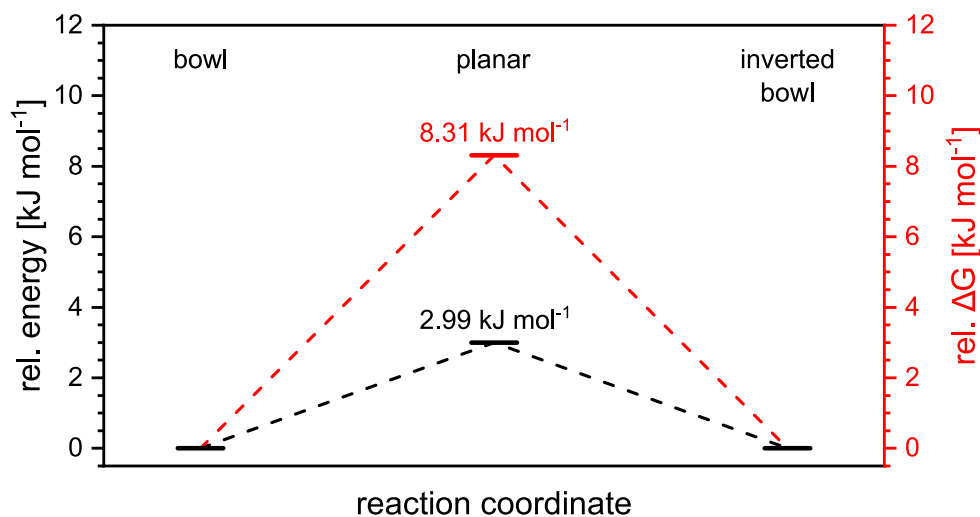


Figure S46: Inversion process of the TIP 2 via a planar transition state with the calculated difference in energy (black) and free enthalpy (red) derived from DFT-calculations (B3LYP/6-311G(d,p)) without dispersion correction.

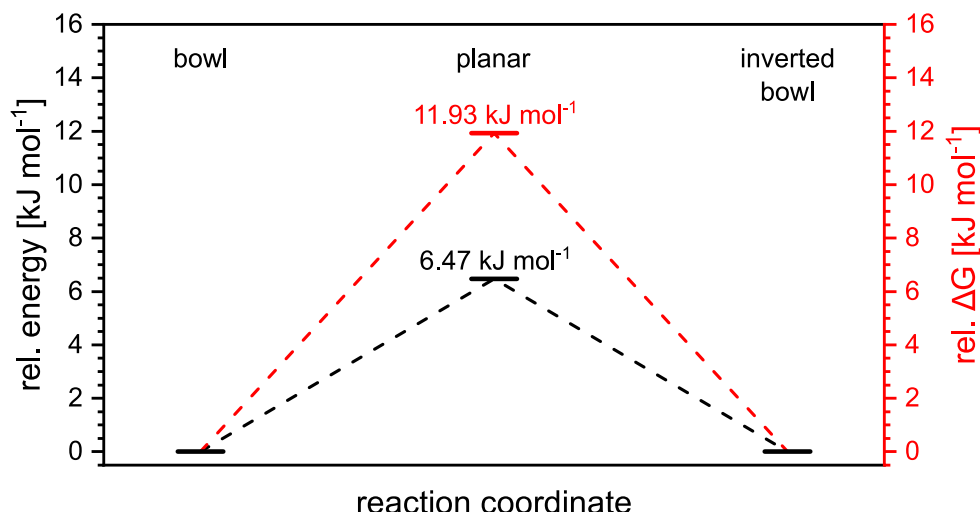


Figure S47: Inversion process of the TIP 2 via a planar transition state with the calculated difference in energy (black) and free enthalpy (red) derived from DFT-calculations (B3LYP/6-311G(d,p)) with dispersion correction (D3BJ).

TD-DFT

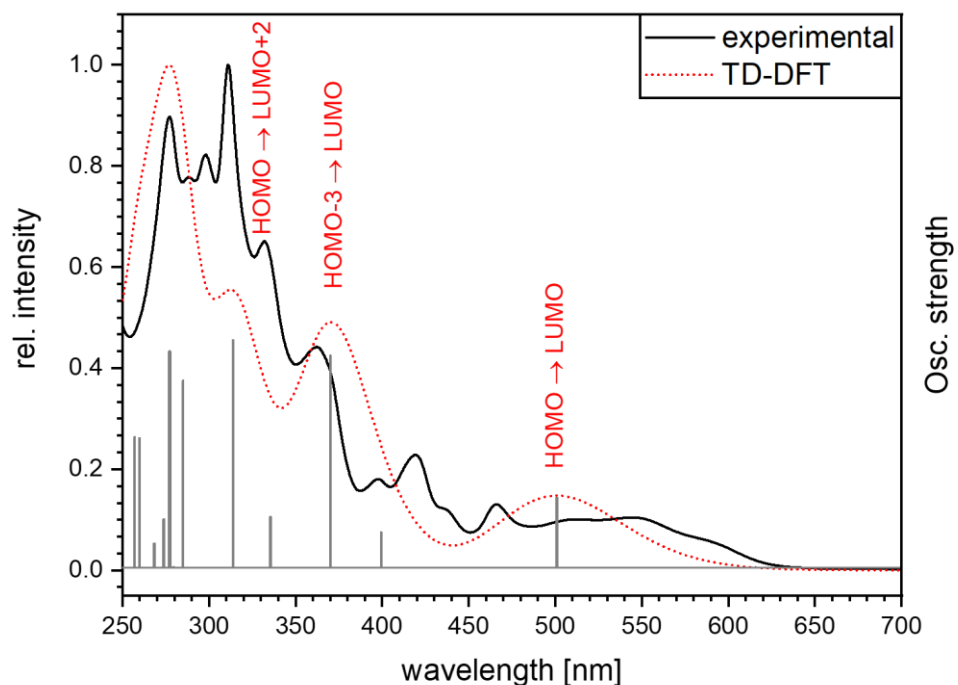


Figure S48: Comparison of the experimental absorption spectrum in CH_2Cl_2 (black solid line) and the TD-DFT calculation (red dotted line, cam-B3LYP/6-311G(d,p)). For the three most intense calculated maxima the major contributions for the transitions are given.

The tailing of the lowest energy adsorption band of TIP **2** till $\lambda_{\text{onset}} = 620 \text{ nm}$ resulting in an optical band gap $E_{\text{gap, opt}} = 2.0 \text{ eV}$. TD-DFT calculations (cam-B3LYP/6-311G(d,p)) reveal the detailed structure of the UV/Vis spectrum. The positions of the absorption maxima of the calculated spectrum corresponds, even if the convoluted spectrum does not fit that well. The most bathochromic absorption was identified as the HOMO-LUMO transition, whereas the other transitions are mostly from the HOMO-4 and lower to the LUMO. As there was no vibronic coupling taken into account for the calculation, a deeper analysis cannot be provided.

MO analysis

Both the planar as well as the bowl-shaped conformer of TIP **2** were analysed in terms of their electronic properties by DFT-methods (B3LYP/6-311G(d,p)) with and without dispersion correction applied. As Figure S 49 shows, it turns out that there's is hardly any difference between both forms.

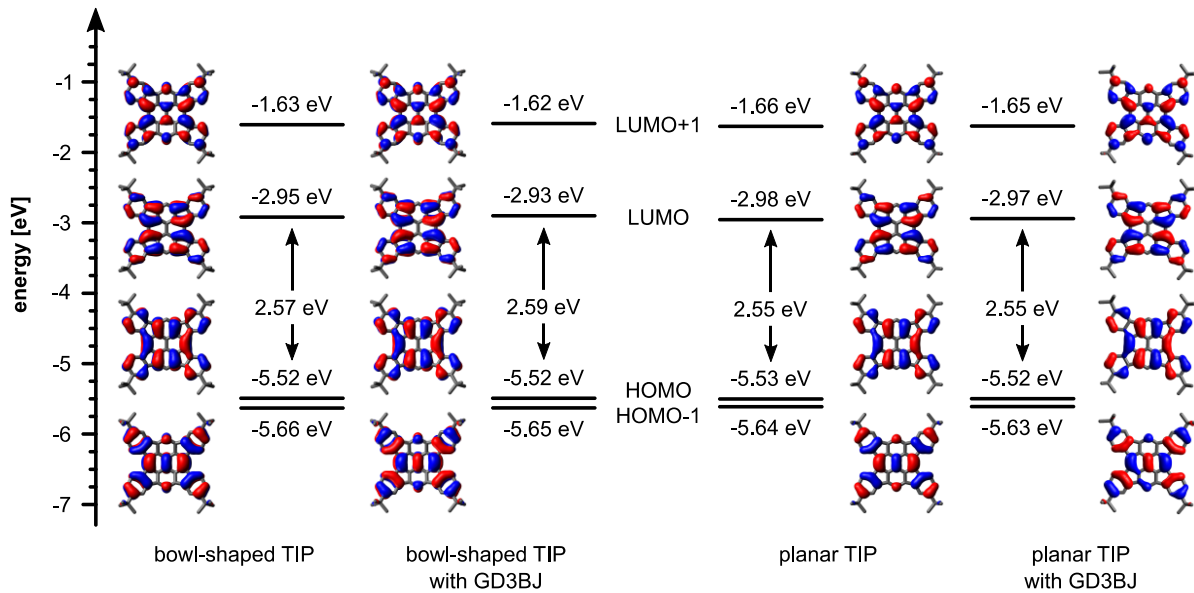


Figure S49: Canonical MOs of the bowl-shaped and planar TIP **2** (B3LYP/6-311G(d,p)) with (D3BJ) and without dispersion correction. The distribution of the MOs is for all geometries identical and the difference in energies is only marginal and lies within the DFT error.

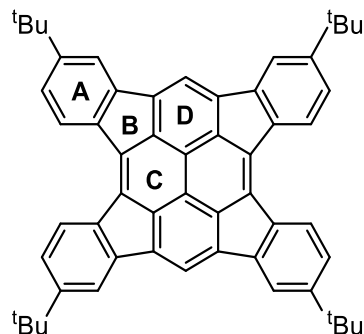
NICS and AICD calculations

We calculated NICS(0) and NICS(1) values to further investigate local aromaticity of tetraindenopyrene **2**. Following the suggestions of Dobrowolski *et al.*, we splitted the NICS(1) values in NICS(+1) and NICS(-1), where NICS(+1) is 1 Å below the outside of the bowl located (convex side) and NICS(-1) 1 Å inside the bowl (concave side).^[S13]

The results of the NICS calculations in Table S1 indicate an aromatic character for the outer ring A as well as the “top” ring D. The former pyrene K-Region (ring C) shows a non-aromatic character, like the parent pyrene. Whereas the NICS(0) value indicated an antiaromatic character for the five-membered ring B, the NICS(1) values tend more to be non-aromatic. Therefore ring B shows also the highest NICS(1)_{bia}, which means the largest difference between NICS(0) and NICS(1)_{av}. An analysis of the NICS(1)_{diff} values mirrors the difference of the two sides of the bowl. This difference is strongest in the middle-part of the molecule (rings C and D) with NICS(1)_{diff} values between 3.5

and 3.9, whereas ring A shows hardly any difference. The NICS analysis was also performed on the geometry obtained from the dispersion corrected optimization. In comparison to the non-corrected geometry, only smaller differences could be observed.

Table S1: Calculated NICS values for the bowl-shaped tetraindenopyrene (HF/6-31+G(d)). For the splitting of the NICS(1) value we followed the suggestions of Dobrowolski *et al.*[S13]



without dispersion correction

Ring	NICS(0)	NICS(-1)	NICS(+1)	NICS(1) _{av}	NICS(1) _{diff}	NICS(1) _{as}	NICS(1) _{bia}
A	-6.9	-8.7	-8.5	-8.6	0.2	0.0	1.7
B	7.7	1.8	3.8	2.8	1.9	1.0	4.9
C	0.6	-4.7	-0.8	-2.8	3.9	-0.8	3.3
D	-7.6	-11.2	-7.6	-9.4	3.5	-0.3	1.8

with dispersion correction (D3BJ)

Ring	NICS(0)	NICS(-1)	NICS(+1)	NICS(1) _{av}	NICS(1) _{diff}	NICS(1) _{as}	NICS(1) _{bia}
A	-7.0	-8.8	-8.6	-8.7	0.3	0.0	1.7
B	7.4	1.3	3.7	2.5	2.4	1.8	4.9
C	0.4	-5.3	-0.6	-3.0	4.7	-0.9	3.4
D	-7.8	-11.7	-7.3	-9.5	4.3	-0.4	1.7

To confirm the NICS analysis, we performed also AICD calculations. The resulting plots are shown in Figures S50 and S51. The ring current analysis fits perfectly to the NICS values. The rings A und D show a clockwise ring current, which is expected for aromatic rings. Ring C shows no uniform ring current and the five-membered ring B

exhibits an anti-clockwise ring current, which indicates a partial antiaromatic character. In Figures S50 and S51b and c views from different positions point out the difference between the two sides of the TIP. More electron density on the inside/concave side is predicted, which is consistent to larger NICS(-1) values in comparison to the NICS(+1). For the dispersion corrected geometry, the overall ring current doesn't change at all, but the isosurface is now nicely distributed above and below the molecule, maybe due to the more curved structure.

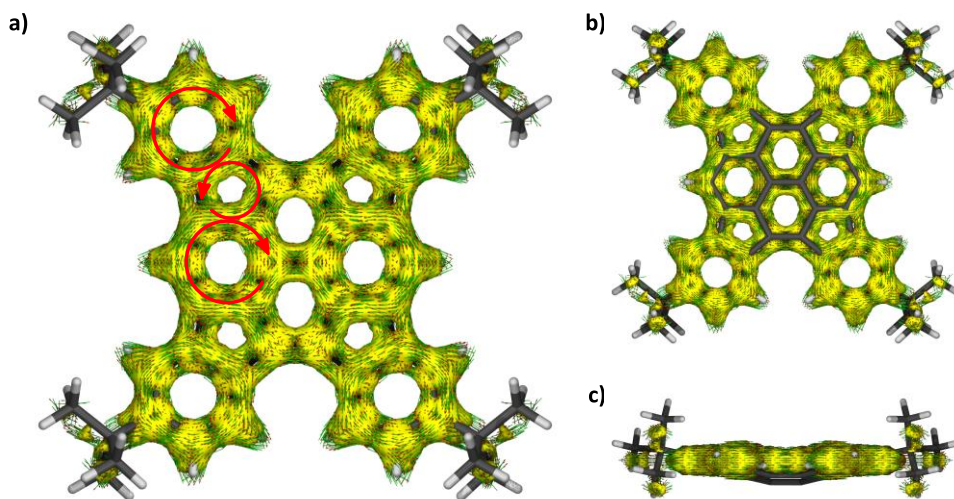


Figure S 50: AICD plots (HF/6-31+G(d)) of the bowl-shaped tetraindenopyrene **2** without dispersion correction from a) the top/concave side with the magnetic field pointing out of the paper plane and red arrows indicating the direction of the ring current. b) View from the convex side and c) from the side. Both pictures show the difference of the isosurface on the concave and convex side of the TIP **2**.

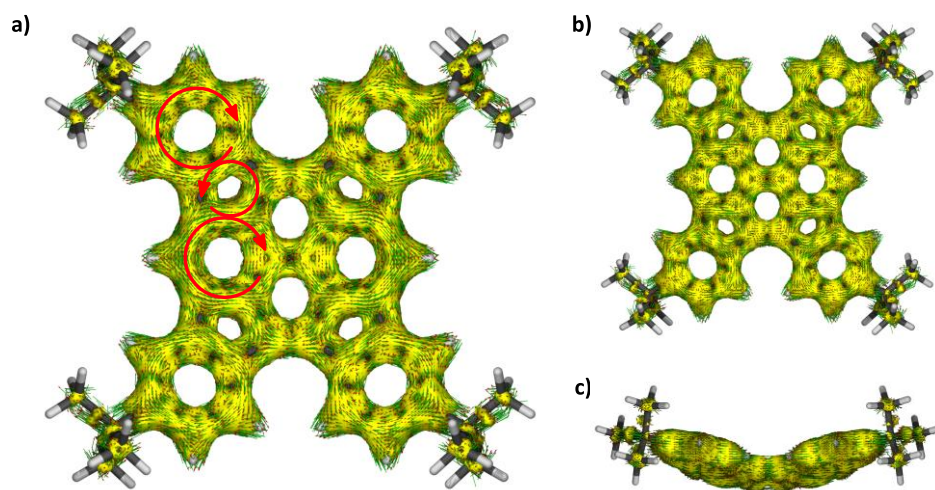


Figure S 51: AICD plots (HF/6-31+G(d)) of the bowl-shaped tetraindenopyrene **2** with dispersion correction (D3BJ) from a) the top/concave side with the magnetic field pointing out of the paper plane and red arrows indicating the direction of the ring current. b) View from the convex side and c) from the side. Both pictures show the difference of the isosurface on the concave and convex side of the TIP **2**.

xyz coordinates of the calculated structures**TIP 2 (bowl conformation) without dispersion correction**

atom	x	y	z	atom	x	y	z
C1	-1.2222	-2.7324	-0.5426	C24	4.7777	1.8861	-0.1646
C2	-0.0001	-3.4330	-0.4108	C25	4.7775	-1.8865	-0.1647
C3	1.2220	-2.7325	-0.5427	C26	5.3870	-3.1125	0.1104
C4	1.2005	-1.3596	-0.8250	C27	3.2735	-4.2475	-0.0159
C5	2.4827	-0.6984	-0.6649	C28	2.6497	-3.0387	-0.2958
C6	2.4825	0.6981	-0.6634	C29	-2.6500	-3.0384	-0.2956
C7	1.2009	1.3598	-0.8266	C30	-3.2739	-4.2473	-0.0159
C8	1.2221	2.7324	-0.5422	C31	-5.3873	-3.1120	0.1105
C9	0.0001	3.4329	-0.4103	C32	-4.7777	-1.8861	-0.1646
C10	-1.2219	2.7325	-0.5421	C33	-4.7776	1.8865	-0.1644
C11	-1.2008	1.3599	-0.8266	C34	-5.3871	3.1125	0.1105
C12	-2.4824	0.6983	-0.6633	C35	-3.2735	4.2476	-0.0157
C13	-2.4827	-0.6982	-0.6647	C36	-2.6497	3.0386	-0.2952
C14	-1.2006	-1.3595	-0.8250	C37	-6.1053	5.5178	1.8681
C15	0.0000	-0.6955	-0.9876	C38	-5.3943	5.6286	0.4988
C16	0.0000	0.6951	-0.9829	C39	-4.6614	4.3098	0.1930
C17	-3.4042	1.8234	-0.3697	C40	-6.4449	5.9016	-0.6033
C18	-3.4044	-1.8231	-0.3700	C41	-4.4369	6.8333	0.5544
C19	3.4042	-1.8234	-0.3702	C42	-4.4374	-6.8330	0.5538
C20	3.4044	1.8231	-0.3699	C43	-5.3947	-5.6281	0.4988
C21	2.6500	3.0384	-0.2954	C44	-4.6617	-4.3094	0.1930
C22	3.2739	4.2473	-0.0158	C45	-6.4458	-5.9008	-0.6029
C23	5.3873	3.1120	0.1103	C46	-6.1051	-5.5175	1.8685

<i>atom</i>	<i>x</i>	<i>y</i>	<i>z</i>	<i>atom</i>	<i>x</i>	<i>y</i>	<i>z</i>
C47	6.4453	-5.9015	-0.6026	H72	-7.1887	5.1039	-0.6623
C48	5.3942	-5.6285	0.4990	H73	-5.0046	7.7411	0.7756
C49	4.6614	-4.3097	0.1930	H74	-3.6823	6.7188	1.3375
C50	4.4368	-6.8332	0.5542	H75	-3.9235	6.9909	-0.3981
C51	6.1046	-5.5177	1.8687	H76	-5.0052	-7.7408	0.7749
C52	4.4375	6.8329	0.5542	H77	-3.6825	-6.7188	1.3367
C53	5.3948	5.6281	0.4987	H78	-3.9244	-6.9905	-0.3990
C54	4.6618	4.3094	0.1929	H79	-7.1895	-5.1029	-0.6615
C55	6.4456	5.9009	-0.6033	H80	-6.9753	-6.8366	-0.3984
C56	6.1056	5.5172	1.8682	H81	-5.9698	-5.9865	-1.5836
H57	-0.0002	-4.4831	-0.1365	H82	-5.3837	-5.3275	2.6680
H58	0.0002	4.4828	-0.1349	H83	-6.8388	-4.7085	1.8818
H59	2.6732	5.1462	0.0347	H84	-6.6312	-6.4492	2.0988
H60	6.4604	3.1245	0.2615	H85	6.9746	-6.8374	-0.3979
H61	6.4601	-3.1250	0.2618	H86	7.1892	-5.1038	-0.6613
H62	2.6727	-5.1464	0.0347	H87	5.9693	-5.9873	-1.5833
H63	-2.6732	-5.1462	0.0347	H88	3.6819	-6.7188	1.3371
H64	-6.4604	-3.1246	0.2616	H89	5.0045	-7.7411	0.7754
H65	-6.4601	3.1251	0.2615	H90	3.9237	-6.9908	-0.3985
H66	-2.6728	5.1464	0.0348	H91	6.6306	-6.4494	2.0992
H67	-6.6314	6.4495	2.0984	H92	6.8383	-4.7086	1.8819
H68	-5.3842	5.3277	2.6679	H93	5.3832	-5.3275	2.6681
H69	-6.8391	4.7088	1.8811	H94	5.0053	7.7407	0.7753
H70	-5.9685	5.9873	-1.5838	H95	3.6828	6.7185	1.3373
H71	-6.9743	6.8375	-0.3989	H96	3.9242	6.9905	-0.3984

atom	x	y	z	atom	x	y	z
H97	7.1893	5.1032	-0.6621	H102	6.6318	6.4489	2.0985
H98	6.9750	6.8368	-0.3988	H103	-5.3907	-0.9964	-0.2212
H99	5.9693	5.9867	-1.5838	H104	-5.3907	0.9969	-0.2211
H100	5.3844	5.3272	2.6679	H105	5.3907	-0.9969	-0.2214
H101	6.8392	4.7081	1.8813	H106	5.3907	0.9964	-0.2213

TIP 2 (bowl conformation) with dispersion correction

atom	x	y	z	atom	x	y	z
C1	-1.2189	-2.7233	-0.6703	C17	-3.3926	1.8058	-0.4600
C2	0.0001	-3.4185	-0.5101	C18	-3.3924	-1.8059	-0.4598
C3	1.2190	-2.7233	-0.6704	C19	3.3925	-1.8057	-0.4603
C4	1.2000	-1.3614	-1.0114	C20	3.3925	1.8059	-0.4603
C5	2.4779	-0.6964	-0.8191	C21	2.6371	3.0192	-0.3687
C6	2.4778	0.6965	-0.8188	C22	3.2494	4.2145	-0.0222
C7	1.2000	1.3616	-1.0119	C23	5.3565	3.0696	0.1343
C8	1.2189	2.7233	-0.6699	C24	4.7571	1.8561	-0.2068
C9	-0.0001	3.4185	-0.5095	C25	4.7569	-1.8558	-0.2060
C10	-1.2190	2.7232	-0.6698	C26	5.3564	-3.0693	0.1351
C11	-1.2001	1.3616	-1.0118	C27	3.2495	-4.2145	-0.0227
C12	-2.4779	0.6964	-0.8185	C28	2.6372	-3.0191	-0.3690
C13	-2.4779	-0.6965	-0.8188	C29	-2.6370	-3.0192	-0.3687
C14	-1.1999	-1.3614	-1.0113	C30	-3.2493	-4.2146	-0.0225
C15	0.0000	-0.6979	-1.1997	C31	-5.3563	-3.0696	0.1353
C16	-0.0001	0.6978	-1.1983	C32	-4.7569	-1.8560	-0.2056

atom	x	y	z	atom	x	y	z
C33	-4.7571	1.8560	-0.2066	H58	-0.0001	4.4508	-0.1761
C34	-5.3566	3.0695	0.1344	H59	2.6489	5.1119	0.0415
C35	-3.2495	4.2145	-0.0221	H60	6.4231	3.0780	0.3229
C36	-2.6372	3.0191	-0.3684	H61	6.4229	-3.0776	0.3243
C37	-6.0117	5.3928	2.0002	H62	2.6490	-5.1119	0.0407
C38	-5.3494	5.5616	0.6161	H63	-2.6489	-5.1121	0.0407
C39	-4.6280	4.2620	0.2365	H64	-6.4228	-3.0780	0.3244
C40	-6.4337	5.8703	-0.4385	H65	-6.4232	3.0780	0.3228
C41	-4.3926	6.7621	0.6859	H66	-2.6490	5.1119	0.0416
C42	-4.3924	-6.7625	0.6841	H67	-6.5288	6.3133	2.2871
C43	-5.3491	-5.5618	0.6160	H68	-5.2618	5.1687	2.7632
C44	-4.6277	-4.2621	0.2367	H69	-6.7435	4.5826	2.0017
C45	-6.4345	-5.8696	-0.4376	H70	-5.9870	5.9903	-1.4288
C46	-6.0100	-5.3937	2.0010	H71	-6.9571	6.7966	-0.1835
C47	6.4346	-5.8697	-0.4374	H72	-7.1755	5.0715	-0.5002
C48	5.3492	-5.5615	0.6162	H73	-4.9526	7.6593	0.9609
C49	4.6279	-4.2619	0.2365	H74	-3.6128	6.6152	1.4377
C50	4.3925	-6.7622	0.6846	H75	-3.9123	6.9542	-0.2771
C51	6.0101	-5.3930	2.0011	H76	-4.9524	-7.6598	0.9590
C52	4.3924	6.7621	0.6858	H77	-3.6119	-6.6164	1.4354
C53	5.3492	5.5616	0.6162	H78	-3.9130	-6.9540	-0.2794
C54	4.6278	4.2620	0.2365	H79	-7.1761	-5.0706	-0.4982
C55	6.4338	5.8703	-0.4381	H80	-6.9579	-6.7959	-0.1825
C56	6.0112	5.3927	2.0005	H81	-5.9887	-5.9893	-1.4284
H57	0.0001	-4.4511	-0.1774	H82	-5.2592	-5.1700	2.7633

atom	x	y	z	atom	x	y	z
H83	-6.7417	-4.5835	2.0036	H95	3.6125	6.6154	1.4375
H84	-6.5268	-6.3144	2.2879	H96	3.9124	6.9542	-0.2773
H85	6.9580	-6.7959	-0.1820	H97	7.1756	5.0715	-0.4995
H86	7.1763	-5.0708	-0.4981	H98	6.9571	6.7966	-0.1829
H87	5.9889	-5.9896	-1.4281	H99	5.9874	5.9902	-1.4285
H88	3.6122	-6.6159	1.4360	H100	5.2610	5.1686	2.7633
H89	4.9526	-7.6594	0.9596	H101	6.7429	4.5824	2.0022
H90	3.9130	-6.9539	-0.2787	H102	6.5282	6.3132	2.2875
H91	6.5270	-6.3135	2.2883	H103	-5.3688	-0.9677	-0.2753
H92	6.7418	-4.5826	2.0034	H104	-5.3693	0.9679	-0.2772
H93	5.2594	-5.1691	2.7633	H105	5.3689	-0.9675	-0.2758
H94	4.9525	7.6593	0.9608	H106	5.3692	0.9680	-0.2776

TIP 2 (planar conformation) without dispersion correction

atom	x	y	z	atom	x	y	z
C1	-2.4928	0.7007	0.0000	C8	2.4928	-0.7007	0.0000
C2	-2.4928	-0.7007	0.0000	C9	2.4928	0.7007	0.0000
C3	-1.2004	-1.3564	0.0000	C10	1.2004	1.3564	0.0000
C4	0.0000	-0.6899	0.0000	C11	1.2290	2.7545	0.0000
C5	0.0000	0.6899	0.0000	C12	0.0000	3.4659	0.0000
C6	-1.2004	1.3564	0.0000	C13	-1.2290	2.7545	0.0000
C7	1.2004	-1.3564	0.0000	C14	-1.2290	-2.7545	0.0000

<i>atom</i>	<i>x</i>	<i>y</i>	<i>z</i>	<i>atom</i>	<i>x</i>	<i>y</i>	<i>z</i>
C15	0.0000	-3.4659	0.0000	C40	4.8168	-1.9290	0.0000
C16	1.2290	-2.7545	0.0000	C41	5.4867	5.7190	0.0000
C17	3.4299	1.8522	0.0000	C42	5.4867	-5.7190	0.0000
C18	-3.4299	1.8522	0.0000	C43	-5.4867	-5.7190	0.0000
C19	-3.4299	-1.8522	0.0000	C44	-5.4867	5.7190	0.0000
C20	3.4299	-1.8522	0.0000	C45	-6.3765	5.8080	1.2620
C21	-4.8168	-1.9290	0.0000	C46	-6.3765	5.8080	-1.2620
C22	-5.4477	-3.1743	0.0000	C47	-4.5360	6.9302	0.0000
C23	-4.7296	-4.3784	0.0000	C48	6.3765	5.8080	-1.2620
C24	-3.3265	-4.3037	0.0000	C49	4.5360	6.9302	0.0000
C25	-2.6781	-3.0765	0.0000	C50	6.3765	5.8080	1.2620
C26	-2.6781	3.0765	0.0000	C51	6.3765	-5.8080	-1.2620
C27	-3.3265	4.3037	0.0000	C52	4.5360	-6.9302	0.0000
C28	-4.7296	4.3784	0.0000	C53	6.3765	-5.8080	1.2620
C29	-5.4477	3.1743	0.0000	C54	-4.5360	-6.9302	0.0000
C30	-4.8168	1.9290	0.0000	C55	-6.3765	-5.8080	1.2620
C31	4.8168	1.9290	0.0000	C56	-6.3765	-5.8080	-1.2620
C32	5.4477	3.1743	0.0000	H57	0.0000	4.5513	0.0000
C33	4.7296	4.3784	0.0000	H58	0.0000	-4.5513	0.0000
C34	3.3265	4.3037	0.0000	H59	-5.4217	-1.0312	0.0000
C35	2.6781	3.0765	0.0000	H60	-6.5311	-3.1977	0.0000
C36	2.6781	-3.0765	0.0000	H61	-2.7322	-5.2082	0.0000
C37	3.3265	-4.3037	0.0000	H62	-2.7322	5.2082	0.0000
C38	4.7296	-4.3784	0.0000	H63	-6.5311	3.1977	0.0000
C39	5.4477	-3.1743	0.0000	H64	-5.4217	1.0312	0.0000

<i>atom</i>	<i>x</i>	<i>y</i>	<i>z</i>	<i>atom</i>	<i>x</i>	<i>y</i>	<i>z</i>
H65	5.4217	1.0312	0.0000	H86	5.7711	5.7499	2.1706
H66	6.5311	3.1977	0.0000	H87	6.9215	6.7569	1.2757
H67	2.7322	5.2082	0.0000	H88	7.1114	5.0008	1.2986
H68	2.7322	-5.2082	0.0000	H89	6.9215	-6.7569	-1.2757
H69	6.5311	-3.1977	0.0000	H90	5.7711	-5.7499	-2.1706
H70	5.4217	-1.0312	0.0000	H91	7.1114	-5.0008	-1.2986
H71	-5.7711	5.7499	2.1706	H92	3.8962	-6.9459	0.8865
H72	-7.1114	5.0008	1.2986	H93	3.8962	-6.9459	-0.8865
H73	-6.9215	6.7569	1.2757	H94	5.1207	-7.8539	0.0000
H74	-6.9215	6.7569	-1.2757	H95	5.7711	-5.7499	2.1706
H75	-5.7711	5.7499	-2.1706	H96	7.1114	-5.0008	1.2986
H76	-7.1114	5.0008	-1.2986	H97	6.9215	-6.7569	1.2757
H77	-3.8962	6.9459	0.8865	H98	-3.8962	-6.9459	0.8865
H78	-3.8962	6.9459	-0.8865	H99	-3.8962	-6.9459	-0.8865
H79	-5.1207	7.8539	0.0000	H100	-5.1207	-7.8539	0.0000
H80	7.1114	5.0008	-1.2986	H101	-5.7711	-5.7499	2.1706
H81	5.7711	5.7499	-2.1706	H102	-7.1114	-5.0008	1.2986
H82	6.9215	6.7569	-1.2757	H103	-6.9215	-6.7569	1.2757
H83	3.8962	6.9459	0.8865	H104	-6.9215	-6.7569	-1.2757
H84	3.8962	6.9459	-0.8865	H105	-5.7711	-5.7499	-2.1706
H85	5.1207	7.8539	0.0000	H106	-7.1114	-5.0008	-1.2986

TIP 2 (planar conformation) with dispersion correction

atom	x	y	z	atom	x	y	z
C1	-2.5011	-0.6244	-0.0011	C23	2.7755	3.0027	-0.0008
C2	-2.4614	0.7749	-0.0011	C24	3.4913	1.7548	-0.0008
C3	-1.1503	1.3945	-0.0015	C25	-4.7499	2.0595	0.0004
C4	0.0295	0.6942	-0.0017	C26	-5.3474	3.3205	0.0010
C5	-0.0098	-0.6856	-0.0015	C27	-3.1968	4.3964	0.0001
C6	-1.2275	-1.3176	-0.0012	C28	-3.4415	-4.1983	-0.0002
C7	1.2472	1.3265	-0.0015	C29	-5.5273	-3.0018	-0.0008
C8	2.5209	0.6336	-0.0011	C30	-4.8590	-1.7767	-0.0010
C9	2.4812	-0.7657	-0.0010	C31	4.7672	-2.0486	0.0001
C10	1.1703	-1.3861	-0.0012	C32	5.3716	-3.3125	0.0007
C11	1.1596	-2.7853	-0.0006	C33	3.2177	-4.3828	0.0004
C12	-0.0894	-3.4616	-0.0004	C34	3.4605	4.2076	-0.0005
C13	-1.2975	-2.7152	-0.0007	C35	5.5465	3.0114	-0.0003
C14	-1.1406	2.7938	-0.0011	C36	4.8785	1.7862	-0.0006
C15	0.1082	3.4703	-0.0010	C37	6.8020	-5.8172	0.0019
C16	1.3168	2.7240	-0.0011	C38	5.2669	-5.8816	0.0015
C17	3.3878	-1.9391	-0.0004	C39	4.6231	-4.4900	0.0009
C18	2.5998	-3.1479	-0.0002	C40	4.8168	-6.6515	-1.2585
C19	-2.7563	-2.9935	-0.0005	C41	4.8161	-6.6507	1.2619
C20	-3.4719	-1.7456	-0.0008	C42	-4.7311	-6.7737	0.0010
C21	-3.3667	1.9495	-0.0005	C43	-5.6421	-5.5361	0.0000
C22	-2.5812	3.1546	-0.0006	C44	-4.8453	-4.2250	-0.0003

atom	x	y	z	atom	x	y	z
C45	-6.5310	-5.5936	-1.2606	H68	2.8962	5.1303	-0.0005
C46	-6.5320	-5.5924	1.2599	H69	6.6296	3.0052	-0.0002
C47	-6.2025	5.9656	-1.2583	H70	5.4520	0.8685	-0.0007
C48	-5.3173	5.8575	0.0016	H71	7.2101	-6.8309	0.0024
C49	-4.5967	4.5030	0.0008	H72	7.1847	-5.3050	0.8882
C50	-4.3372	7.0411	0.0017	H73	7.1851	-5.3056	-0.8846
C51	-6.2014	5.9645	1.2624	H74	3.7322	-6.7728	-1.2924
C52	4.7496	6.7832	0.0001	H75	5.2667	-7.6485	-1.2738
C53	5.6608	5.5458	0.0001	H76	5.1231	-6.1227	-2.1645
C54	4.8642	4.2345	-0.0002	H77	5.2660	-7.6476	1.2781
C55	6.5504	5.6030	-1.2600	H78	5.1220	-6.1212	2.1677
C56	6.5500	5.6026	1.2605	H79	3.7315	-6.7720	1.2952
H57	-0.1204	-4.5460	0.0001	H80	-5.3443	-7.6782	0.0011
H58	0.1390	4.5547	-0.0006	H81	-4.0932	-6.8058	0.8879
H59	-5.3745	1.1758	0.0007	H82	-4.0923	-6.8066	-0.8853
H60	-6.4291	3.3759	0.0017	H83	-7.2383	-4.7627	-1.2936
H61	-2.5812	5.2857	0.0000	H84	-7.1049	-6.5248	-1.2773
H62	-2.8774	-5.1211	0.0001	H85	-5.9206	-5.5504	-2.1661
H63	-6.6104	-2.9954	-0.0010	H86	-7.1060	-6.5235	1.2770
H64	-5.4323	-0.8589	-0.0016	H87	-5.9224	-5.5485	2.1660
H65	5.3916	-1.1648	0.0001	H88	-7.2394	-4.7614	1.2916
H66	6.4515	-3.3599	0.0011	H90	-6.9560	5.1762	-1.2908
H67	2.6077	-5.2786	0.0006	H91	-5.5962	5.8877	-2.1643

atom	x	y	z		H99	4.1110	6.8154	0.8866
H92	-3.6979	7.0370	0.8882		H100	4.1114	6.8157	-0.8866
H93	-4.8977	7.9791	0.0019		H101	7.2578	4.7722	-1.2924
H94	-3.6981	7.0372	-0.8850		H102	7.1242	6.5343	-1.2766
H95	-6.7215	6.9268	1.2798		H103	5.9406	5.5595	-2.1659
H96	-6.9548	5.1751	1.2949		H104	7.1238	6.5339	1.2776
H97	-5.5944	5.8861	2.1678		H105	5.9398	5.5588	2.1662
H98	5.3626	7.6878	0.0004		H106	7.2574	4.7718	1.2928

Compound 2 without *tert*-butyl (bowl conformation) w/o dispersion correction

atom	x	y	z		atom	x	y	z
C1	-1.2187	-2.7247	-0.2867		C13	-2.4788	-0.6971	-0.4328
C2	0.0002	-3.4210	-0.1311		C14	-1.2003	-1.3608	-0.6178
C3	1.2190	-2.7246	-0.2866		C15	0.0001	-0.6971	-0.8015
C4	1.2005	-1.3607	-0.6178		C16	0.0000	0.6970	-0.7995
C5	2.4790	-0.6968	-0.4327		C17	-3.3981	1.8091	-0.0858
C6	2.4788	0.6971	-0.4317		C18	-3.3979	-1.8096	-0.0862
C7	1.2004	1.3610	-0.6174		C19	3.3982	-1.8092	-0.0862
C8	1.2187	2.7247	-0.2856		C20	3.3979	1.8095	-0.0854
C9	-0.0002	3.4210	-0.1302		C21	2.6369	3.0256	0.0047
C10	-1.2190	2.7246	-0.2857		C22	3.2565	4.2199	0.3371
C11	-1.2004	1.3608	-0.6174		C23	5.3803	3.0613	0.4784
C12	-2.4788	0.6968	-0.4318		C24	4.7659	1.8473	0.1496

atom	x	y	z	atom	x	y	z
C25	4.7661	-1.8470	0.1490	H42	-0.0003	4.4564	0.1929
C26	5.3805	-3.0607	0.4783	H43	2.6817	5.1364	0.4081
C27	3.2568	-4.2196	0.3368	H44	6.4486	3.0861	0.6581
C28	2.6372	-3.0254	0.0038	H45	6.4488	-3.0855	0.6582
C29	-2.6369	-3.0257	0.0038	H46	2.6820	-5.1361	0.4078
C30	-3.2563	-4.2198	0.3371	H47	-2.6814	-5.1362	0.4082
C31	-5.3800	-3.0611	0.4795	H48	-6.4481	-3.0858	0.6600
C32	-4.7657	-1.8473	0.1497	H49	-6.4491	3.0853	0.6572
C33	-4.7661	1.8467	0.1490	H50	-2.6825	5.1361	0.4076
C34	-5.3808	3.0606	0.4776	H51	-5.3671	-0.9530	0.0740
C35	-3.2572	4.2195	0.3366	H52	-5.3671	0.9522	0.0736
C36	-2.6373	3.0253	0.0043	H53	5.3673	-0.9527	0.0731
C37	-4.6364	4.2330	0.5733	H54	5.3670	0.9529	0.0745
C38	-4.6353	-4.2334	0.5752	H55	5.1277	5.1648	0.8296
C39	4.6359	-4.2331	0.5742	H56	5.1278	-5.1641	0.8303
C40	4.6357	4.2336	0.5741	H57	-5.1271	-5.1644	0.8316
H41	0.0002	-4.4565	0.1917	H58	-5.1285	5.1641	0.8288

Compound 2 without *tert*-butyl (bowl conformation) with dispersion correction

atom	x	y	z	atom	x	y	z
C1	-1.2217	-2.7333	-0.2324	C3	1.2217	-2.7333	-0.2325
C2	0.0000	-3.4348	-0.1046	C4	1.2010	-1.3591	-0.5066

atom	x	y	z	atom	x	y	z
C5	2.4834	-0.6988	-0.3519	C28	2.6485	-3.0439	0.0055
C6	2.4834	0.6987	-0.3519	C29	-2.6486	-3.0438	0.0055
C7	1.2011	1.3591	-0.5072	C30	-3.2784	-4.2502	0.2754
C8	1.2217	2.7333	-0.2327	C31	-5.4083	-3.0998	0.3897
C9	0.0001	3.4348	-0.1049	C32	-4.7852	-1.8747	0.1234
C10	-1.2217	2.7333	-0.2326	C33	-4.7851	1.8748	0.1234
C11	-1.2011	1.3591	-0.5071	C34	-5.4081	3.0999	0.3901
C12	-2.4834	0.6988	-0.3519	C35	-3.2781	4.2503	0.2757
C13	-2.4835	-0.6987	-0.3518	C36	-2.6484	3.0439	0.0055
C14	-1.2011	-1.3591	-0.5066	C37	-4.6643	4.2745	0.4678
C15	0.0000	-0.6946	-0.6626	C38	-4.6646	-4.2744	0.4673
C16	0.0000	0.6945	-0.6621	C39	4.6644	-4.2744	0.4676
C17	-3.4092	1.8260	-0.0680	C40	4.6645	4.2743	0.4676
C18	-3.4092	-1.8259	-0.0679	H41	-0.0001	-4.4869	0.1612
C19	3.4092	-1.8260	-0.0679	H42	0.0001	4.4868	0.1613
C20	3.4093	1.8259	-0.0682	H43	2.7057	5.1695	0.3332
C21	2.6485	3.0438	0.0053	H44	6.4820	3.1313	0.5353
C22	3.2783	4.2502	0.2755	H45	6.4819	-3.1314	0.5357
C23	5.4082	3.0998	0.3899	H46	2.7056	-5.1696	0.3331
C24	4.7852	1.8747	0.1232	H47	-2.7058	-5.1696	0.3330
C25	4.7851	-1.8748	0.1236	H48	-6.4820	-3.1313	0.5351
C26	5.4082	-3.0998	0.3901	H49	-6.4818	3.1315	0.5355
C27	3.2782	-4.2503	0.2755	H50	-2.7055	5.1696	0.3333

atom	x	y	z	atom	x	y	z
H51	-5.3869	-0.9784	0.0622	H55	5.1621	5.2149	0.6747
H52	-5.3870	0.9787	0.0618	H56	5.1621	-5.2151	0.6745
H53	5.3869	-0.9785	0.0625	H57	-5.1623	-5.2150	0.6740
H54	5.3870	0.9785	0.0615	H58	-5.1619	5.2151	0.6749

7. TFT characteristics

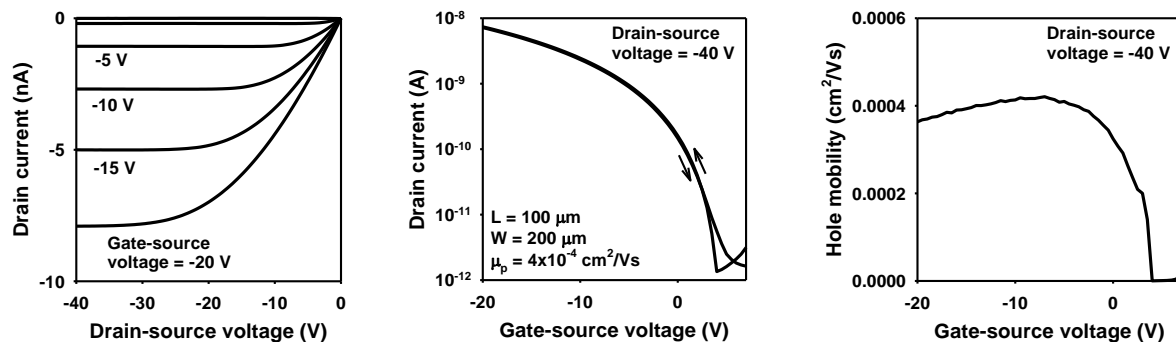


Figure S52: Current-voltage characteristics of a p-channel TFT based on a vacuum-deposited layer of TIP **2** as the semiconductor (substrate temperature during the semiconductor deposition: 80 °C; semiconductor thickness: 30 nm). The substrate is a heavily doped silicon wafer, and the gate dielectric is a combination of a 100-nm-thick layer of thermally grown silicon dioxide (SiO_2), an 8-nm-thick layer of aluminum oxide (Al_2O_3) grown by atomic layer deposition (ALD) and a self-assembled monolayer (SAM) of pentadecylfluoroctadecylphosphonic acid.

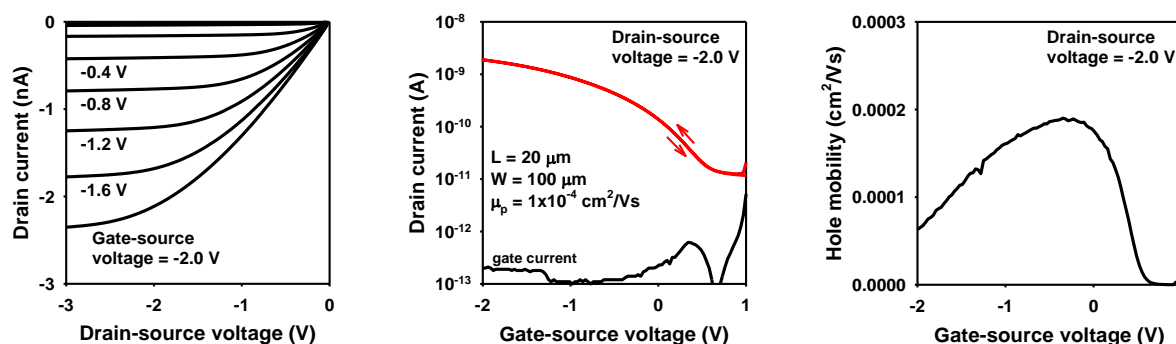


Figure S53: Current-voltage characteristics of a p-channel TFT based on a vacuum-deposited layer of TIP **2** as the semiconductor (substrate temperature during the semiconductor deposition: 80 °C; semiconductor thickness: 30 nm). The substrate is 125-μm-thick flexible polyethylene naphthalate (PEN), and the gate dielectric is a combination of a 3.6-nm-thick layer of aluminum oxide (AlO_x) obtained by plasma oxidation of the surface of the aluminum gate electrode and a 2.1-nm-thick self-assembled monolayer (SAM) of pentadecylfluoroctadecylphosphonic acid.

8. Crystallographic information

Single crystals of **5** suitable for SCXRD analysis were obtained by vapor diffusion of *n*-pentane into a saturated CH₂Cl₂ solution of **5**.

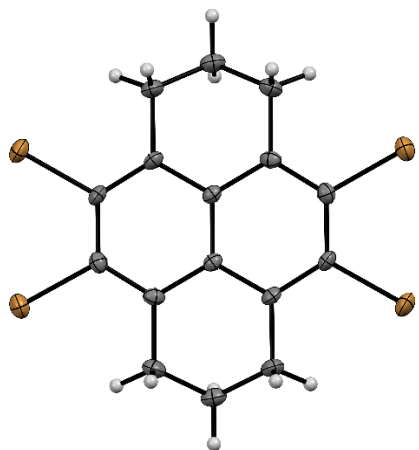


Table S2: Crystal data and structure refinement for **5**.

CCDC number	1992741					
Empirical formula	C ₁₆ H ₁₂ Br ₄					
Formula weight	523.90					
Temperature	200(2) K					
Wavelength	0.71073 Å					
Crystal system	orthorhombic					
Space group	Pnna					
Z	4					
Unit cell dimensions	a = 7.3263(5) Å	α = 90 deg.	b = 11.4960(8) Å	β = 90 deg.	c = 17.3499(12) Å	γ = 90 deg.
Volume	1461.26(17) Å ³					
Density (calculated)	2.38 g/cm ³					
Absorption coefficient	11.00 mm ⁻¹					
Crystal shape	plate					
Crystal size	0.058 x 0.040 x 0.015 mm ³					
Crystal colour	colourless					
Theta range for data collection	2.1 to 33.7 deg.					
Index ranges	-10≤h≤9, -17≤k≤17, -23≤l≤26					
Reflections collected	13294					
Independent reflections	2630 (R(int) = 0.0548)					
Observed reflections	1536 (I > 2σ(I))					
Absorption correction	Semi-empirical from equivalents					
Max. and min. transmission	0.88 and 0.72					
Refinement method	Full-matrix least-squares on F ²					
Data/restraints/parameters	2630 / 0 / 91					
Goodness-of-fit on F ²	0.97					
Final R indices (I>2sigma(I))	R1 = 0.034, wR2 = 0.057					
Largest diff. peak and hole	0.56 and -0.78 eÅ ⁻³					

Single crystals of **6** suitable for SCXRD analysis were obtained by vapor diffusion of *n*-pentane into a saturated CH₂Cl₂ solution of **6**.

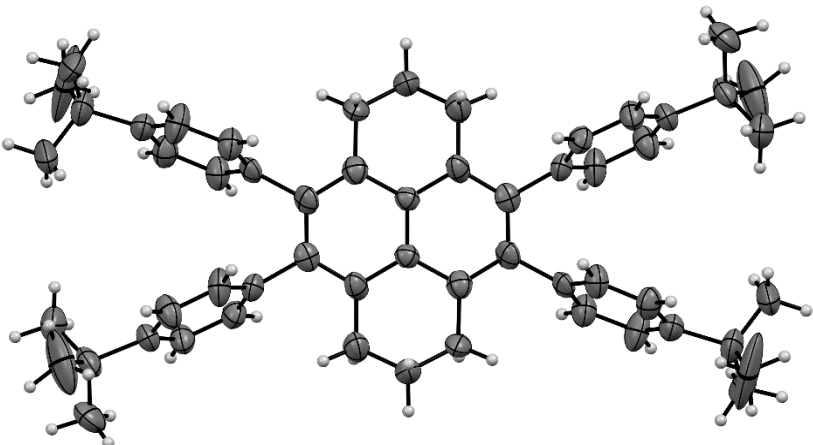


Table S3: Crystal data and structure refinement for **6**.

CCDC number	1992741		
Empirical formula	C ₅₆ H ₆₄		
Formula weight	737.07		
Temperature	200(2) K		
Wavelength	1.54178 Å		
Crystal system	monoclinic		
Space group	P2 ₁ /c		
Z	2		
Unit cell dimensions	a = 15.235(6) Å	α = 90 deg.	
	b = 10.695(3) Å	β = 119.30(3) deg.	
	c = 15.558(9) Å	γ = 90 deg.	
Volume	2210.7(17) Å ³		
Density (calculated)	1.11 g/cm ³		
Absorption coefficient	0.46 mm ⁻¹		
Crystal shape	brick		
Crystal size	0.055 x 0.040 x 0.018 mm ³		
Crystal colour	colourless		
Theta range for data collection	3.3 to 46.6 deg.		
Index ranges	-14≤h≤14, -9≤k≤10, -9≤l≤14		
Reflections collected	9818		
Independent reflections	1939 (R(int) = 0.1975)		
Observed reflections	922 (I > 2σ(I))		
Absorption correction	Semi-empirical from equivalents		
Max. and min. transmission	1.37 and 0.70		
Refinement method	Full-matrix least-squares on F ²		
Data/restraints/parameters	1939 / 297 / 259		
Goodness-of-fit on F ²	1.12		
Final R indices (I>2sigma(I))	R1 = 0.116, wR2 = 0.299		
Largest diff. peak and hole	0.32 and -0.30 eÅ ⁻³		

9. References

- [S1] a) H. E. Gottlieb, V. Kotlyar, A. Nudelman, *J. Org. Chem.* **1997**, 62, 7512-7515; b) G. R. Fulmer, A. J. M. Miller, N. H. Sherden, H. E. Gottlieb, A. Nudelman, B. M. Stoltz, J. E. Bercaw, K. I. Goldberg, *Organometallics* **2010**, 29, 2176-2179.
- [S2] M. J. Frisch, G. W. Trucks, H. B. Schlegel, G. E. Scuseria, M. A. Robb, J. R. Cheeseman, G. Scalmani, V. Barone, G. A. Petersson, H. Nakatsuji, X. Li, M. Caricato, A. V. Marenich, J. Bloino, B. G. Janesko, R. Gomperts, B. Mennucci, H. P. Hratchian, J. V. Ortiz, A. F. Izmaylov, J. L. Sonnenberg, Williams, F. Ding, F. Lipparini, F. Egidi, J. Goings, B. Peng, A. Petrone, T. Henderson, D. Ranasinghe, V. G. Zakrzewski, J. Gao, N. Rega, G. Zheng, W. Liang, M. Hada, M. Ehara, K. Toyota, R. Fukuda, J. Hasegawa, M. Ishida, T. Nakajima, Y. Honda, O. Kitao, H. Nakai, T. Vreven, K. Throssell, J. A. Montgomery Jr., J. E. Peralta, F. Ogliaro, M. J. Bearpark, J. J. Heyd, E. N. Brothers, K. N. Kudin, V. N. Staroverov, T. A. Keith, R. Kobayashi, J. Normand, K. Raghavachari, A. P. Rendell, J. C. Burant, S. S. Iyengar, J. Tomasi, M. Cossi, J. M. Millam, M. Klene, C. Adamo, R. Cammi, J. W. Ochterski, R. L. Martin, K. Morokuma, O. Farkas, J. B. Foresman, D. J. Fox, Wallingford, CT, **2016**.
- [S3] a) W. Kohn, L. J. Sham, *Phys. Rev.* **1965**, 140, A1133-A1138; b) R. G. Parr, W. Yang, *Density-functional theory of atoms and molecules*, 1. Aufl., Oxford Univ. Press, New York, NY, **1994**; c) W. Koch, *A Chemist's Guide to Density Functional Theory*, 2. Aufl., Wiley-VCH, Weinheim, **2001**; d) P. Hohenberg, W. Kohn, *Phys. Rev.* **1964**, 136, B864-B871.
- [S4] a) A. D. Becke, *J. Chern. Phys.* **1993**, 98, 1372-1377; b) C. Lee, W. Yang, R. G. Parr, *Phys. Rev. B* **1988**, 37, 785-789; c) P. J. Stephens, F. J. Devlin, C. F. Chabalowski, M. J. Frisch, *J. Phys. Chem.* **1994**, 98, 11623-11627; d) S. H. Vosko, L. Wilk, M. Nusair, *Can. J. Phys.* **1980**, 58, 1200-1211.
- [S5] R. Krishnan, J. S. Binkley, R. Seeger, J. A. Pople, *J. Chem. Phys.* **1980**, 72, 650-654.
- [S6] S. Grimme, S. Ehrlich, L. Goerigk, *J. Comput. Chem.* **2011**, 32, 1456-1465.
- [S7] N. M. O'boyle, A. L. Tenderholt, K. M. Langner, *J. Comput. Chem.* **2008**, 29, 839-845.
- [S8] a) J. A. Gaunt, *Math. Proc. Camb. Phil. Soc.* **1928**, 24, 328-342; b) D. R. Hartree, *Math. Proc. Camb. Phil. Soc.* **1928**, 24, 426-437; c) J. C. Slater, *Phys. Rev.* **1928**, 32, 339-348; d) V. Fock, *Z. Physik* **1930**, 61, 126-148; e) V. Fock, *Z. Physik* **1930**, 62, 795-805; f) J. C. Slater, *Phys. Rev.* **1930**, 35, 210-211; g) H. A. Bethe, W. L. Bragg, *Proc. R. Soc. Lond. A* **1935**, 150, 552-575; hC. C. J. Roothaan, *Rev. Mod. Phys.* **1951**, 23, 69-89.
- [S9] T. Clark, J. Chandrasekhar, G. W. Spitznagel, P. V. R. Schleyer, *J. Comput. Chem.* **1983**, 4, 294-301.
- [S10] a) F. London, *J. Phys. Radium* **1937**, 8, 397-409; b) R. McWeeny, *Phys. Rev.* **1962**, 126, 1028-1034; c) R. Ditchfield, *Mol. Phys.* **1974**, 27, 789-807; d) K. Wolinski, J. F. Hinton, P. Pulay, *J. Am. Chem. Soc.* **1990**, 112, 8251-8260.
- [S11] a) J. R. Cheeseman, G. W. Trucks, T. A. Keith, M. J. Frisch, *J. Chem. Phys.* **1996**, 104, 5497-5509; b) T. A. Keith, R. F. W. Bader, *Chem. Phys. Lett.* **1992**, 194, 1-8; c) T. A. Keith, R. F. W. Bader, *Chem. Phys. Lett.* **1993**, 210, 223-231.
- [S12] a) D. Geuenich, K. Hess, F. Köhler, R. Herges, *Chem. Rev.* **2005**, 105, 3758-3772; b) R. Herges, D. Geuenich, *J. Phys. Chem. A* **2001**, 105, 3214-3220.
- [S13] J. C. Dobrowolski, P. F. J. Lipiński, *RSC Adv.* **2016**, 6, 23900-23904.
- [S14] D. Zhao, Q. Wu, Z. Cai, T. Zheng, W. Chen, J. Lu, L. Yu, *Chem. Mater.* **2016**, 28, 1139-1146.

- [S15] L. Zöphel, R. Berger, P. Gao, V. Enkelmann, M. Baumgarten, M. Wagner, K. Müllen, *Chem. Eur. J.* **2013**, 19, 17821-17826.
- [S16] a) H. A. Wegner, H. Reisch, K. Rauch, A. Demeter, K. A. Zachariasse, A. de Meijere, L. T. Scott, *J. Org. Chem.* **2006**, 71, 9080-9087; b) H. A. Wegner, H. Reisch, K. Rauch, A. Demeter, K. A. Zachariasse, A. de Meijere, L. T. Scott, *J. Org. Chem.* **2007**, 72, 1870-1870.
- [S17] a) R. B. Martin, *Chem. Rev.* **1996**, 96, 3043-3064; b) Y. Tobe, N. Utsumi, K. Kawabata, A. Nagano, K. Adachi, S. Araki, M. Sonoda, K. Hirose, K. Naemura, *J. Am. Chem. Soc.* **2002**, 124, 5350-5364; c) Y. Nakamura, T. Nakazato, T. Kamatsuka, H. Shinokubo, Y. Miyake, *Chem. Eur. J.* **2019**, 25, 10571-10574.